RESEARCH MEMORANDUM

MEASUREMENT OF STATIC FORCES ON EXTERNALLY CARRIED BOMBS

OF FINENESS RATIOS 7.1 AND 10.5 IN THE FLOW FIELD

OF A SWEPT-WING FIGHTER-BOMBER CONFIGURATION

AT A MACH NUMBER OF 1.6

By Douglas J. Geier and Harry W. Carlson

Langley Aeronautical Laboratory Langley Field, Va.

Classification changed to Unclassified by authority of NASA classification change notice number 43 dated 12-29-65

NATIONAL ADVISORY COMMITTEE FOR AERONAUTICS

WASHINGTON
January 31, 1957

NATIONAL ADVISORY COMMITTEE FOR AERONAUTICS

RESEARCH MEMORANDUM

MEASUREMENT OF STATIC FORCES ON EXTERNALLY CARRIED BOMBS

OF FINENESS RATIOS 7.1 AND 10.5 IN THE FLOW FIELD

OF A SWEPT-WING FIGHTER-BOMBER CONFIGURATION

AT A MACH NUMBER OF 1.6

By Douglas J. Geier and Harry W. Carlson

SUMMARY

As a continuation of an extensive program to investigate interfer ence and bomb-release problems (first reported in NACA Research Memorandum L56I18), forces and moments have been measured at a Mach number of 1.6 in the Langley 4- by 4-foot supersonic pressure tunnel on bombs of fineness ratios 7.0 and 10.5 in the presence of a swept-wing fighter-bomber airplane configuration for a large number of positions under the fuselage. The results can be used to calculate bomb-drop paths. These paths, however, are not presented in this report. The force results show that the wing has a large effect on the interference pattern of the bomb and that maximum moments occur when the bomb fins are in a region believed to be just within the wing flow field behind the leading-edge shock.

INTRODUCTION

With the development of supersonic bombing airplanes, the problems of bomb release have become increasingly important. In addition to the higher dynamic pressures, the extremely turbulent circulatory flow in the bomb bay, as well as the nonuniform flow field surrounding the airplane, can cause bomb-release motions that endanger both the bomb and the airplane.

A study of the release problems can be made by measuring static forces on the bomb throughout the drop region and calculating the resultant motions. Although one set of measurements applies only to one configuration at one Mach number, a rather complete investigation of the various factors affecting bomb motion can be performed by simply varying the appropriate parameter in a series of drop calculations. Such calculations are readily performed by automatic computing machines.

The results of such a test program performed in the Langley 4- by 4-foot supersonic pressure tunnel at a Mach number of 1.6 are presented in reference 1 which used bombs with fineness ratios of 2.36, 4, and 7. In that report, measured forces and moments on bombs of three fineness ratios and on a fighter-bomber airplane model are presented for a number of positions of the bomb under an open bomb bay. Data for bomb trajectories were calculated and presented to illustrate the procedure and demonstrate the type of analysis that can be made.

As an extension of the tests discussed in reference 1, forces and moments have been measured on streamlined bombs of fineness ratios 7.0 and 10.5 and on a fighter-bomber airplane model for a number of positions of the bomb under the closed bomb bay (simulating an external carriage-bomb-airplane configuration) and under the 45° swept wing. These data are presented in this report with only a limited analysis in order to expedite publication.

SYMBOLS

c_D	drag coefficient of wing-fuselage combination, $\frac{\text{Drag}}{\text{qS}}$
$\mathtt{c}_{\mathtt{L}}$	lift coefficient of wing-fuselage combination, $\frac{\text{Lift}}{\text{qS}}$
C _m	pitching-moment coefficient of wing-fuselage combination about the quarter chord of \bar{c} , $\frac{\text{Pitching moment}}{\text{qS}\bar{c}}$
c_{D_b}	drag coefficient of bomb, $\frac{\text{Drag}}{\text{qF}}$
$c_{\mathbf{L_b}}$	lift coefficient of bomb, $\frac{\text{Lift}}{\text{qF}}$
c_{m_b}	pitching-moment coefficient of bomb about bomb nose, Pitching moment qF1
c_{n_b}	yawing-moment coefficient of bomb, $\frac{\text{Yawing moment}}{\text{qFl}}$
c_{y_b}	side-force coefficient of bomb, $\frac{\text{Side force}}{qF}$

ē	mean aerodynamic chord of wing, in.
S	total area of wing, sq ft
F	frontal area of bomb, sq ft
ı	bomb length, in.
q	dynamic pressure, lb/sq ft
x	longitudinal distance between bomb midpoint and fuselage at station 20 (fig. 1(b))
y	spanwise position of bomb midpoint measured from fuselage center, in.
z	vertical distance between bomb midpoint and horizontal line through fuselage center line at station 20 (fig. 1(b)).
ΔC _{Db}	bomb-interference drag coefficient, bomb drag minus isolated bomb drag
$\Delta c_{\mathbf{L}_{\mathbf{b}}}$	bomb-interference lift coefficient, bomb lift minus isolated bomb lift
α _{wf}	angle of attack of wing-fuselage center line referenced to free-stream direction, deg
α _b	angle of attack of bomb center line referenced to free- stream direction

MODELS AND TEST METHODS

The general arrangement of models, along with fuselage coordinates and wing dimensional data, is shown in figure 1. The wing-fuselage combination was designed to simulate a swept-wing fighter-bomber airplane. A detailed description of the airplane configuration and model setup is given in reference 1. All data in the present report refer to a highwing fighter-bomber configuration except where otherwise indicated.

The bombs used in this investigation (fig. 2) were made of metal and had fineness ratios of 7.0 and 10.5. These two bombs were tested at three spanwise stations: y = 0 under the fuselage center line, and y = 3 inches and y = 6 inches under the wing.

The nominal ranges of angles and positions used in the investigation and a convenient index to the bomb and wing-fuselage configurations involved are presented in table I.

PRECISION OF TEST DATA

The repeatability or relative accuracies are estimated from an inspection of repeat test points, zero shifts, and static-deflection calibration to be as follows:

х.																				•				•		•	٠.	٠.		•		±0.05
у.																					•			•	•	•	•		•	•	•	±0.10 ±0.10
z.		•					•					•		•		•		•			•	ě		•	•	•	•	•	•	•	•	±0.10
$C_{D_{\mathbf{b}}}$		•	•		•	•		•	•	•	•	•		•	•	•	•	•	•	•	•	•	ė	•	•	٠	•		•	•	•	±0.01
																																±0.03
C _m		•				• .	•					•		•;	•			•	•	•	•.	٠.	•	•	•		. •		•			±0.03
																																±0.10
ωb	•	•	. •	•	•	•	•	•	•	•	Ī	•	•	•	·	•	Ī	. •	•	•	•	•		_	-	•	-	•			•	±0.001
$c_{ m D}$	•	•	•	•	•	•	•	•	•	•	•	•	•	•	٠	•	•	•	•	•	•	•	•	•	•	•	•	•	•	•	•	±0.001
$\mathtt{c}_{\mathtt{L}}$				•	•		•		•	•	•	•	•	•	•	•	•	•	•		•	•	•	•	•	•	•	•	•	•	•	±0.002
$C_{\mathbf{m}}$						٠.	•	•	•	•	•	•	•	•	•	•	•	•	•	•	•	•	•	•	•	•	•	٠.		· ·	•	±0.001
$\alpha_{\mathbf{wf}}$	•	•		•	•	•	•	•	•	•	•	•	•	•	•	•	•	•	•	•	•	•	•	•	•	•	•	•	•	•	•	±0.10

PRESENTATION AND DISCUSSION OF DATA

Isolated Bomb

Lift, drag, and pitching-moment data for the two bombs are presented in figure 3 for bomb angles of attack up to 15° . Data are included for bombs without fins. It should be noted that bomb pitching moments in all cases are computed about the bomb nose.

Isolated Wing-Fuselage Data

The aerodynamic characteristics of the wing-fuselage combination are presented in figure $4\,$.

During the run used to obtain isolated wing-fuselage data, a large zero shift occurred in the chord-force component. The data for this single run therefore may contain errors in excess of those quoted previously. Damage to the balance in this last run of the test prevented

NACA RM L56K30

the making of a repeat run. The wing-fuselage data have therefore been presented along with the data from reference 2, which were taken on a half model of a geometrically similar wing-fuselage configuration. The dashed lines in figure 4 represent the data taken from reference 2 and are believed to be more accurate.

Basic Data Plots

Drag, lift, and pitching-moment coefficients for bombs 3 and 4 in the presence of the wing-fuselage combination are presented in figures 5 to 1). Bomb side-force and yawing-moment coefficients in addition to the drag, lift, and pitching-moment coefficients are presented in figures 9 to 14 for the under-wing position. Table I gives a convenient index to the contents of the basic-data figures.

Figures 16 and 17 show the forces on the wing-fuselage combination in the presence of the bombs. In figure 16 the wing-fuselage lift, drag, and pitching-moment coefficients in the presence of bomb 3 are plotted for three spanwise positions (y = 0, 3, and 6) and for three airplane angles of attack.

Figure 17 shows wing-fuselage coefficients for two spanwise positions (y = 0 and 6) in the presence of bomb 4.

Contour Plots

The drag, lift, and pitching-moments coefficients for bombs 3 and 4 in the presence of the wing-fuselage combination are presented in contourmap form in figures 18 to 26. Contour plots are shown only for an airplane angle of attack of 40 and for bombs with fins when three or more chordwise positions were used.

From an inspection of the bomb-pitching-moment contour maps for under-fuselage and under-wing positions, it will be noted that the maximum change in moments due to interference occurs when the bomb fins are located in a region believed to be just within the wing flow field behind the leading-edge shock. The moments are slightly larger at under-wing positions (fig. 2(b)) than at under-fuselage positions (fig. 20), the maximum interference moment being the same as that of the isolated bomb at 5° angle of attack.

Analysis Plots

In the analysis plots (figs. 27 to 31) interference lift and drag are presented. Pitching moments are not presented because previous examination of all data exhibited pitching-moment trends similar to the lift trends, for the reason that the moments were taken about the bomb nose.

Figure 27 shows the effect of the wing on bomb-interference lift and drag at y = 0. Data taken with wing on and off show, in general, that the wing is the major cause of interference forces on the bombs.

Figures 28 and 29 present a comparison of interference lift and drag at three spanwise stations for bomb 3 and at two spanwise stations for bomb 4. The shapes of the corresponding curves at the various spanwise stations are generally similar. The bomb vertical position at which minimum interference is encountered (apparently occurring as the bomb fins emerge from the wing flow field) is slightly different at each of the three spanwise stations. These changes, but not the absolute value of the vertical position, can be explained by a consideration of the envelope which bounds the Mach cones emanating from the leading edge of the wing. Actually, a bow wave occurs ahead of the leading edge as discussed in reference 3. Again it is shown that the wing is the major cause of interference forces on the bomb.

A comparison of the bomb-interference lift and drag patterns due to a low-winged fighter-bomber airplane and the high-winged fighter-bomber airplane (bay closed) is presented in figure 30. The changing of wings from high to low shifts the interference pattern down approximately 2 inches.

Interference lift and drag of bomb 3 under a closed bomb bay is compared with the interference lift and drag of bomb 3 under an open bomb bay in figure 31. The bomb bay seems to have small effect on the interference drag, but changes the shape of the interference lift curve considerably. This is probably due to the shock reflection from the closed bomb bay as well as the flow field created by the open bomb bay. The open-bomb-bay data were taken from reference 2.

CONCLUDING REMARKS

Forces and moments have been measured in the Langley 4- by 4-foot supersonic pressure tunnel at a Mach number of 1.6 on bombs of two fineness ratios (7.0 and 10.5) and on a swept-wing fighter-bomber airplane configuration for a large number of positions of the bomb under a closed bomb bay and under a swept wing. The bomb data have been presented in contour-map form, suitable for use in trajectory calculations.

NACA RM L56K30 7

The results show that, in general, the wing has a large effect on the interference pattern of the bomb, whereas the fuselage has a small effect, even for under-fuselage positions. The maximum moments occur when the bomb fins are in a region believed to be just within the wing flow field behind the leading-edge shock.

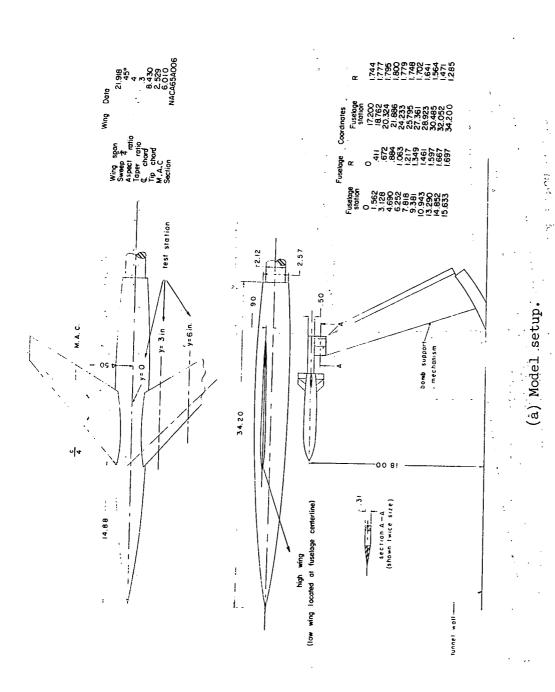
Langley Aeronautical Laboratory,
National Advisory Committee for Aeronautics,
Langley Field, Va., November 13, 1956.

REFERENCES

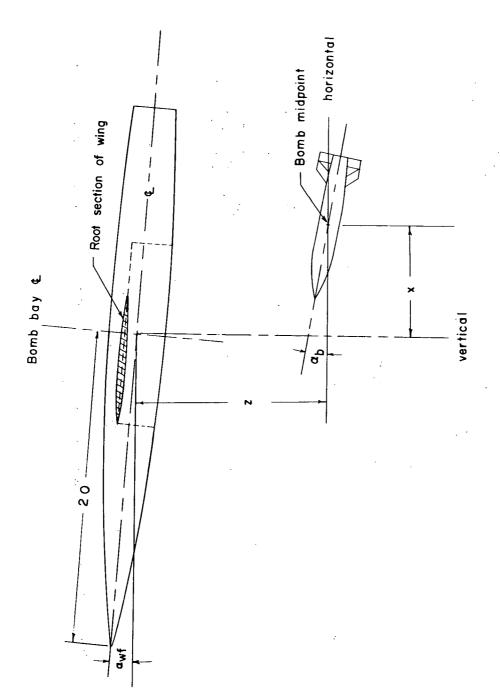
- 1. Smith, Norman F., and Carlson, Harry W.: Measurement of Static Forces on Internally Carried Bombs of Three Fineness Ratios in Flow Field of a Swept-Wing Fighter-Bomber Configuration at a Mach Number of 1.61 With Illustrative Drop-Path Calculations. NACA RM L56118, 1956.
- 2. Smith, Norman F., and Carlson, Harry W.: The Origin and Distribution of Supersonic Store Interference From Measurement of Individual Forces on Several Wing-Fuselage-Store Configurations. III.- Swept-Wing Fighter-Bomber Configuration With Large and Small Stores. Mach Number, 1.61. NACA RM L55HO1, 1955.
- 3. Smith, Norman F., and Carlson, Harry W.: The Origin and Distribution of Supersonic Store Interference From Measurement of Individual Forces on Several Wing-Fuselage-Store Configurations. I.- Swept-Wing Heavy-Bomber Configuration With Large Store (Nacelle). Lift and Drag; Mach Number, 1.61. NACA RM L55Al3a, 1955.

TABLE I - INDEX TO MODEL CONFIGURATION AND FIGURES

. 1		· · ·	г		<u> </u>	- 					
Basic data, fig. no.	2	9	2	80	6	10	11	12	1.5	77.	15
z range, in.	0 to 10	0 to 10	0 to 14	0 to 14	0 to 10	0 to 10	0 to 10	0 to 10	0 to 14	0 to 14	0 to 14
x values, in.	-0.4, 1.6, 3.6 -0.15, 1.85, 3.85 -0.27, 1.73, 3.73										
α _b , deg	0±10 0±5, ±10, ±15 0±10										
αwf, deg	0.78	0.78	0 4 8	0 # 8	0.40	0 = 0	O = 0	0.700	0 + 8	0.78	0,700
Span station, in.	0	0	0	0	. 9	9	ĸ		9	9	0
Wing	High	Off	High	High	High	High	High	H1gh	High	High	Low
Fins	On	e G	o	JJ0	e S	JJO	e, O	JJ0	On	Off	u _O
Pomb	:0	5	ā	-7	3	3	5	3	. 	4	#



All dimensions are in inches. Figure 1.- Drawing of models, wing data, and fuselage coordinates.



(b) Sketch showing x- and z-coordinate systems for bomb orientation.

Figure 1.- Concluded.

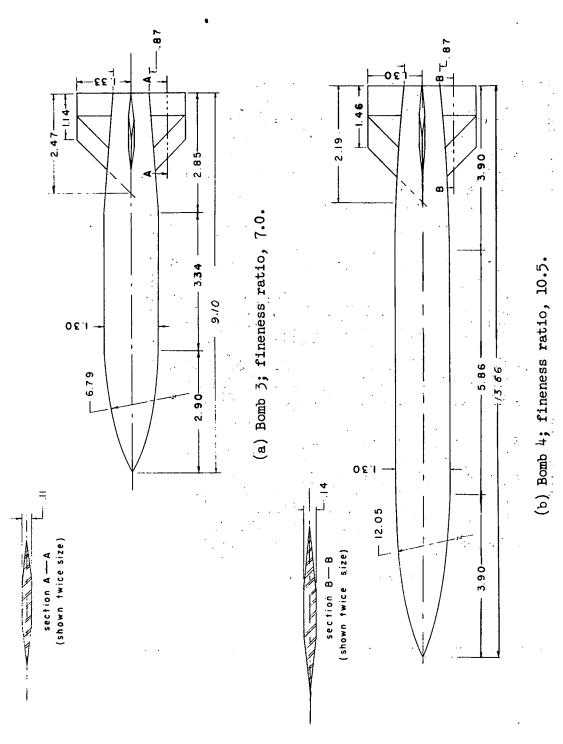


Figure 2.- Details and dimensions of bomb 3 and bomb 4. All dimensions are in inches.

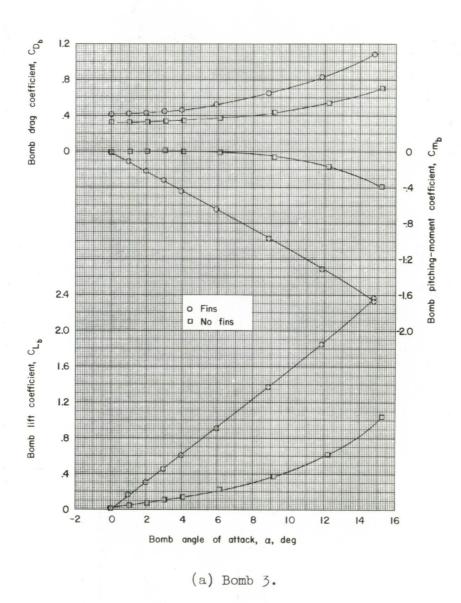


Figure 3.- Aerodynamic characteristics of the isolated bomb.

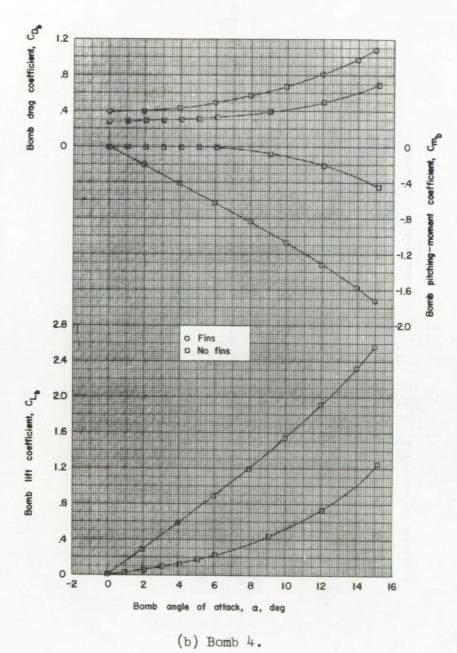


Figure 3.- Concluded.

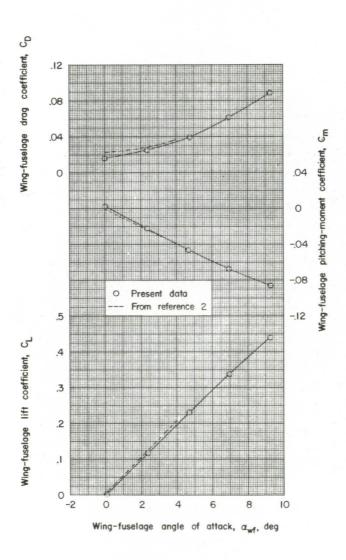
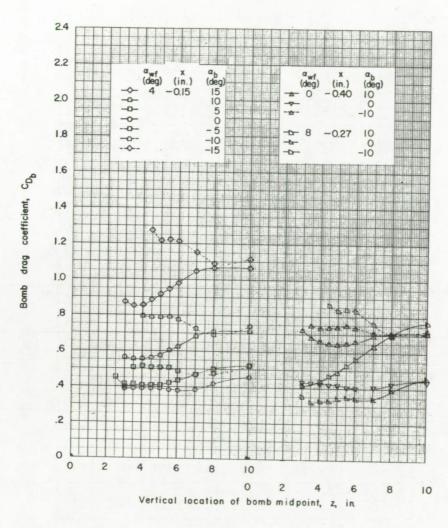
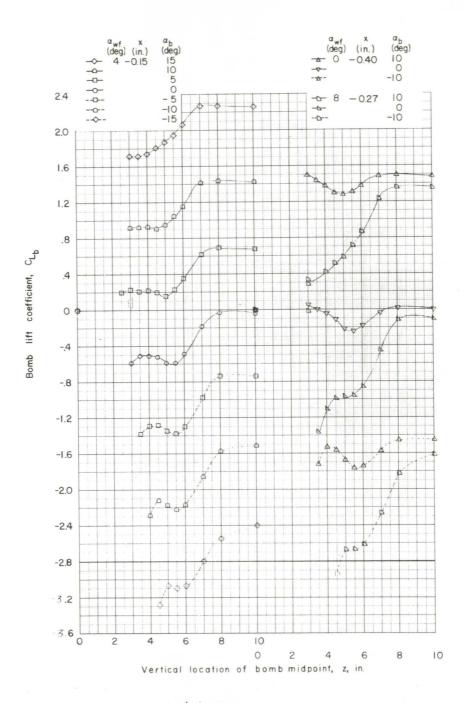


Figure 4.- Aerodynamic characteristics of isolated wing-fuselage combination with high wing.



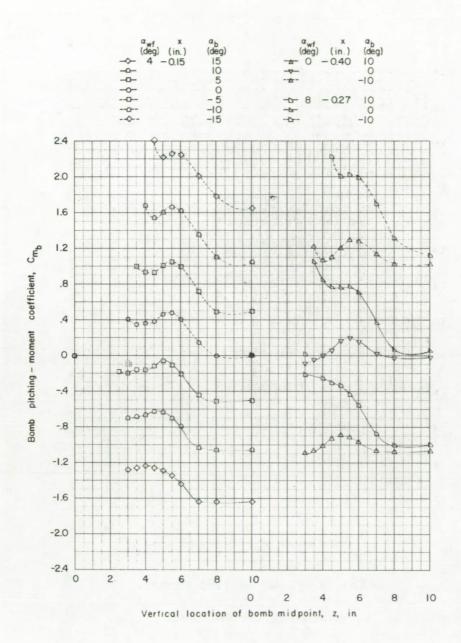
(a) x = -0.15 to -0.40 inch.

Figure 5.- Force data for bomb 3 in presence of wing-fuselage combination. Fins on; under-fuselage position; y = 0.



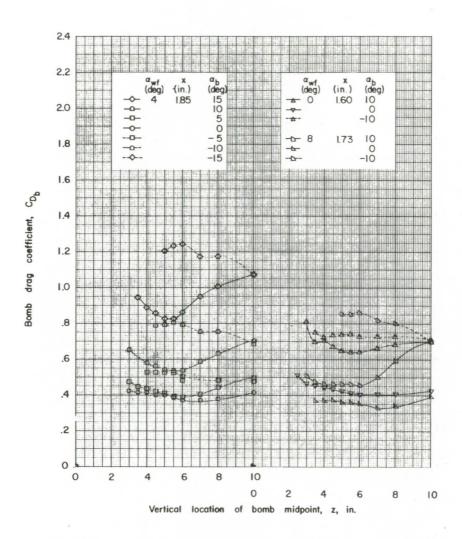
(a) Continued.

Figure 5.- Continued.

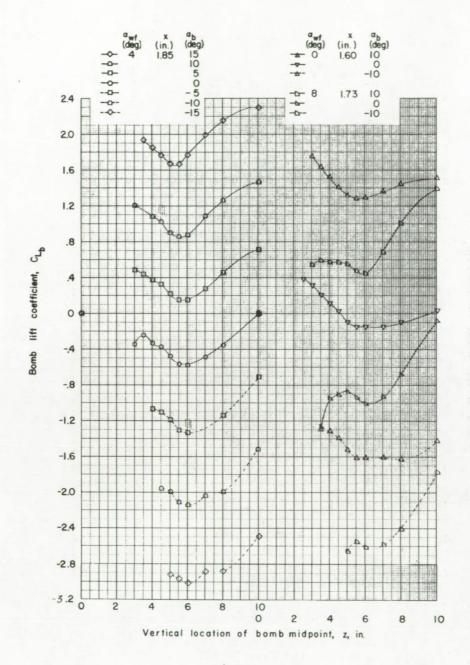


(a) Concluded.

Figure 5.- Continued.

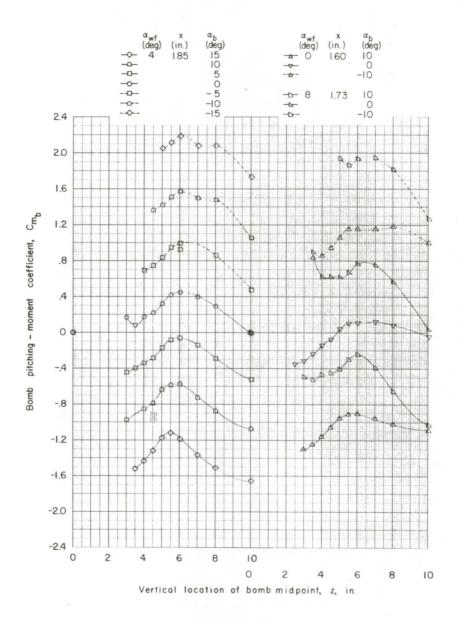


(b) x = 1.60 to 1.85 inches. Figure 5.- Continued.



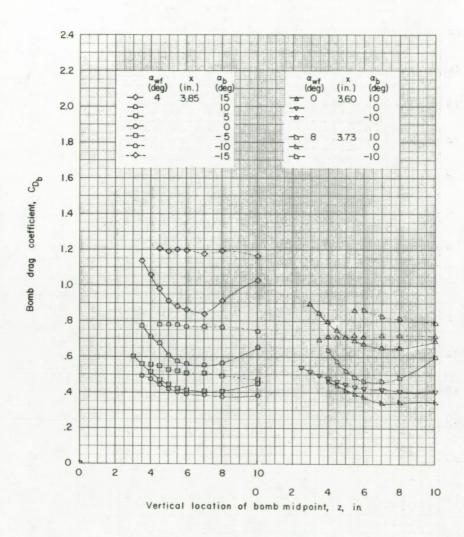
(b) Continued.

Figure 5.- Continued.

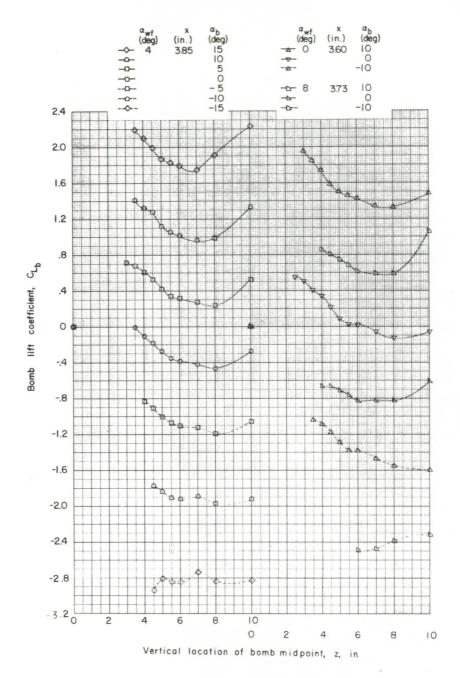


(b) Concluded.

Figure 5.- Continued.

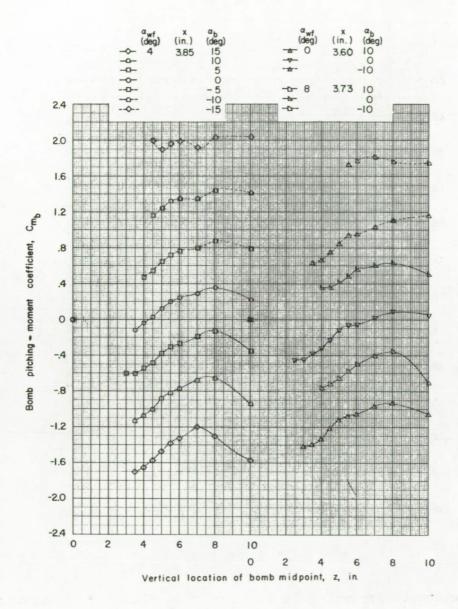


(c) x = 3.60 to 3.85 inches. Figure 5.- Continued.



(c) Continued.

Figure 5.- Continued.



(c) Concluded.

Figure 5.- Concluded.

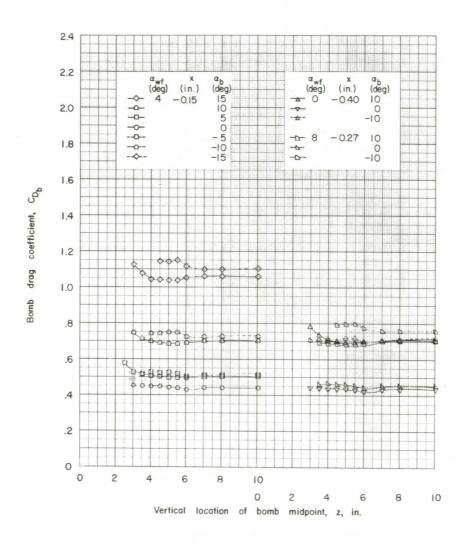


Figure 6.- Force data for bomb 3 in presence of fuselage. Fins on; underfuselage position; y = 0; wing off; x = -0.15 to -0.40 inch.

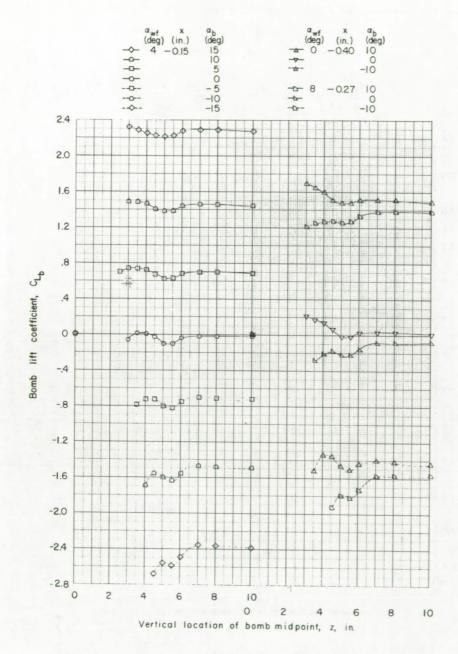


Figure 6.- Continued.

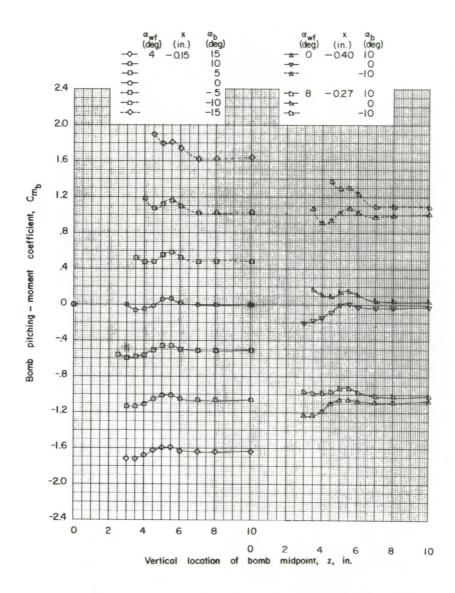
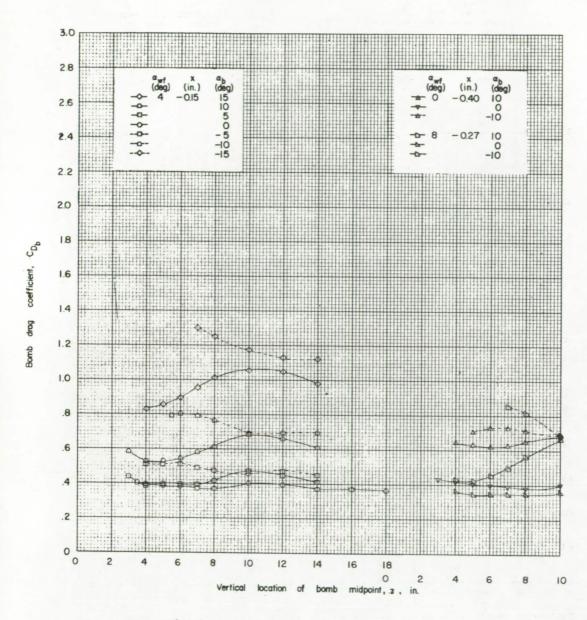
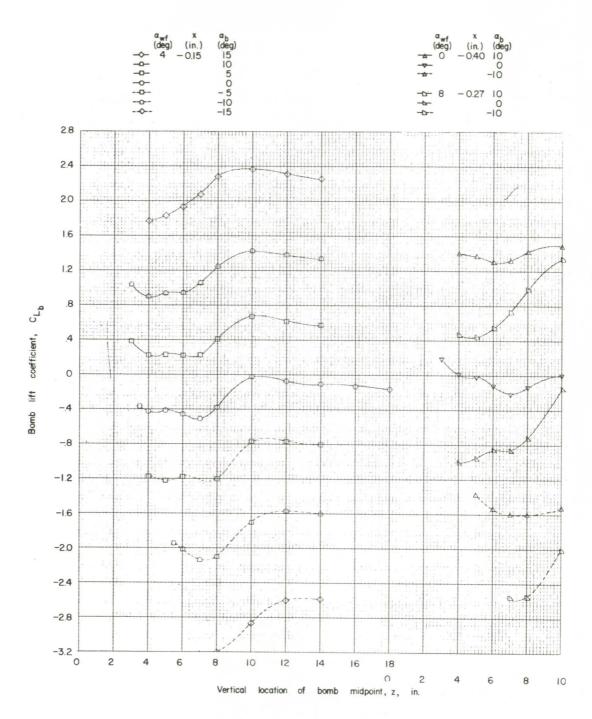


Figure 6.- Concluded.



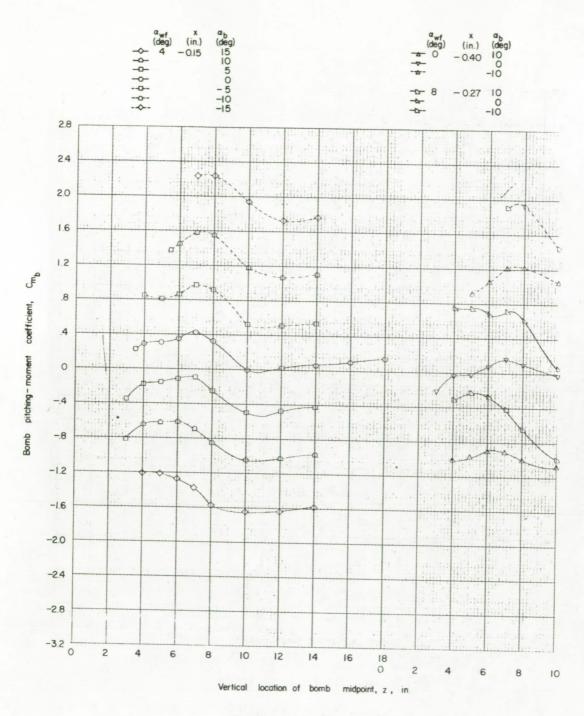
(a) x = -0.15 to -0.40 inch.

Figure 7.- Force data for bomb 4 in presence of wing-fuselage combination. Under-fuselage position; y = 0.



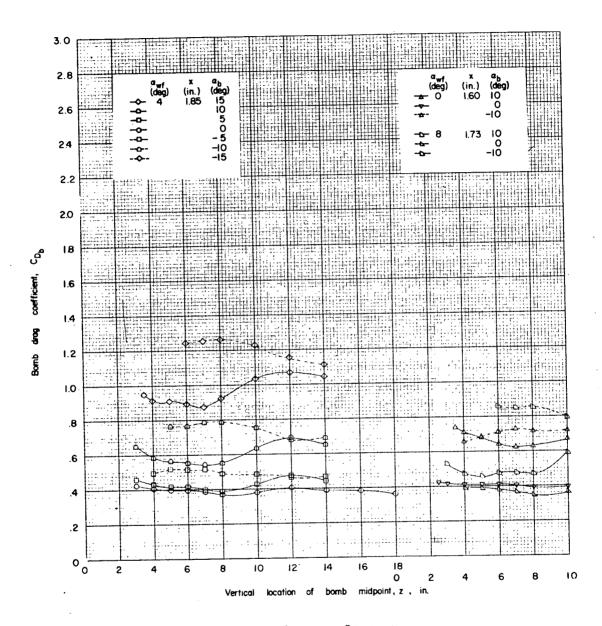
(a) Continued.

Figure 7.- Continued.

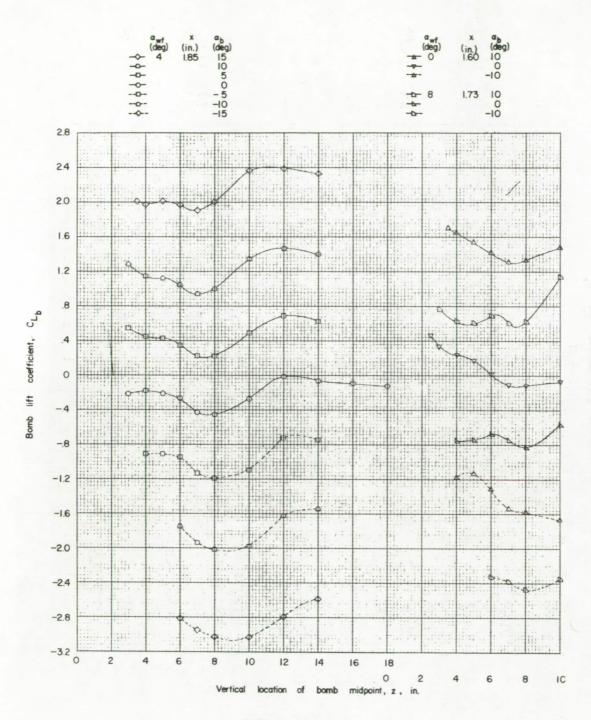


(a) Concluded.

Figure 7.- Continued.

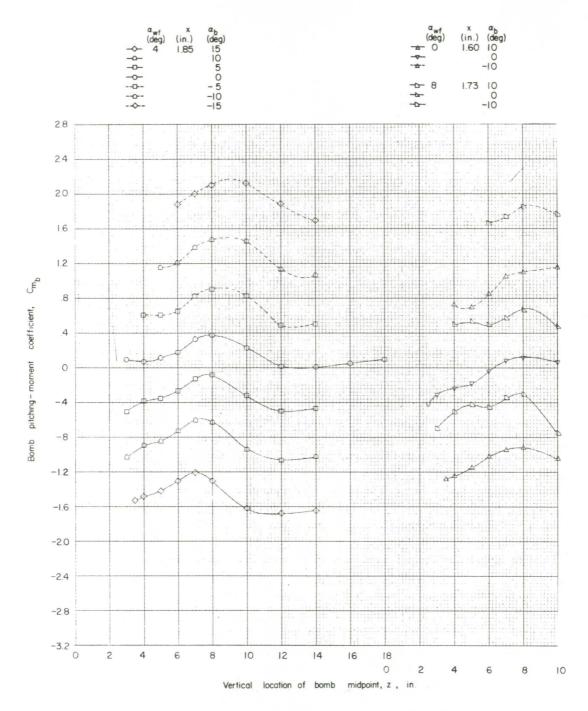


(b) x = 1.60 to 1.85 inches. Figure 7.- Continued.



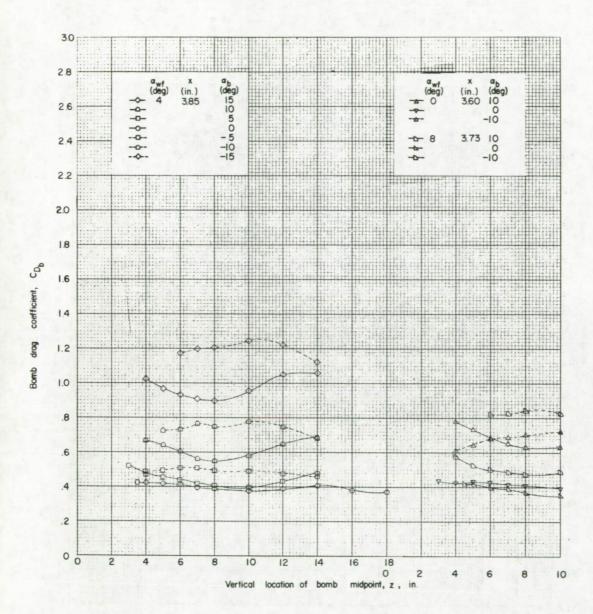
(b) Continued.

Figure 7 .- Continued.



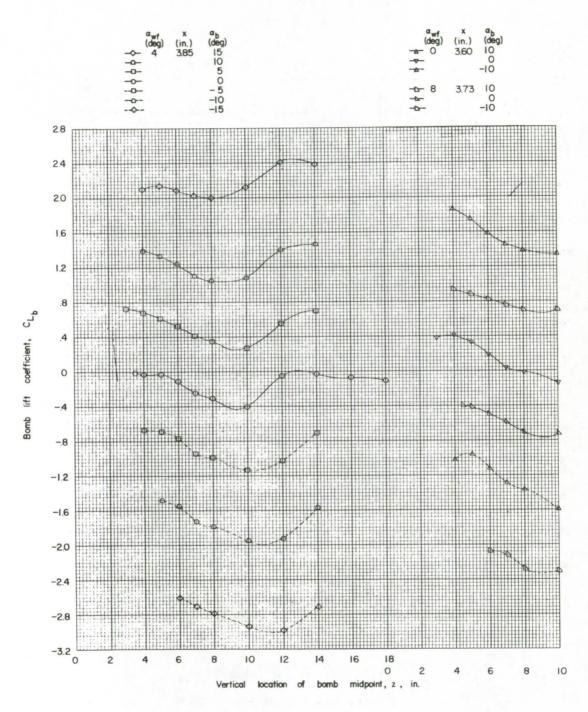
(b) Concluded.

Figure 7.- Continued.



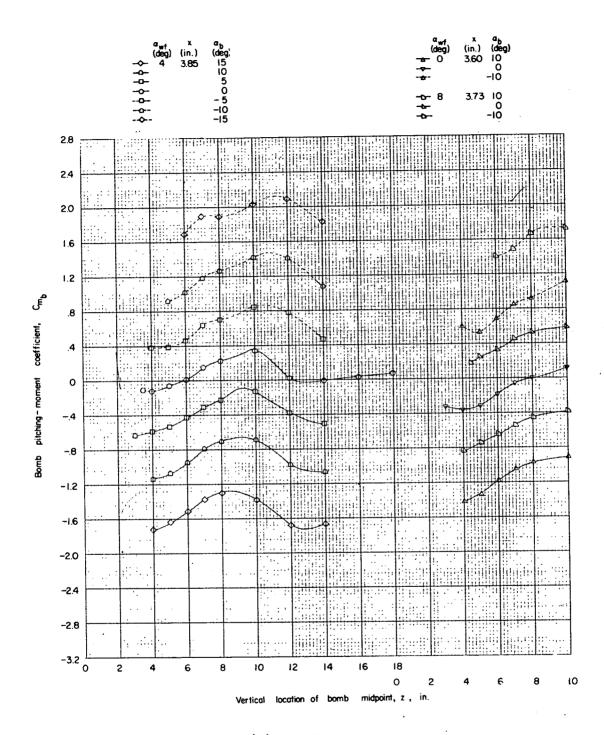
(c) x = 3.60 to 3.85 inches.

Figure 7.- Continued.



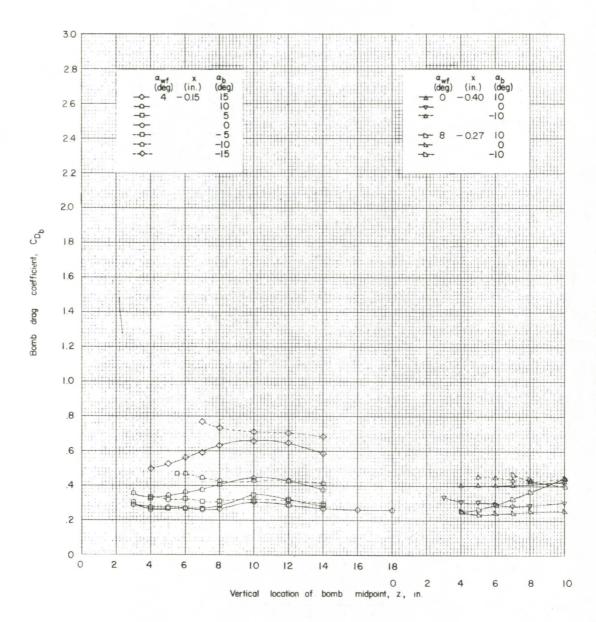
(c) Continued.

Figure 7.- Continued.



(c) Concluded.

Figure 7.- Concluded.



(a) x = -0.15 to -0.40 inch.

Figure 8.- Force data for bomb 4 in presence of wing-fuselage combination. Under-fuselage position; y = 0.

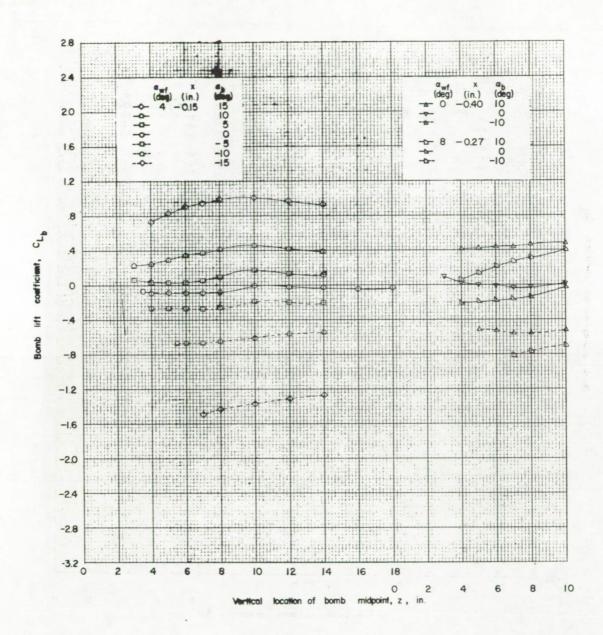
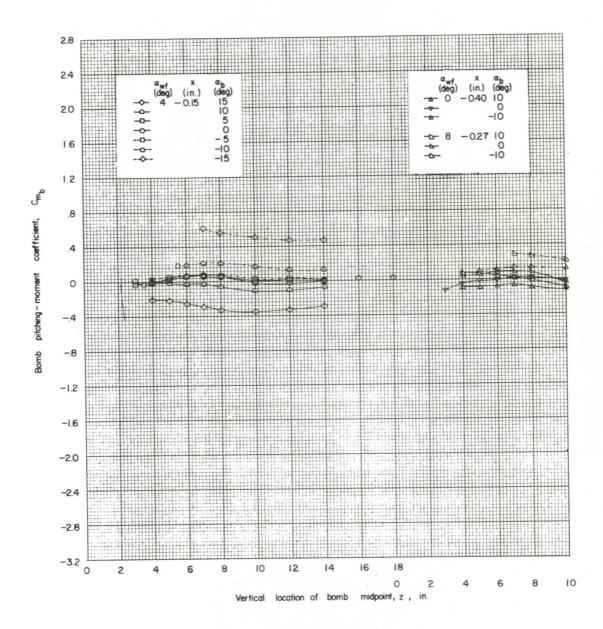
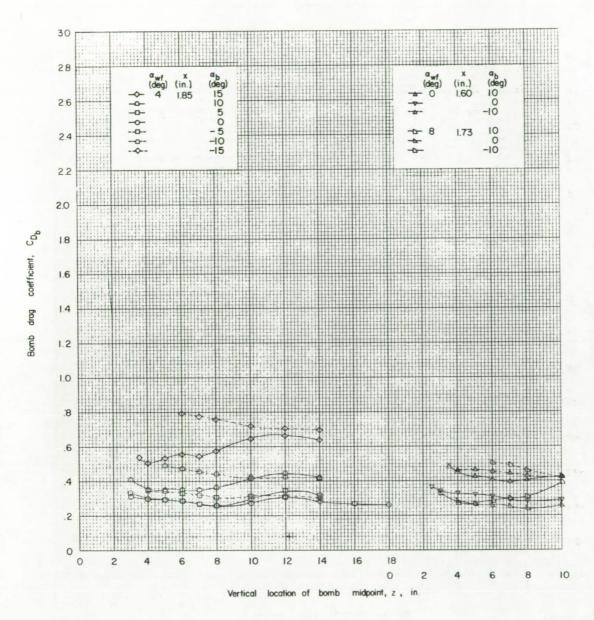


Figure 8.- Continued.



(a) Concluded.

Figure 8.- Continued.



(b) x = 1.60 to 1.85 inches. Figure 8.- Continued.

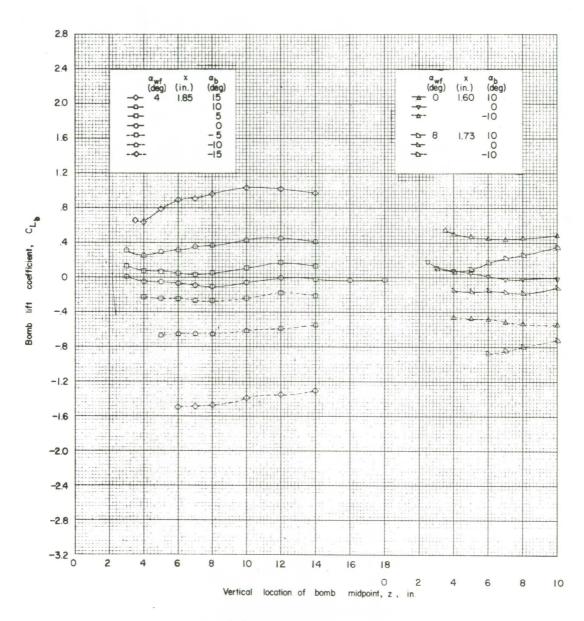
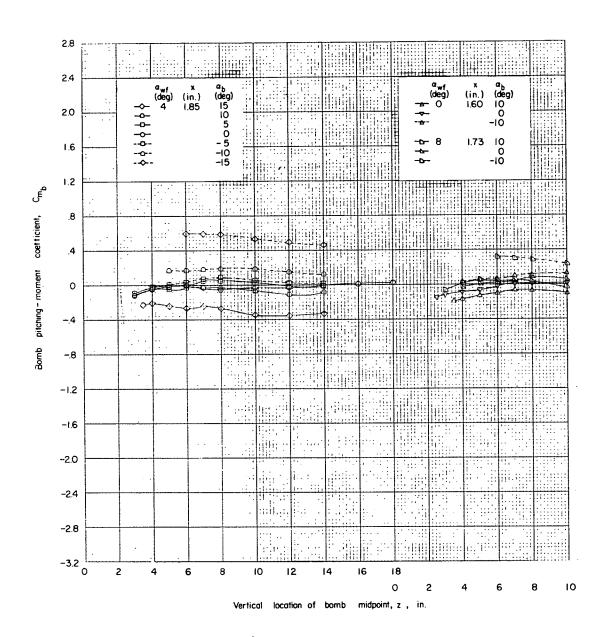
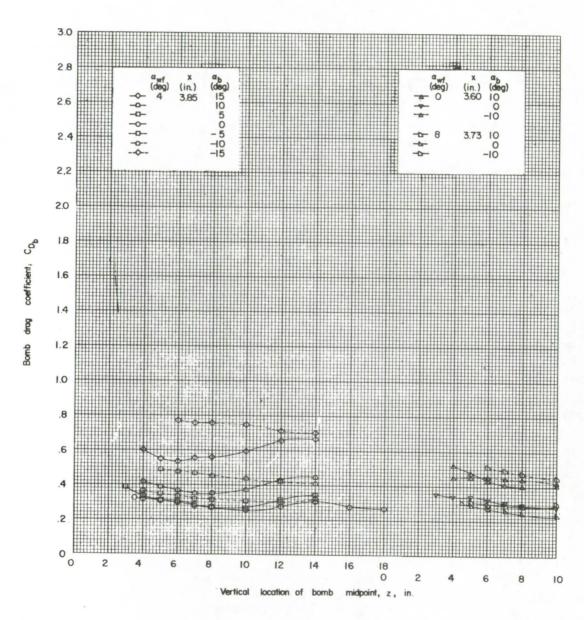


Figure 8.- Continued.



(b) Concluded.

Figure 8.- Continued.



(c) x = 3.60 to 3.85 inches. Figure 8.- Continued.

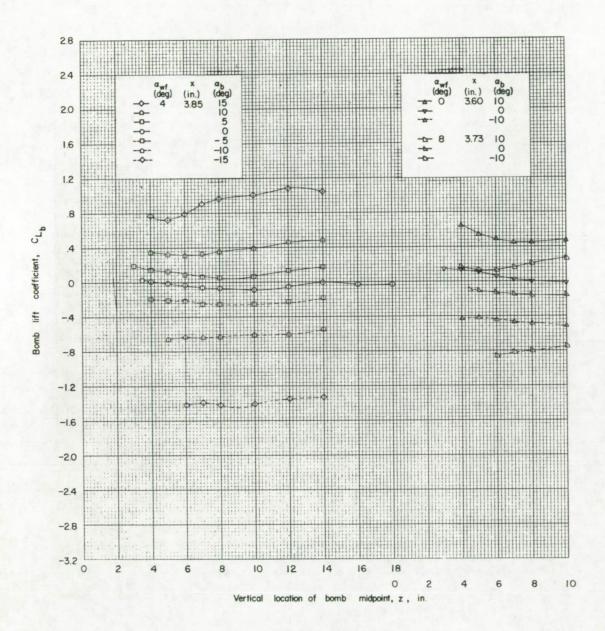
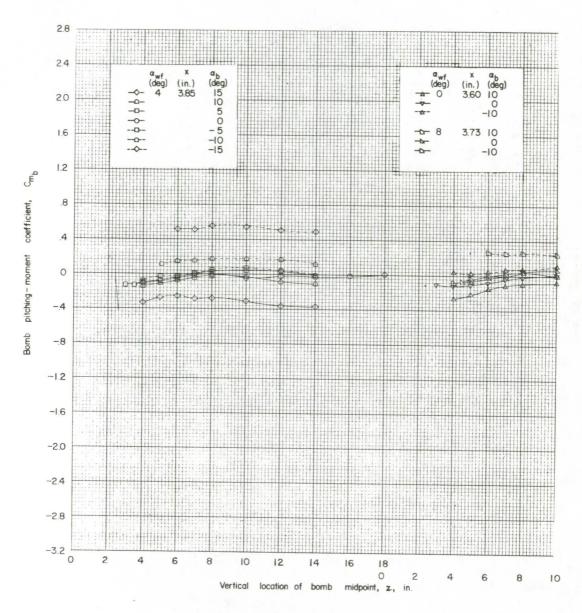
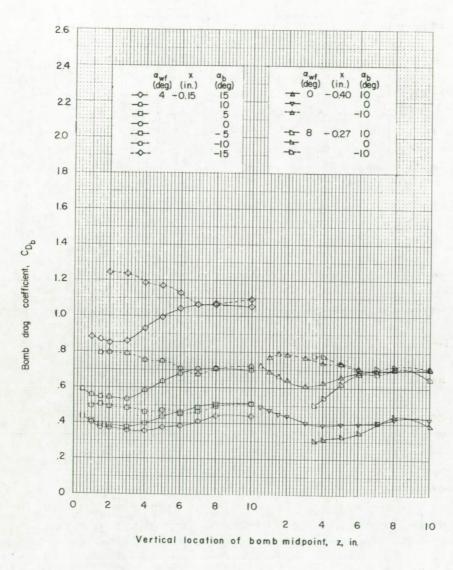


Figure 8.- Continued.



(c) Concluded.

Figure 8.- Concluded.



(a) x = -0.15 to -0.40 inch.

Figure 9.- Force data for bomb 3 in presence of wing-fuselage combination. Fins on; under-wing position; y = 6 inches.

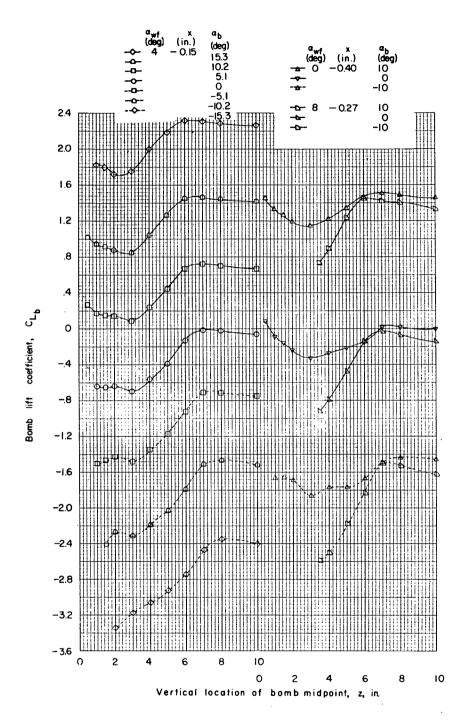
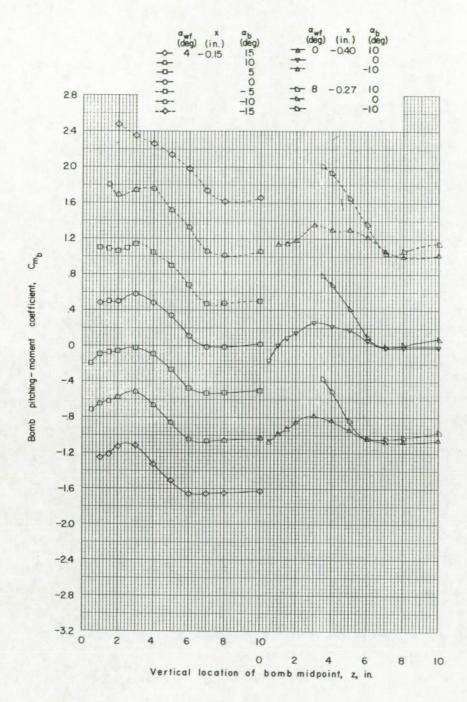


Figure 9.- Continued.



(a) Continued.

Figure 9.- Continued.

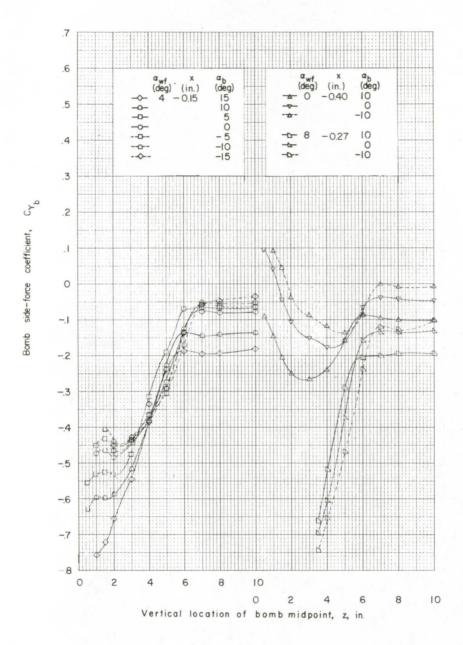
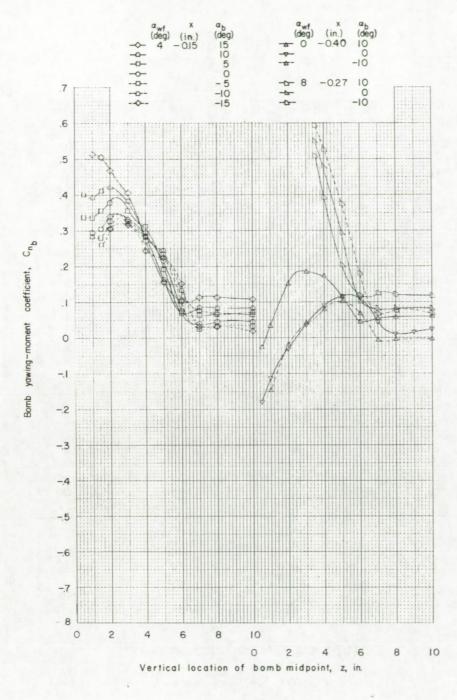
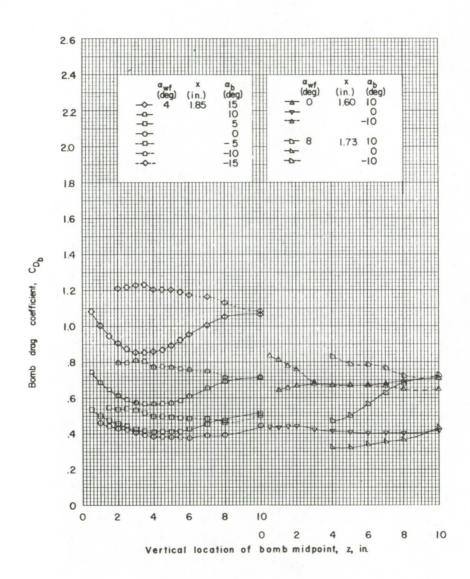


Figure 9.- Continued.



(a) Concluded.

Figure 9.- Continued.



(b) x = 1.60 to 1.85 inches. Figure 9.- Continued.

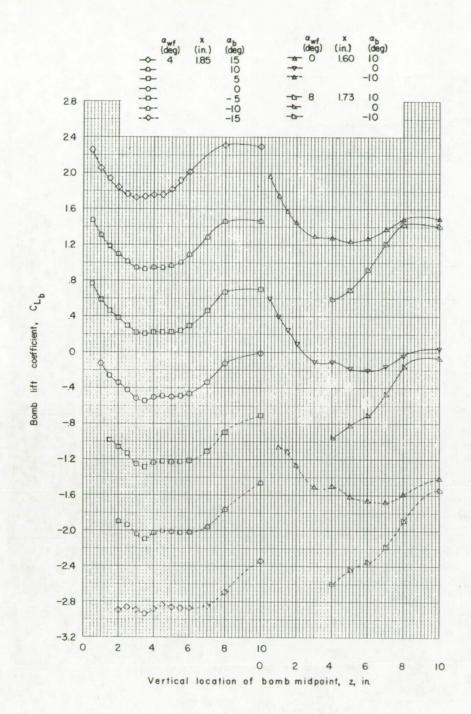
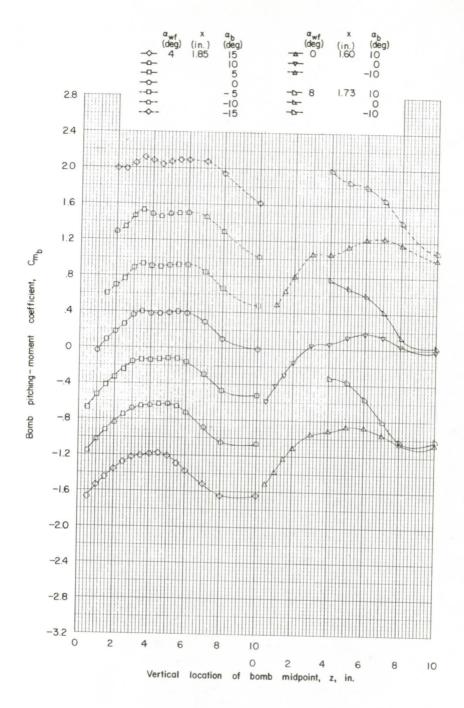


Figure 9.- Continued.



(b) Continued.

Figure 9.- Continued.

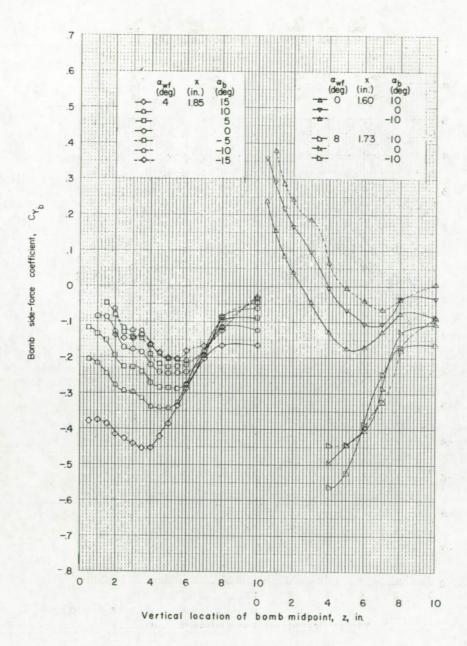
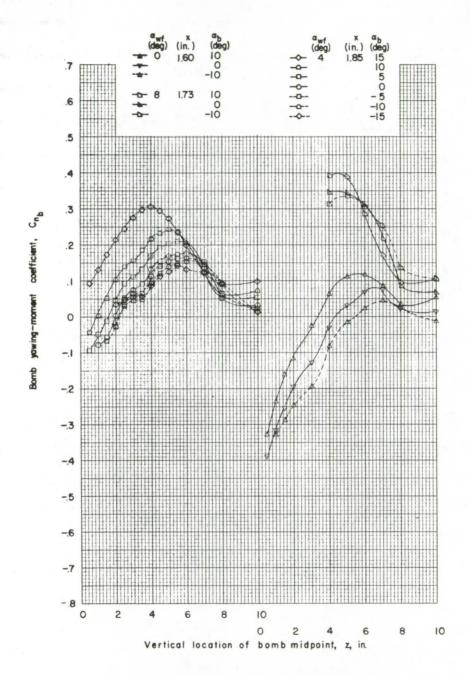
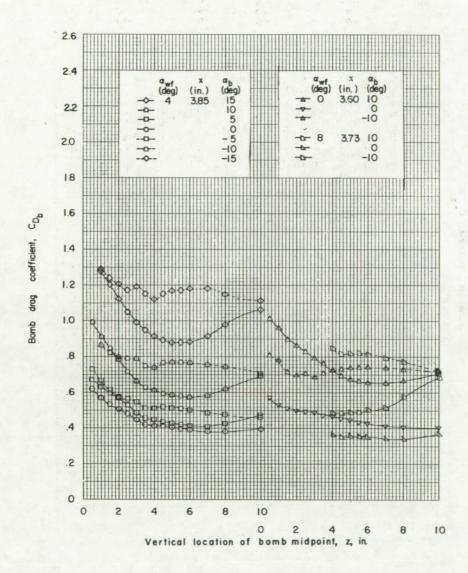


Figure 9.- Continued.



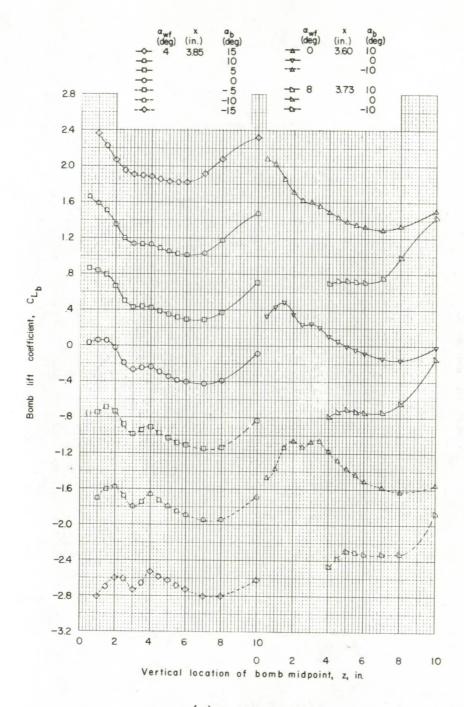
(b) Concluded.

Figure 9.- Continued.



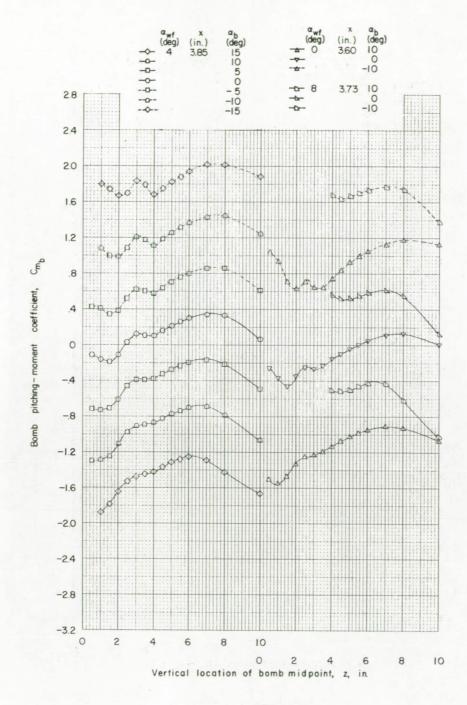
(c) x = 3.60 to 3.85 inches.

Figure 9.- Continued.



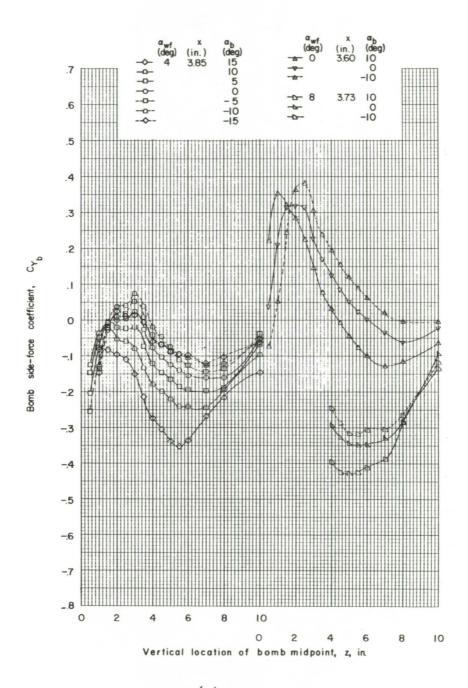
(c) Continued.

Figure 9.- Continued.



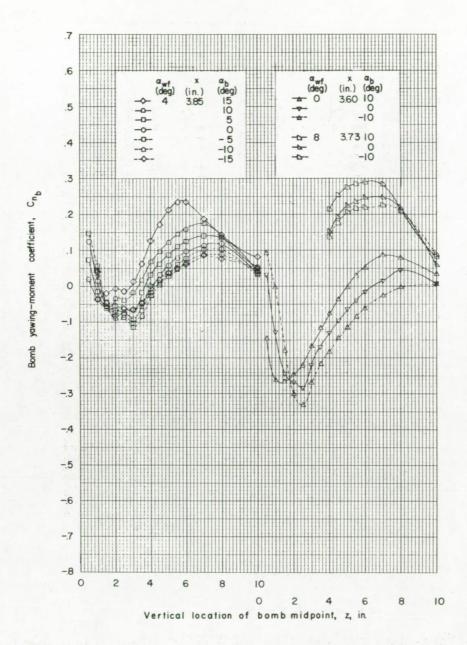
(c) Continued.

Figure 9.- Continued.



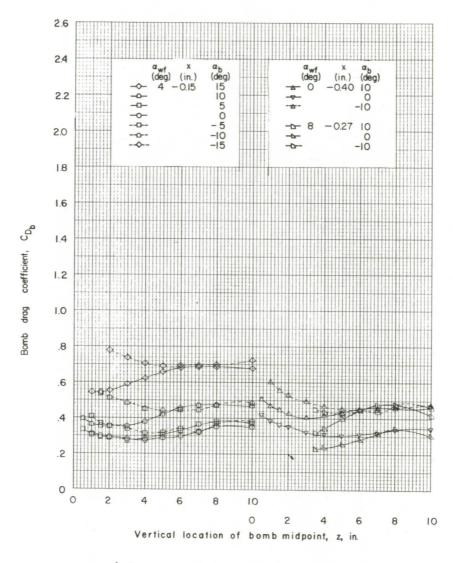
(c) Continued.

Figure 9.- Continued.



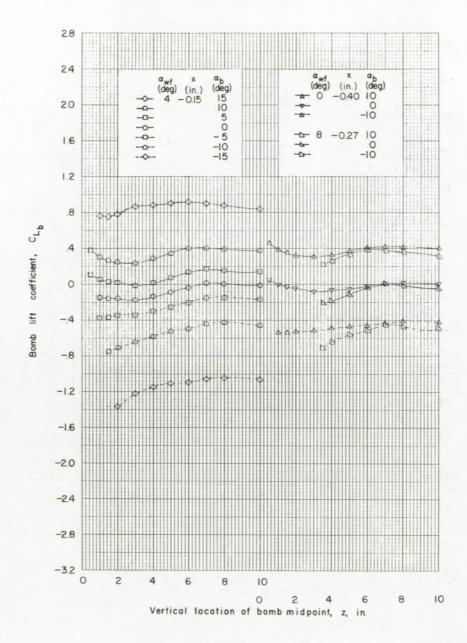
(c) Concluded.

Figure 9.- Concluded.



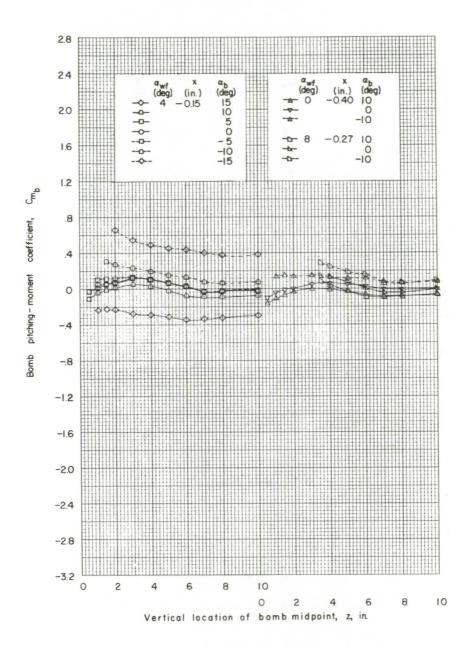
(a) x = -0.15 to -0.40 inch.

Figure 10.- Force data for bomb 3 in presence of wing-fuselage combination. Fins off; under-wing position; y = 6 inches.



(a) Continued.

Figure 10. - Continued.



(a) Continued.

Figure 10.- Continued.

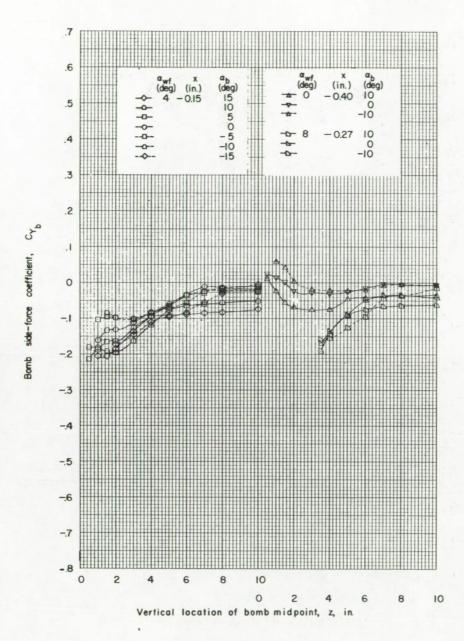
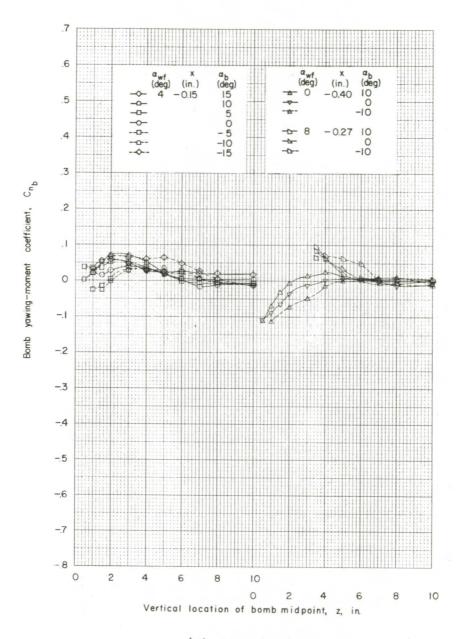
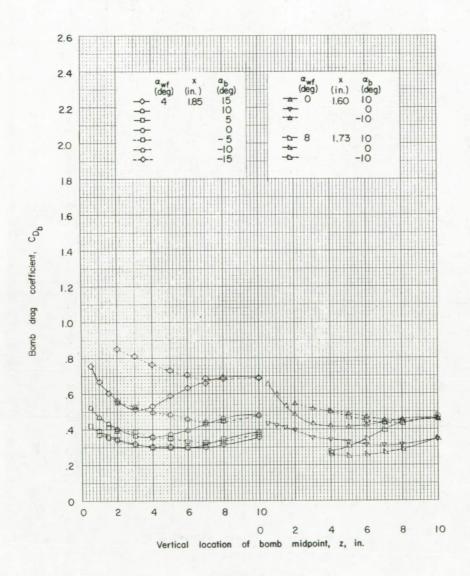


Figure 10.- Continued.



(a) Concluded.

Figure 10.- Continued.



(b) x = 1.60 to 1.85 inches.

Figure 10. - Continued.

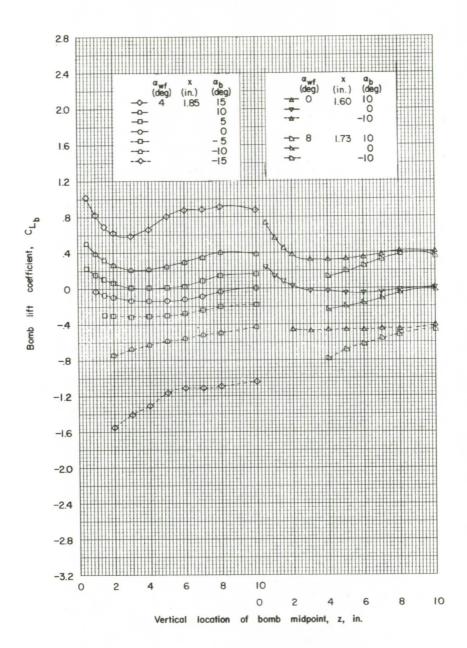


Figure 10.- Continued.

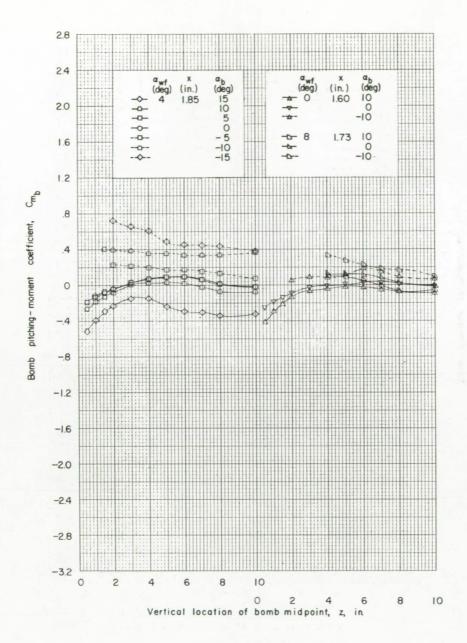
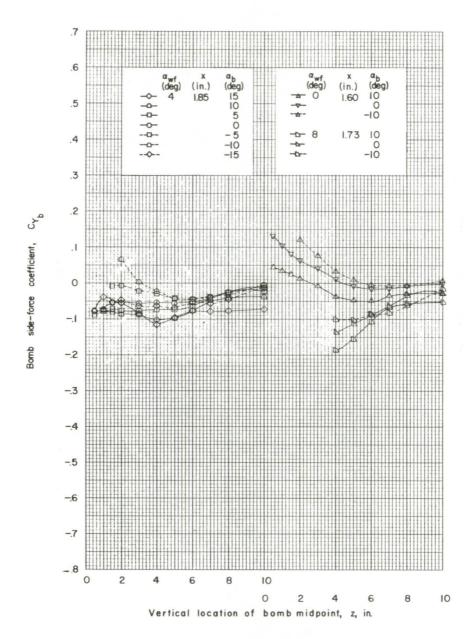
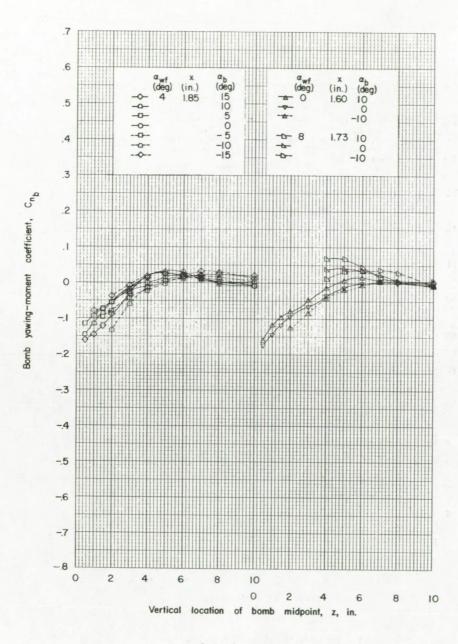


Figure 10.- Continued.



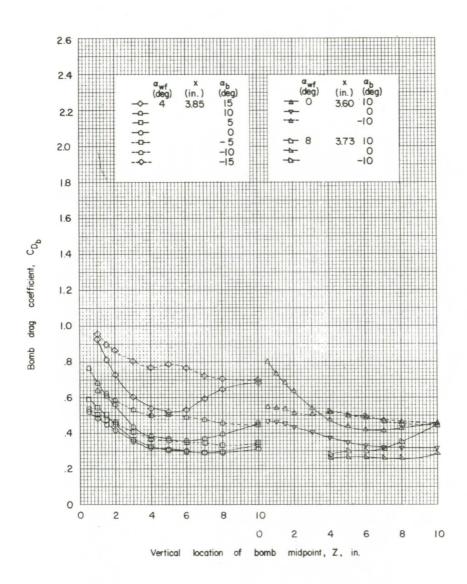
(b) Continued.

Figure 10.- Continued.



(b) Concluded.

Figure 10.- Continued.



(c) x = 3.60 to 3.85 inches.

Figure 10.- Continued.

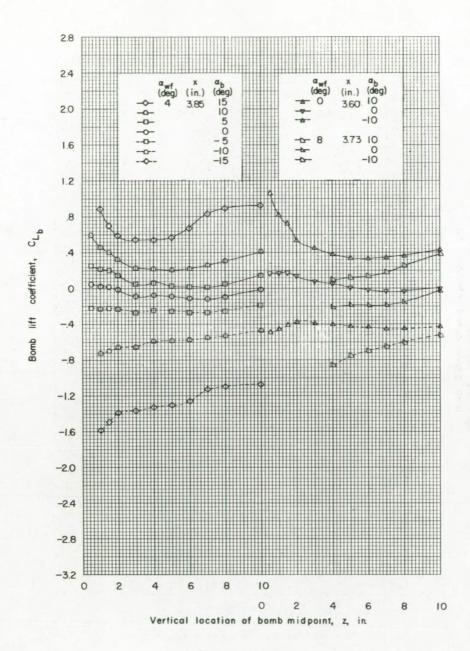
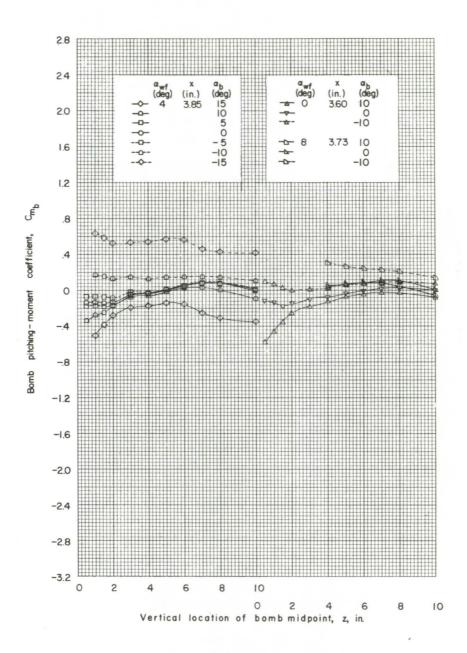
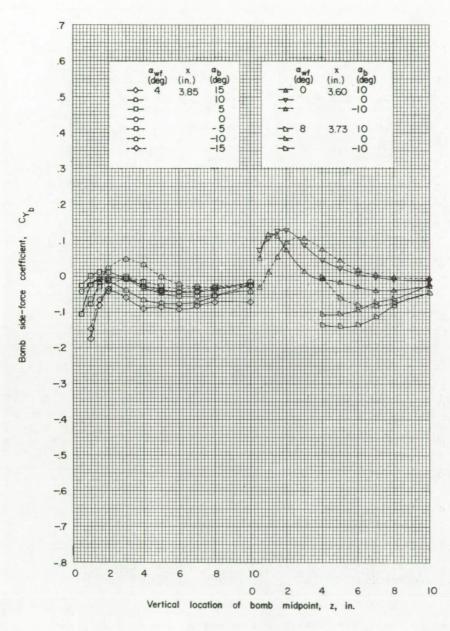


Figure 10.- Continued.



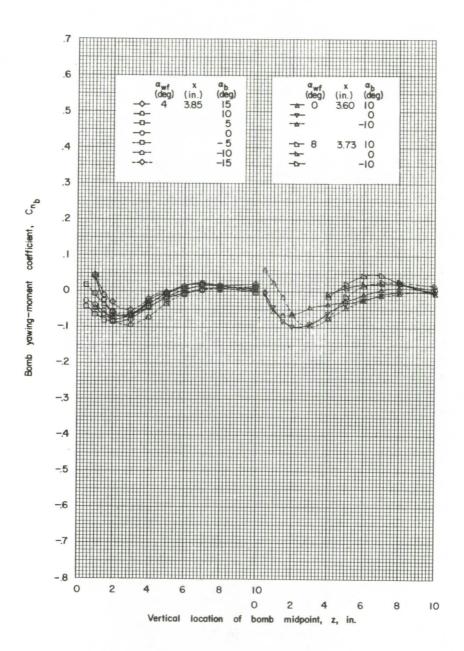
(c) Continued.

Figure 10.- Continued.



(c) Continued.

Figure 10.- Continued.



(c) Concluded.

Figure 10.- Concluded.

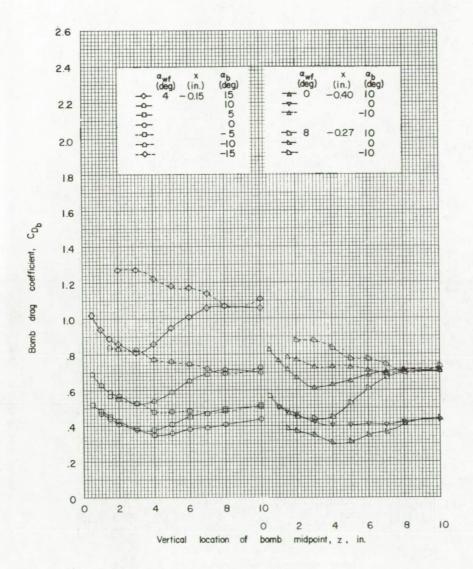


Figure 11.- Force data for bomb 3 in presence of wing-fuselage combination. Fins on; under-wing position; y = 3 inches; x = -0.15 to -0.40 inch.

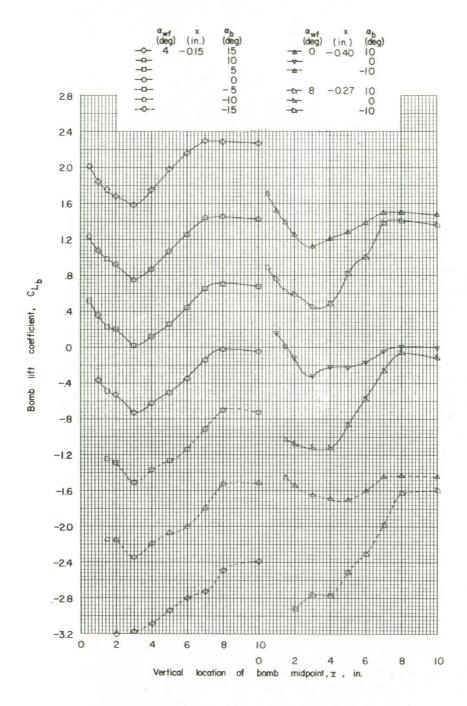


Figure 11.- Continued.

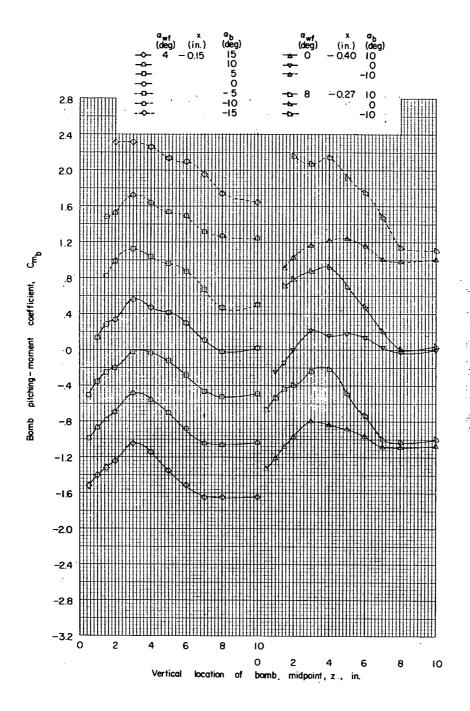


Figure 11.- Continued.

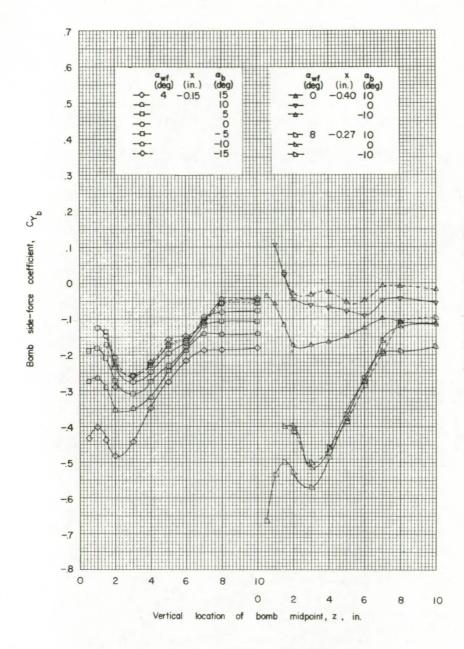


Figure 11.- Continued.

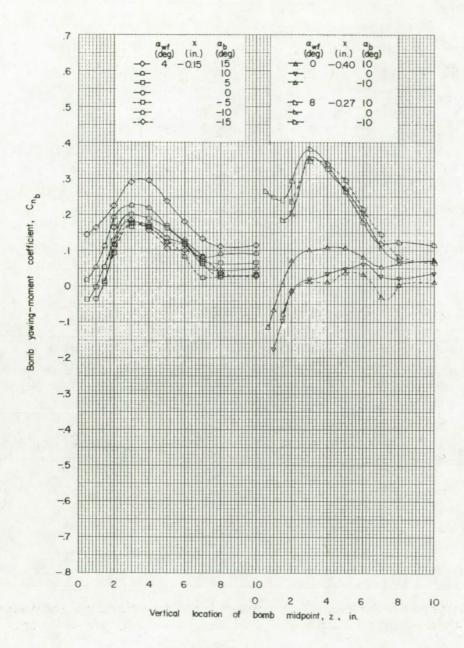


Figure 11.- Concluded.

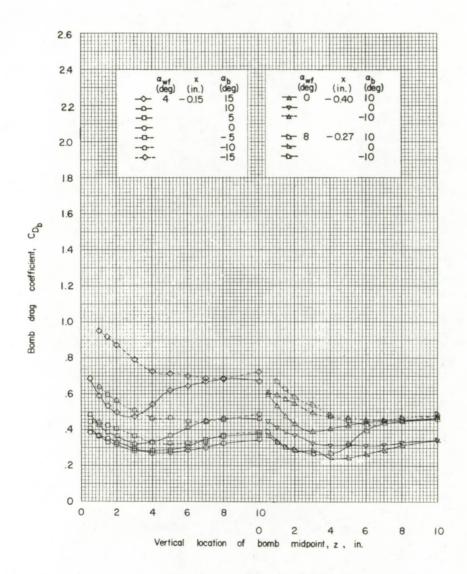


Figure 12.- Force data for bomb 3 in presence of wing-fuselage combination. Fins off; under-wing position; y=3 inches; x=-0.15 to -0.40 inch.

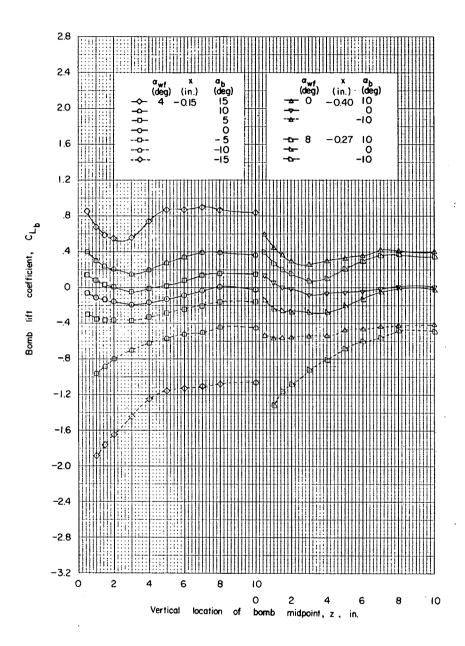


Figure 12.- Continued.

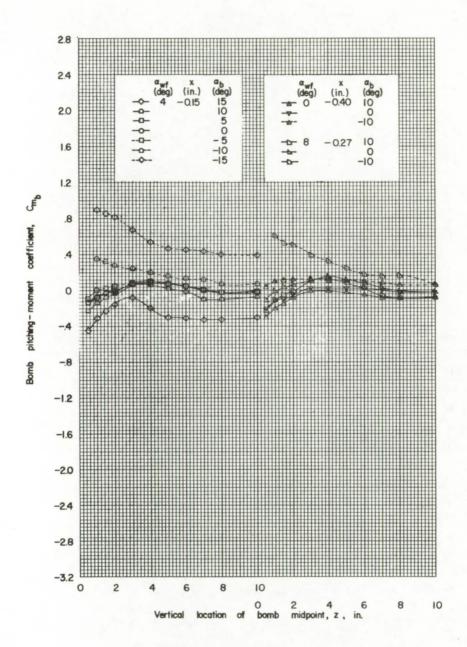


Figure 12.- Continued.

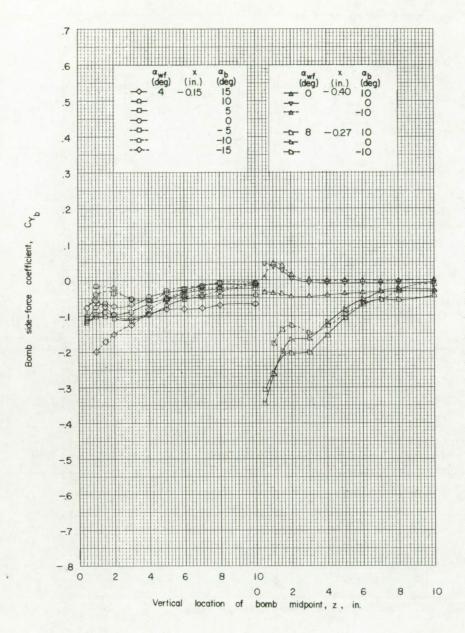


Figure 12.- Continued.

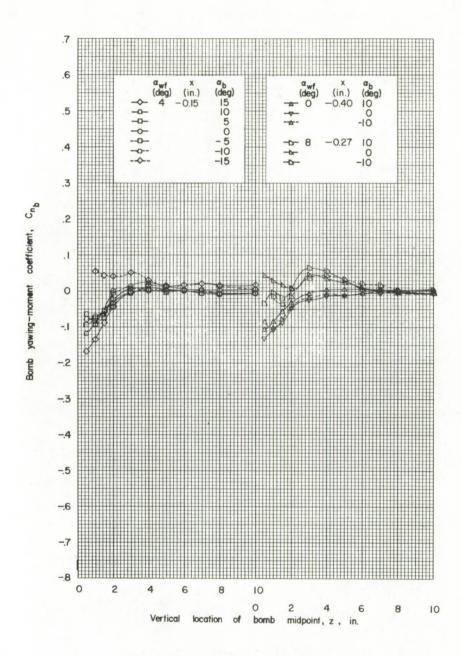
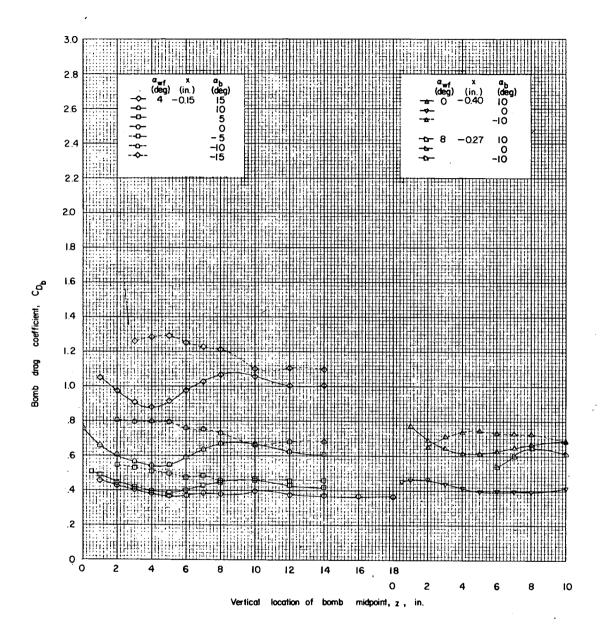


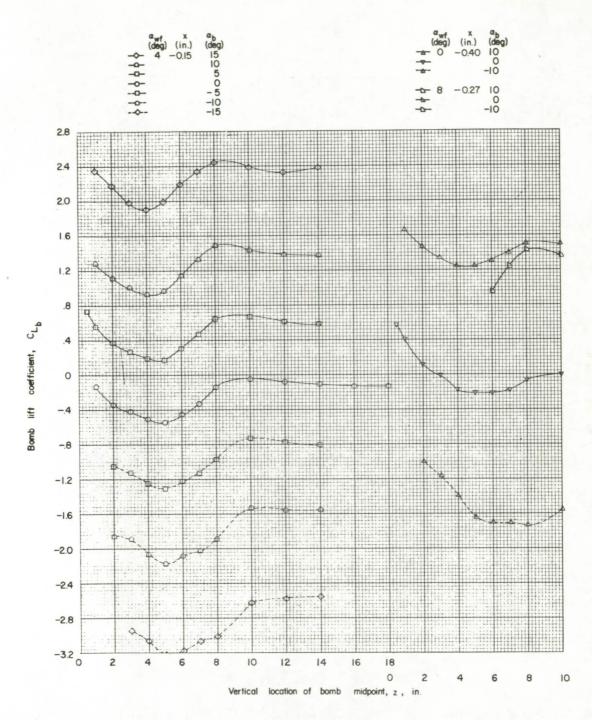
Figure 12.- Concluded.

85



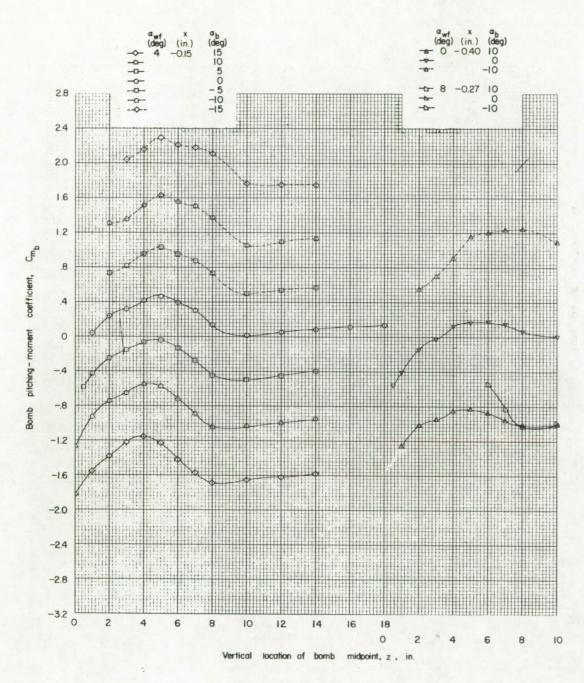
(a) x = -0.15 to -0.40 inch.

Figure 13.- Force data for bomb 4 in presence of wing-fuselage combination. Fins on; under-wing position; y = 6 inches.



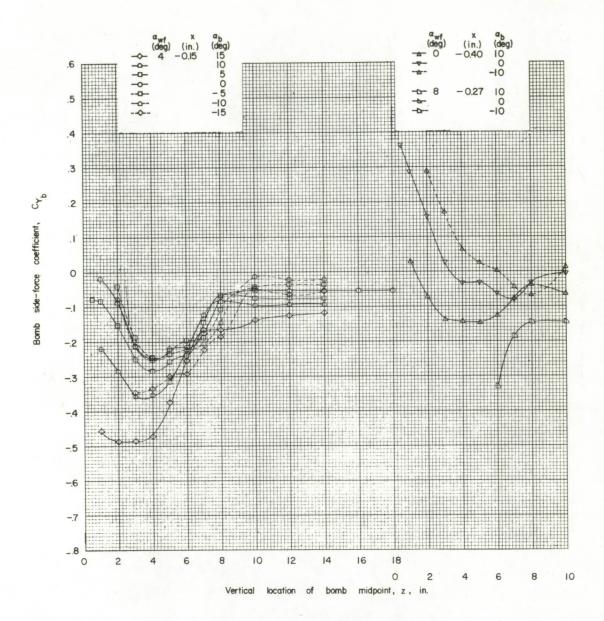
(a) Continued.

Figure 13.- Continued.



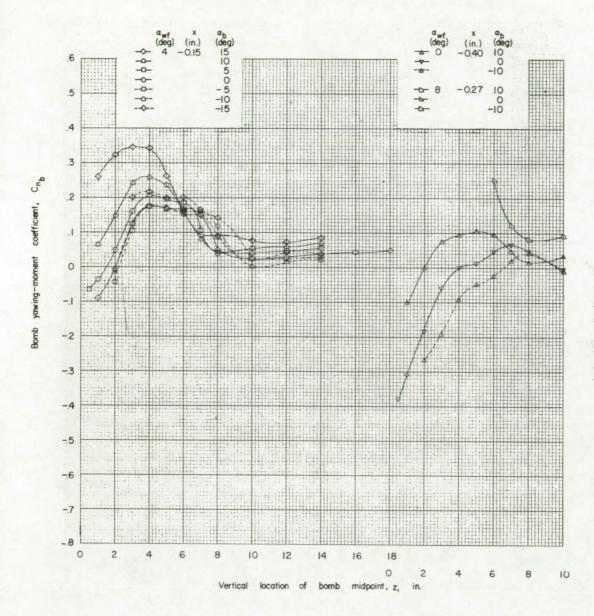
(a) Continued.

Figure 13.- Continued.



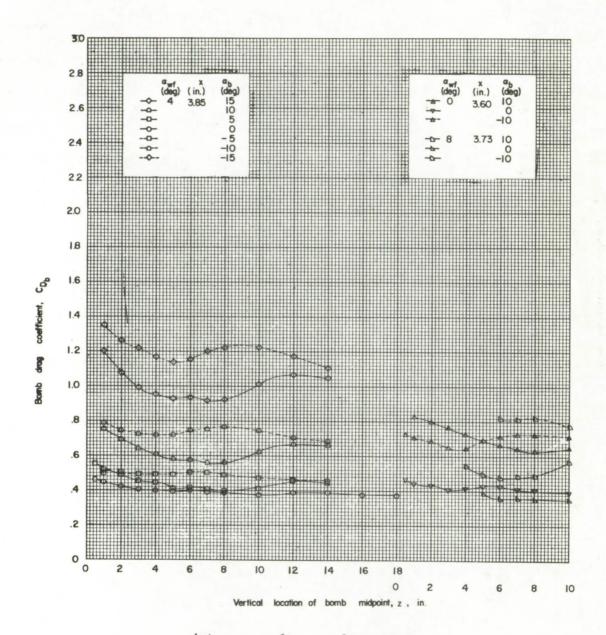
(a) Continued.

Figure 13.- Continued.

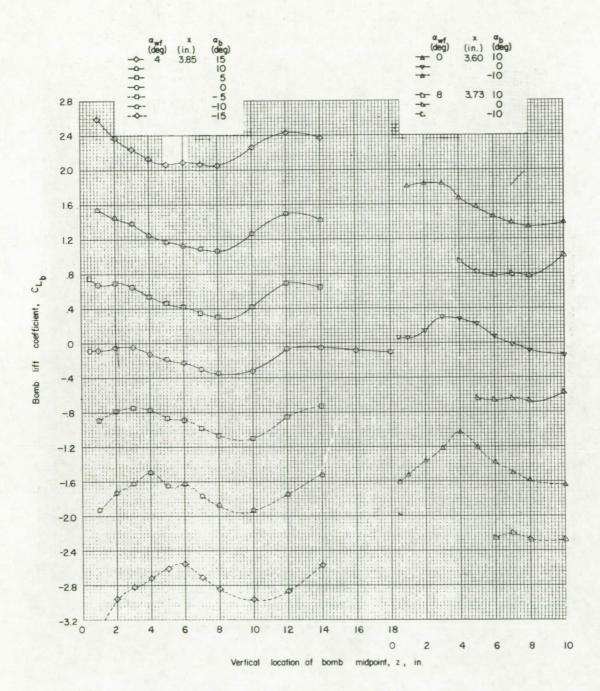


(a) Concluded.

Figure 13.- Continued.

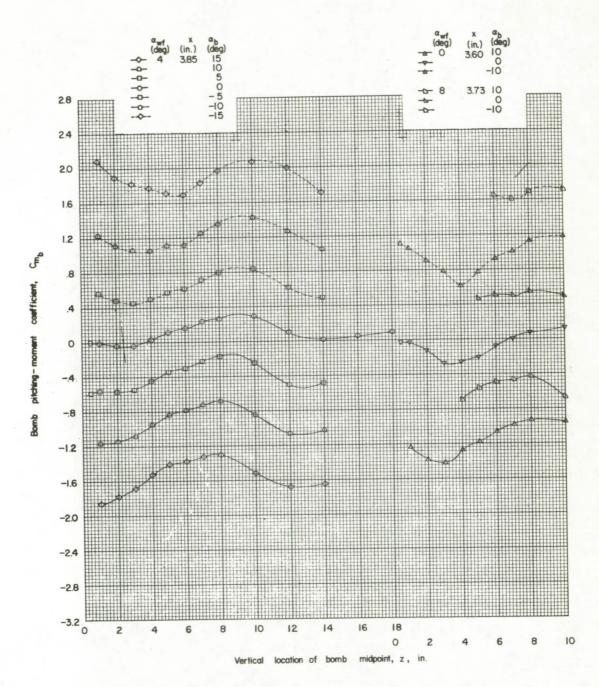


(b) x = 3.60 to 3.85 inches. Figure 13.- Continued.



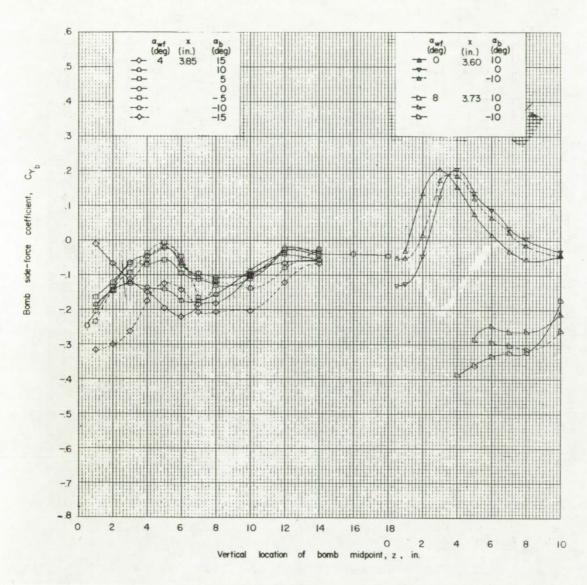
(b) Continued.

Figure 13.- Continued.



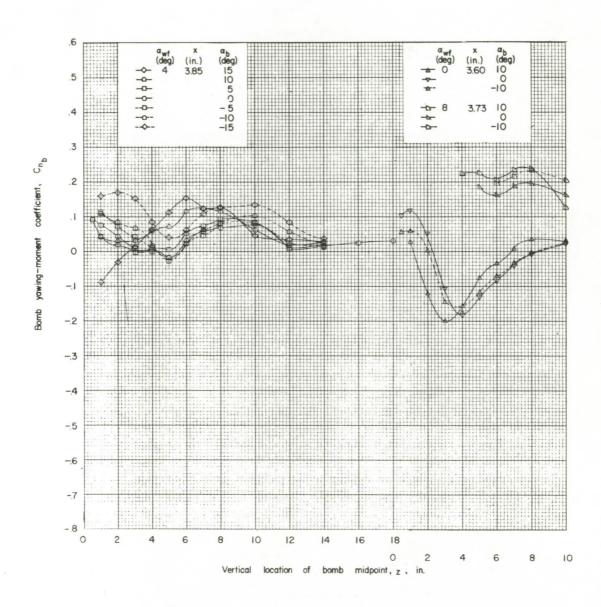
(b) Continued.

Figure 13.- Continued.



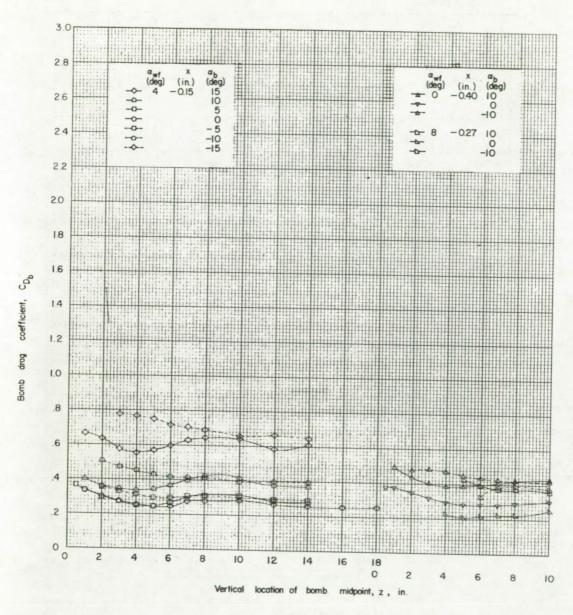
(b) Continued.

Figure 13.- Continued.



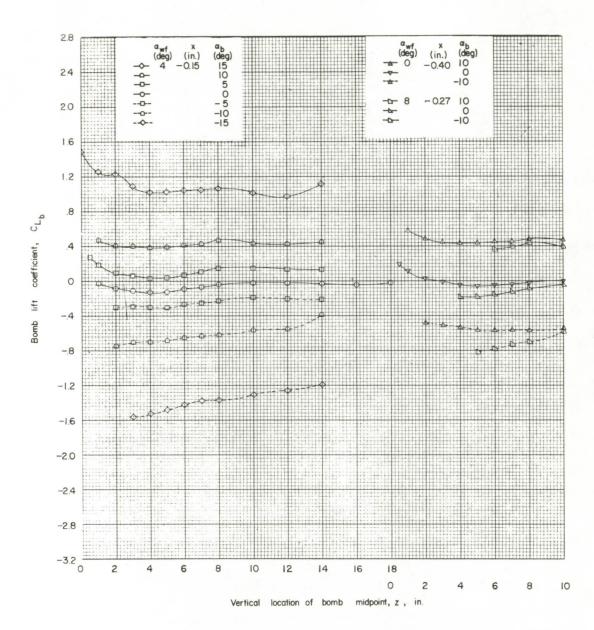
(b) Concluded.

Figure 13.- Concluded.



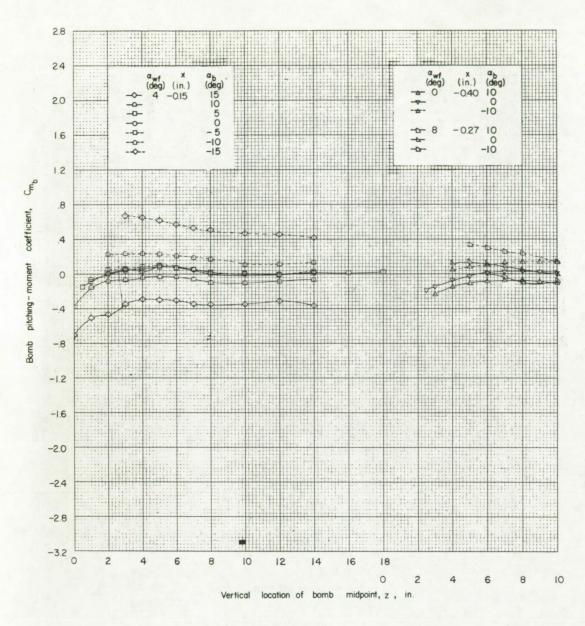
(a) x = -0.15 to -0.40 inch.

Figure 14.- Force data for bomb 4 in presence of wing-fuselage combination. Fins off; under-wing position; y = 6 inches.



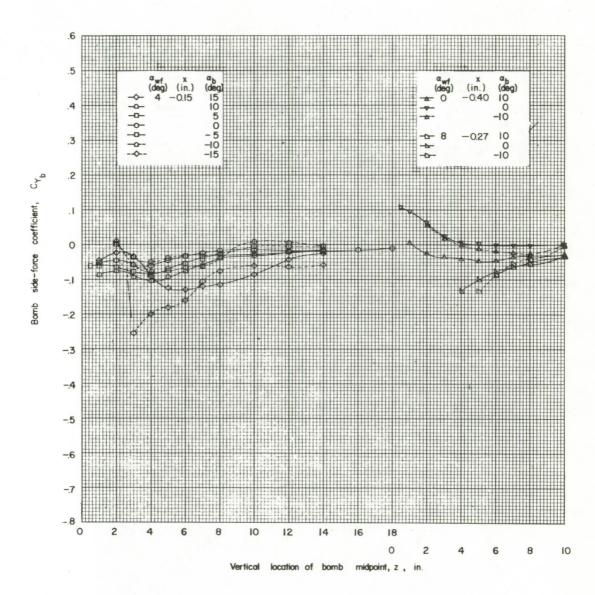
(a) Continued.

Figure 14.- Continued.



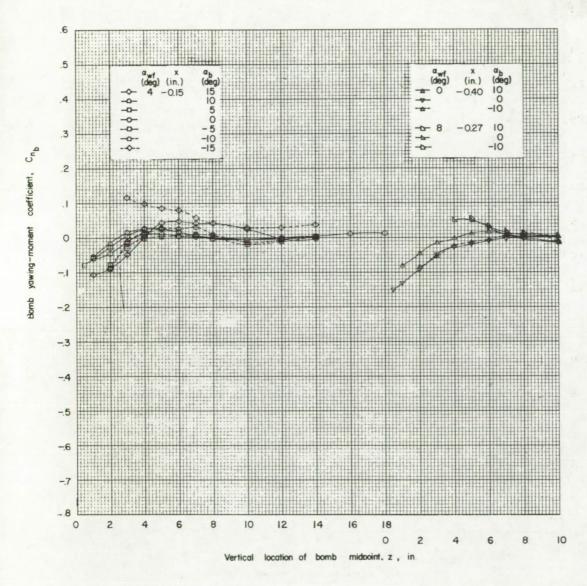
(a) Continued.

Figure 14.- Continued.



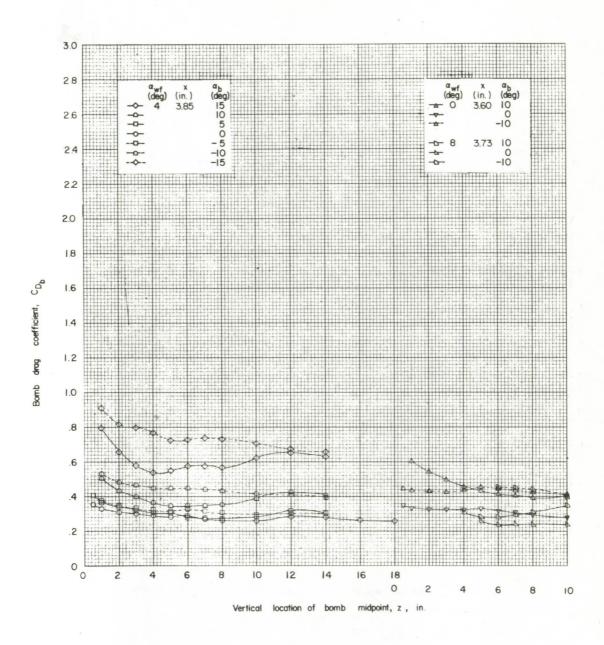
(a) Continued.

Figure 14.- Continued.

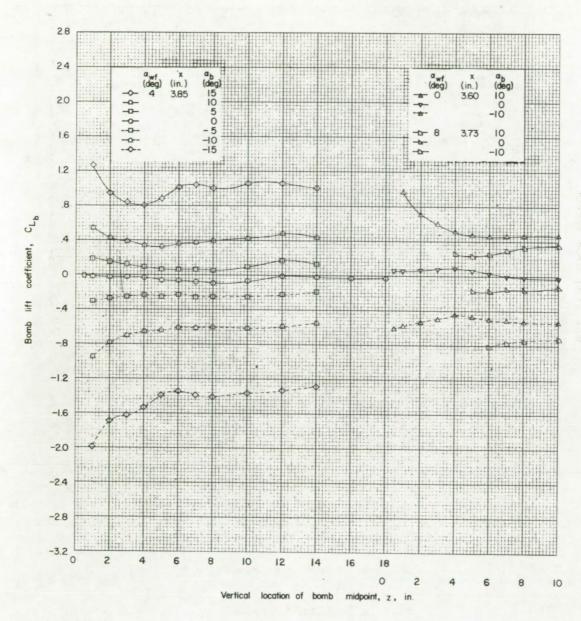


(a) Concluded.

Figure 14.- Continued.

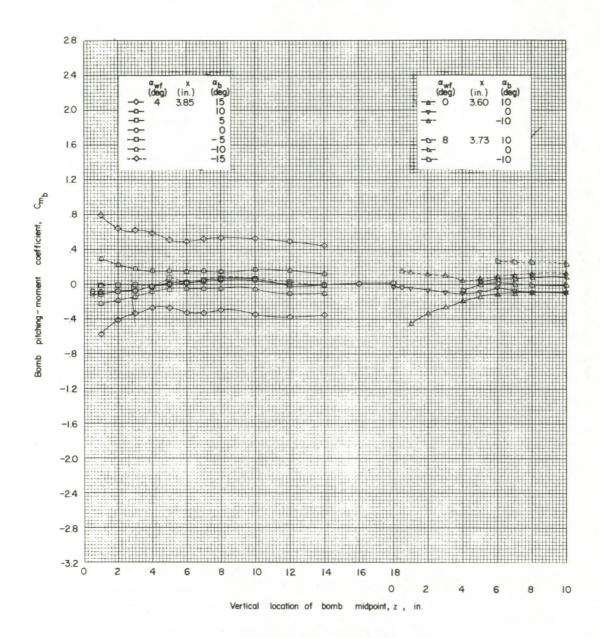


(b) x = 3.60 to 3.85 inches. Figure 14.- Continued.



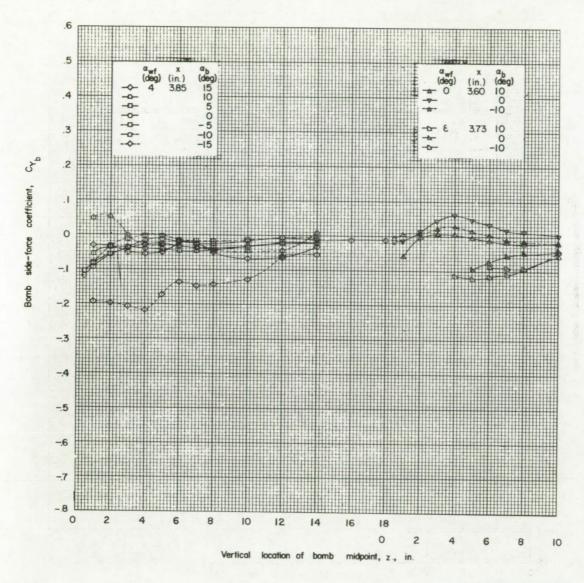
(b) Continued.

Figure 14.- Continued.



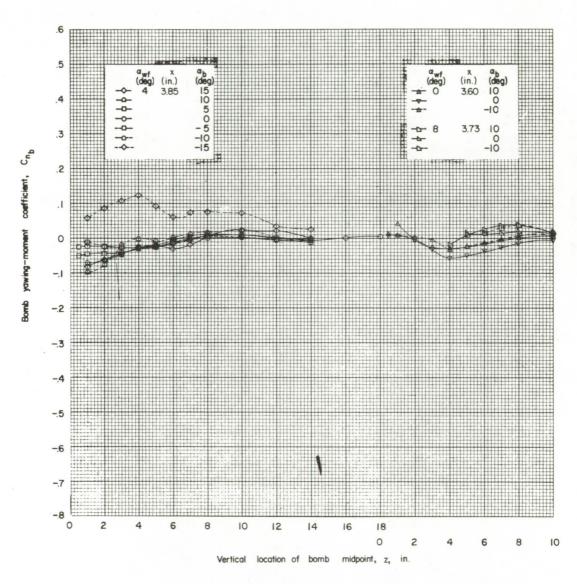
(b) Continued.

Figure 14.- Continued.



(b) Continued.

Figure 14.- Continued.



(b) Concluded.

Figure 14. - Concluded.

NACA RM L56K30 105

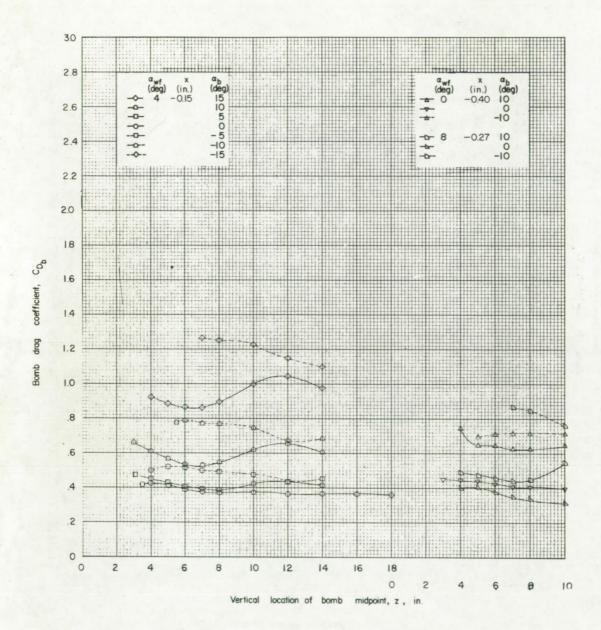


Figure 15.- Force data for bomb 4 in presence of low-winged fighter-bomber configuration. Under-fuselage position; y = 0; x = -0.15 to -0.40 inch.

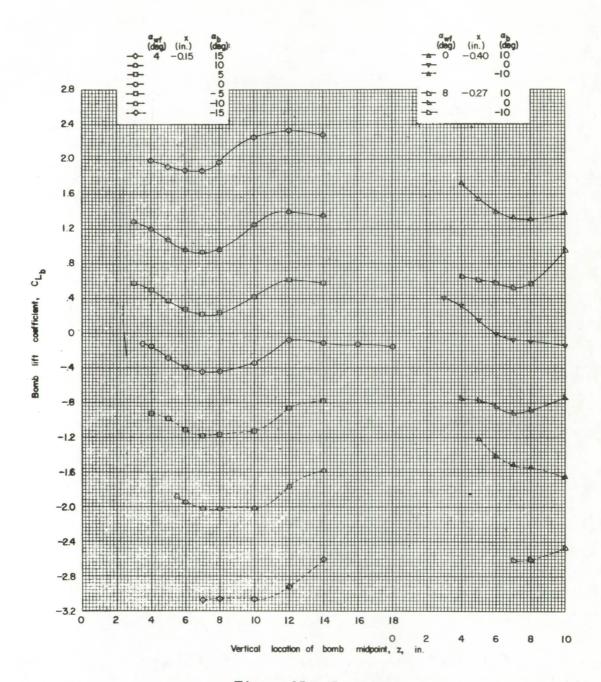


Figure 15 .- Continued.

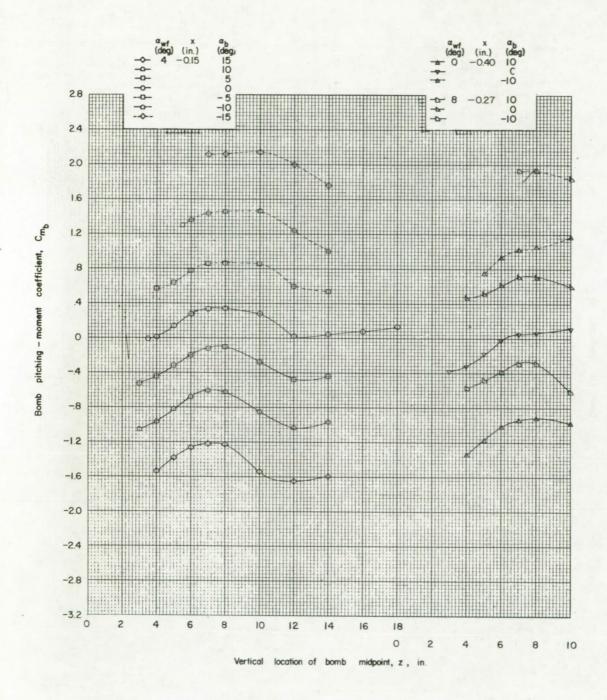


Figure 15.- Concluded.

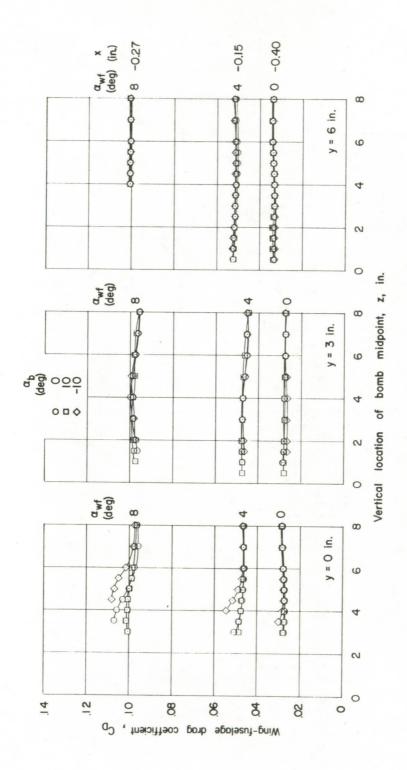


Figure 16.- Wing-fuselage forces in presence of bomb 3.

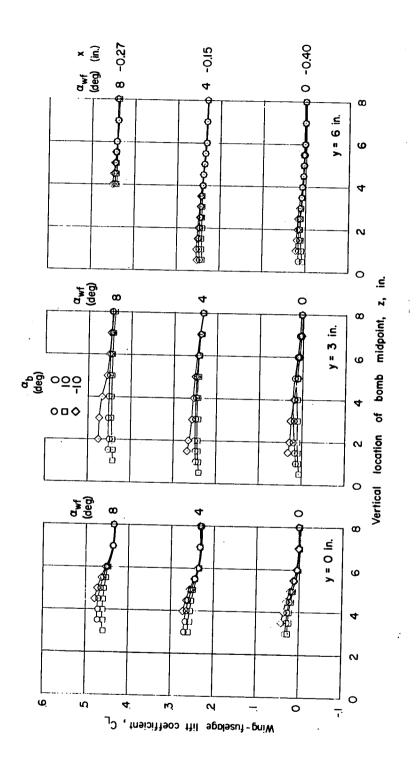


Figure 16:- Continued.

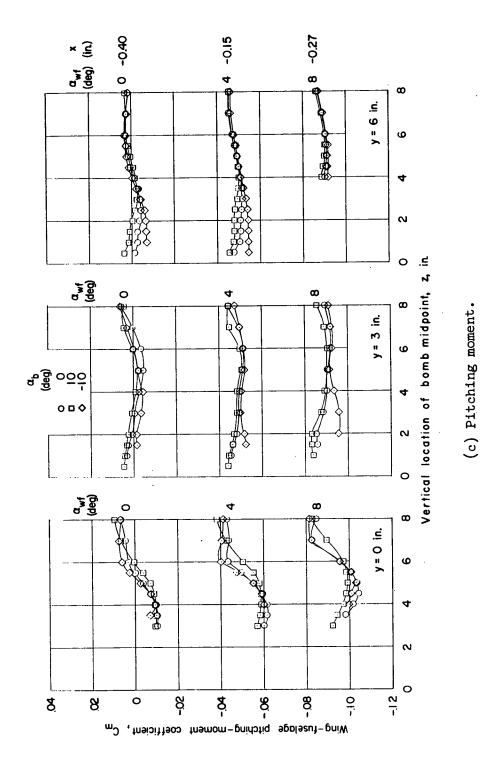
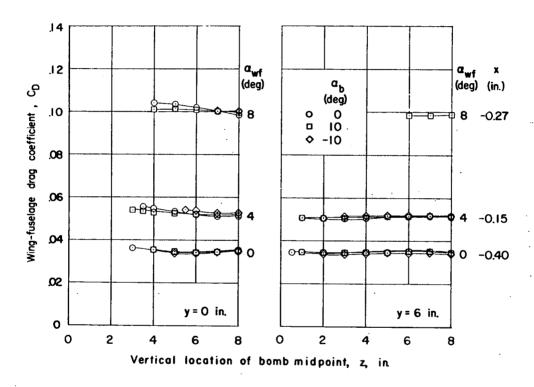
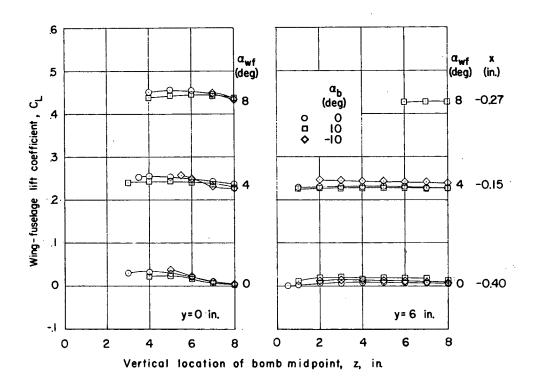


Figure 16.- Concluded.



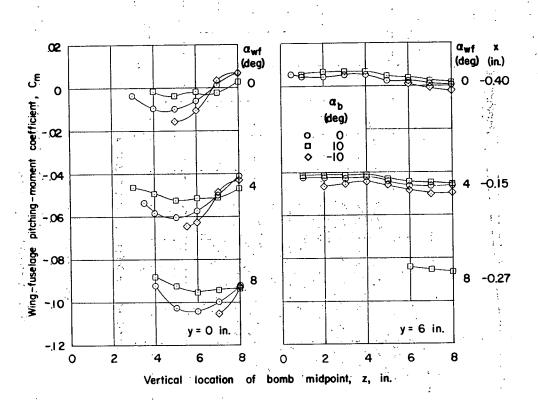
(a) Drag.

Figure 17.- Wing-fuselage forces in presence of bomb 4.



(b) Lift.

Figure 17.- Continued.



(c) Pitching moment.

Figure 17.- Concluded.

11.00

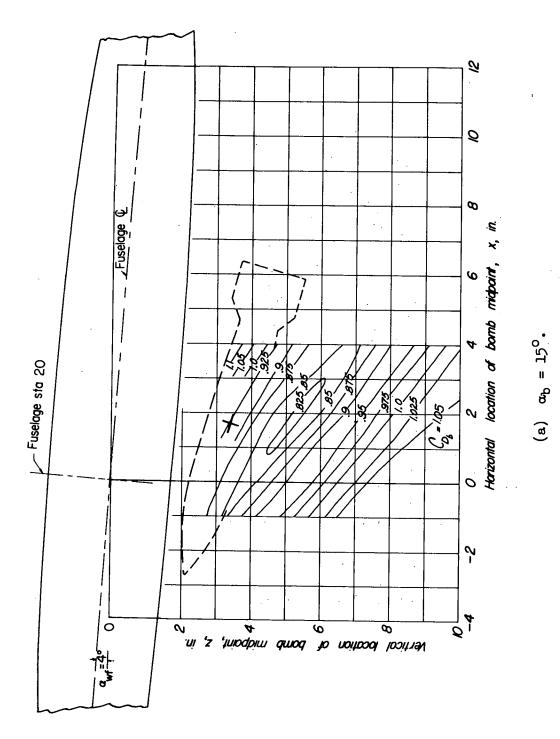


Figure 18.- Contour plot of drag of bomb 3 in presence of wing-fuselage combination. y=0.

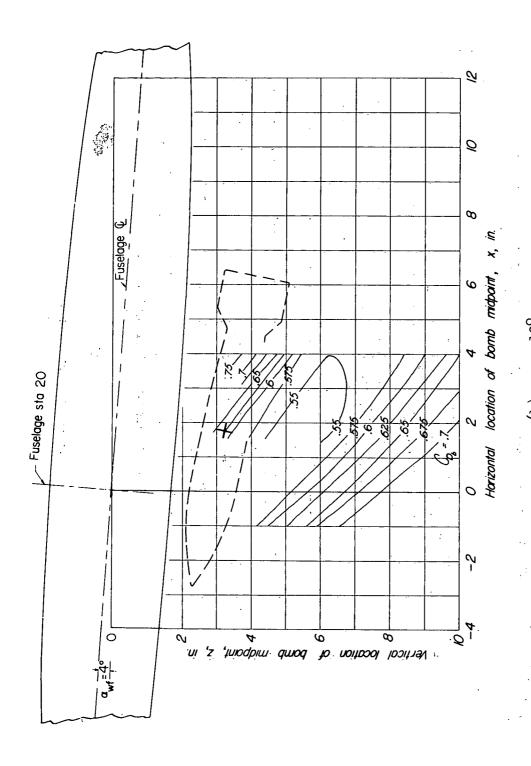


Figure 18.- Continued.

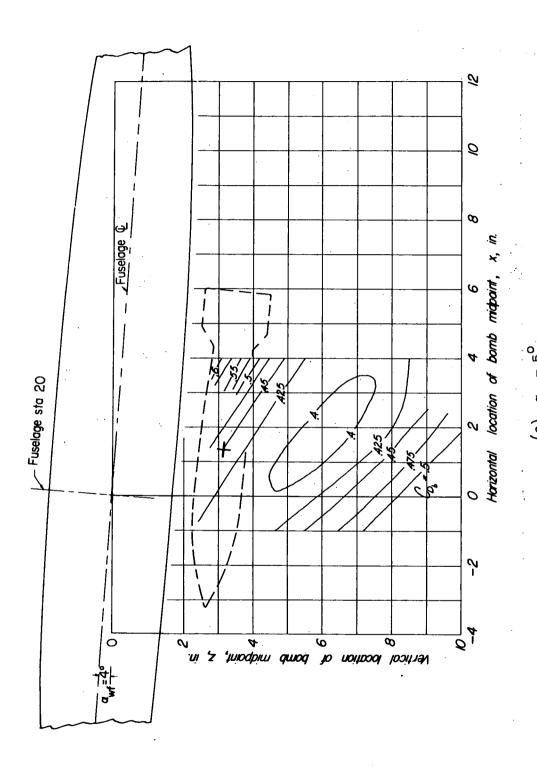


Figure 18.- Continued.

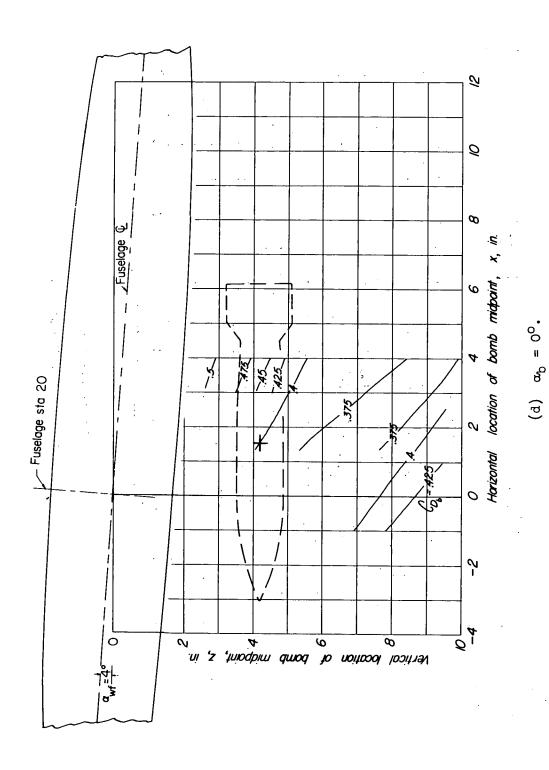


Figure 18.- Continued.

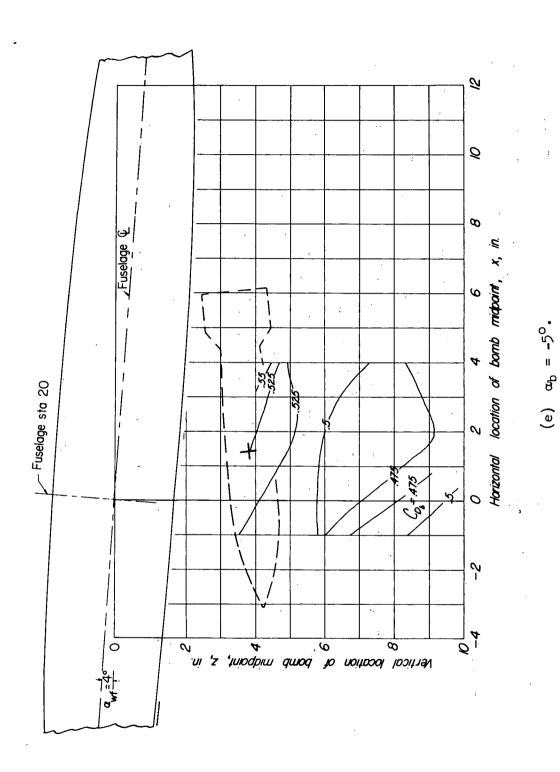


Figure 18.- Continued.

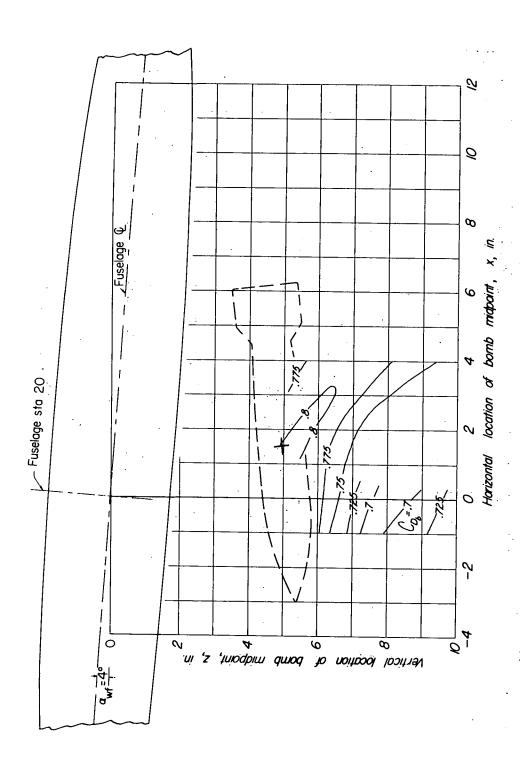


Figure 18.- Continued.

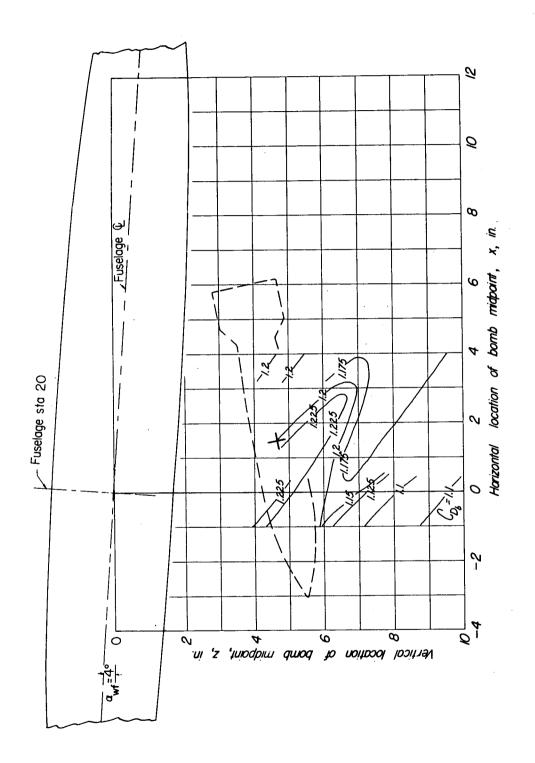


Figure 18.- Concluded.

(g) $\alpha_{\rm b} = -15^{\rm o}$.

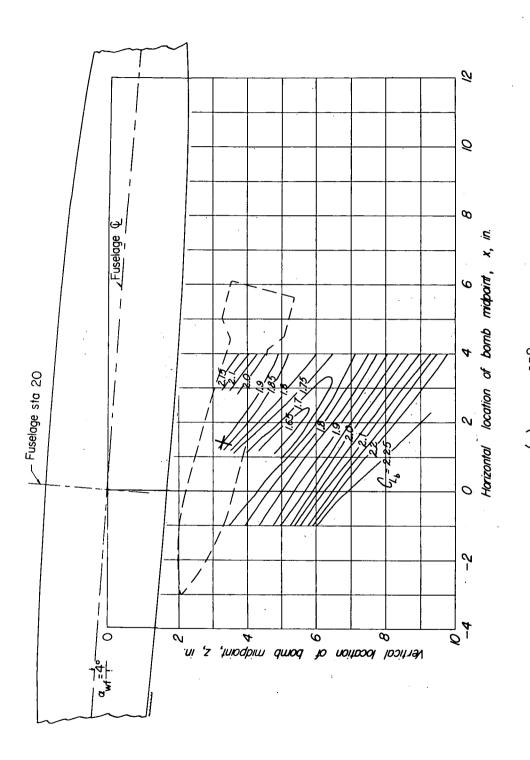


Figure 19.- Contour plot of lift of bomb 3 in presence of wing-fuselage combination. y = 0.

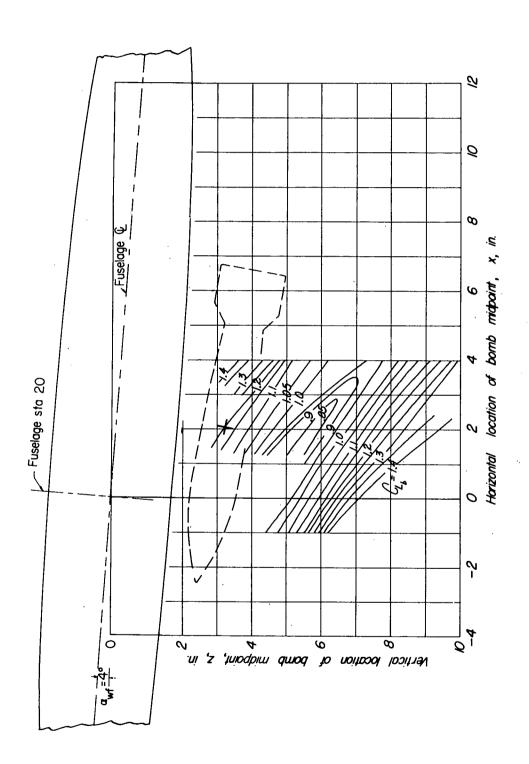


Figure 19.- Continued.

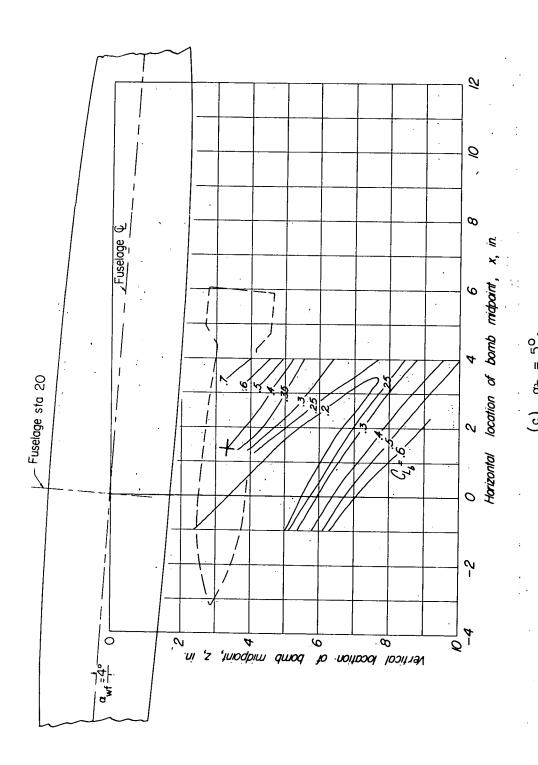


Figure 19.- Continued.

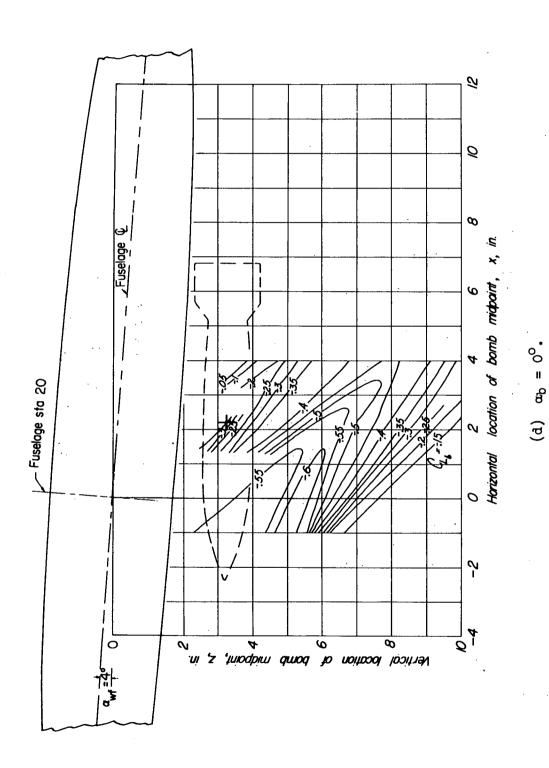


Figure 19.- Continued:

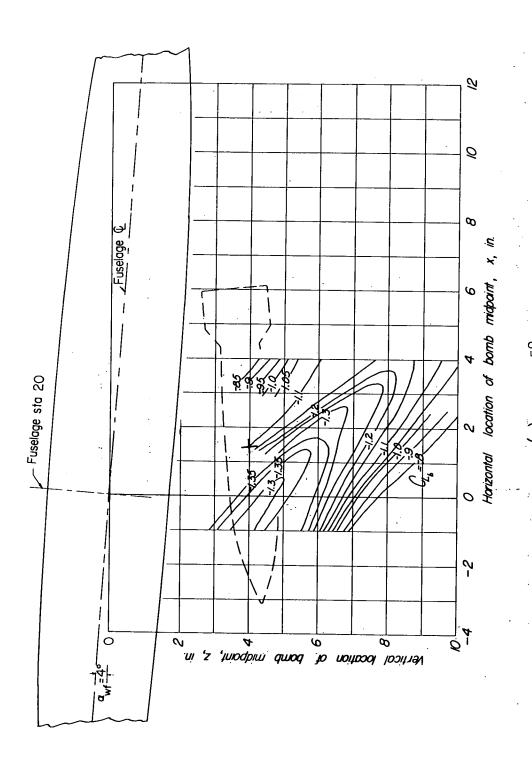


Figure 19.- Continued.

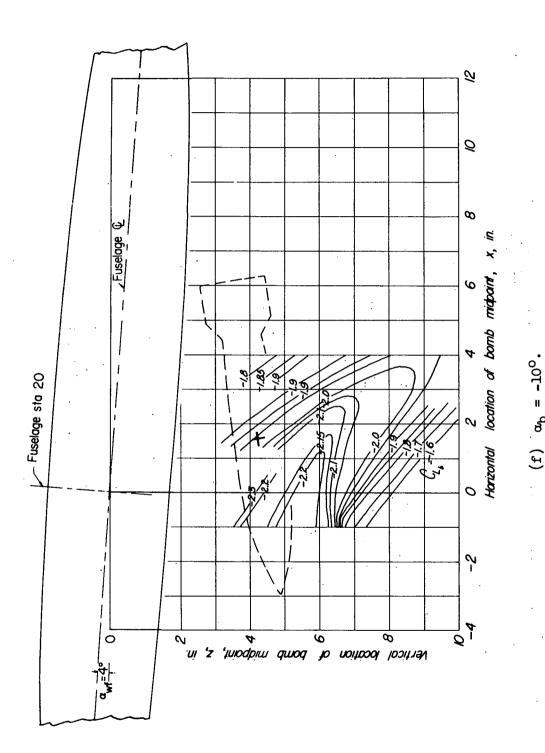
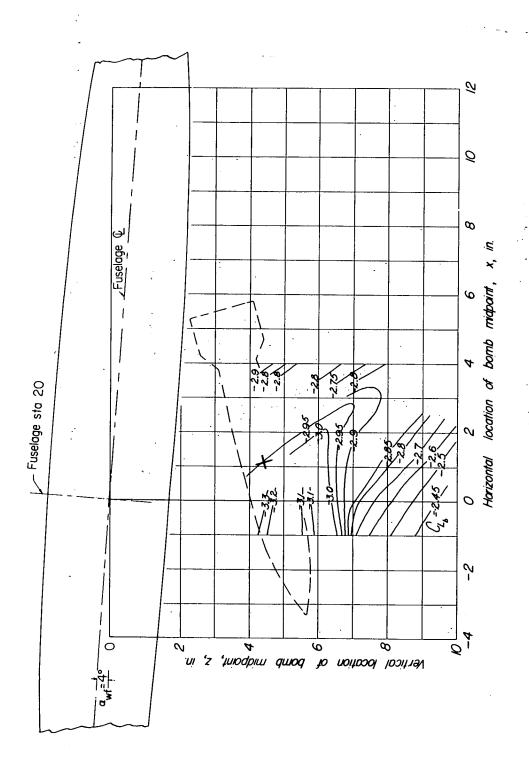


Figure 19.- Continued.



 $\cdot C = q_{D} (8)$

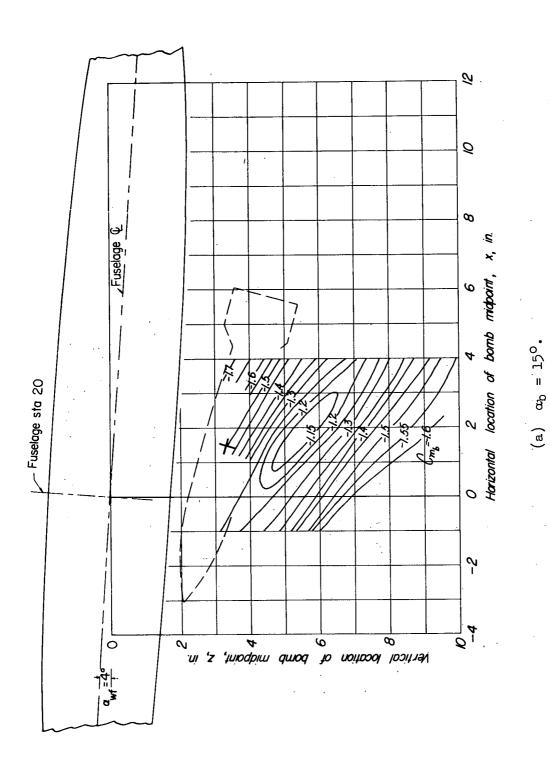


Figure 20.- Contour plot of pitching moment of bomb 3 in presence of wing-fuselage combination. y = 0.

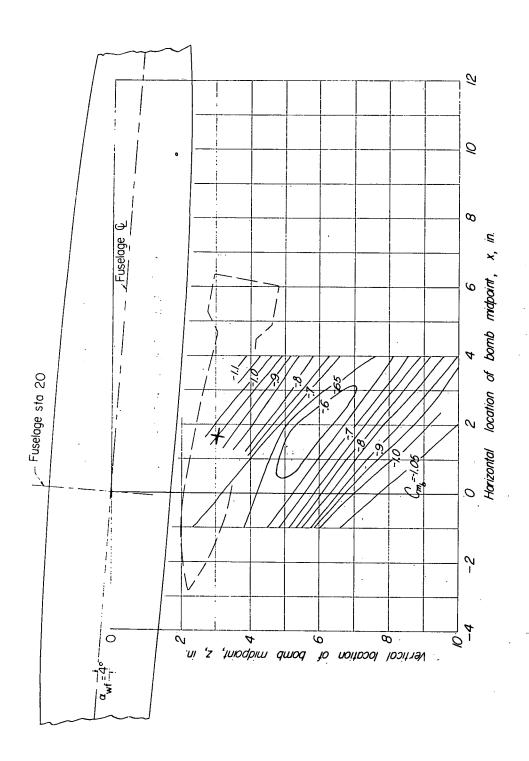


Figure 20.- Continued.

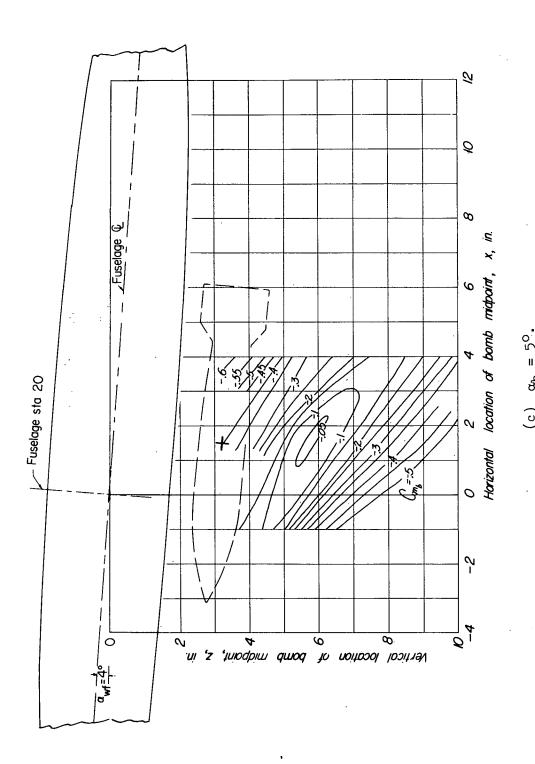


Figure 20.- Continued.

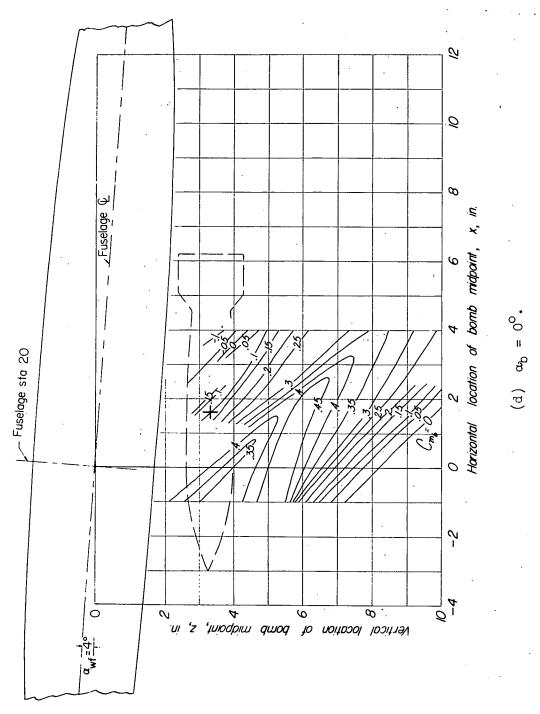


Figure 20.- Continued.

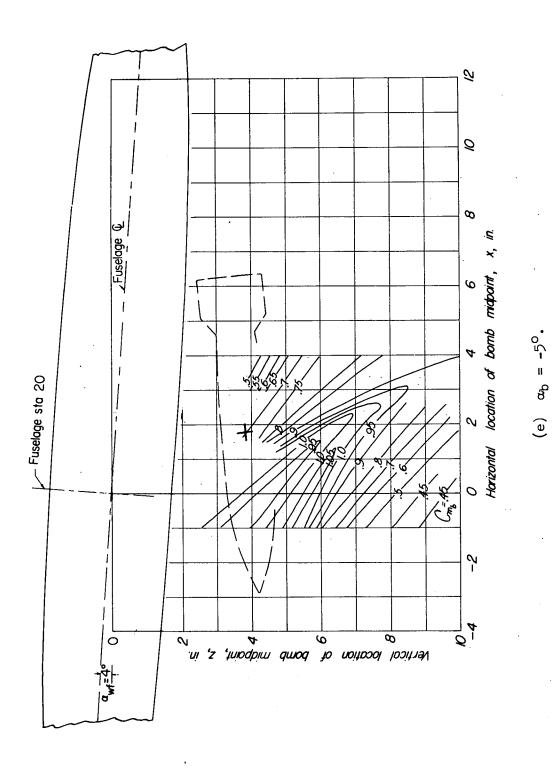


Figure 20.- Continued.

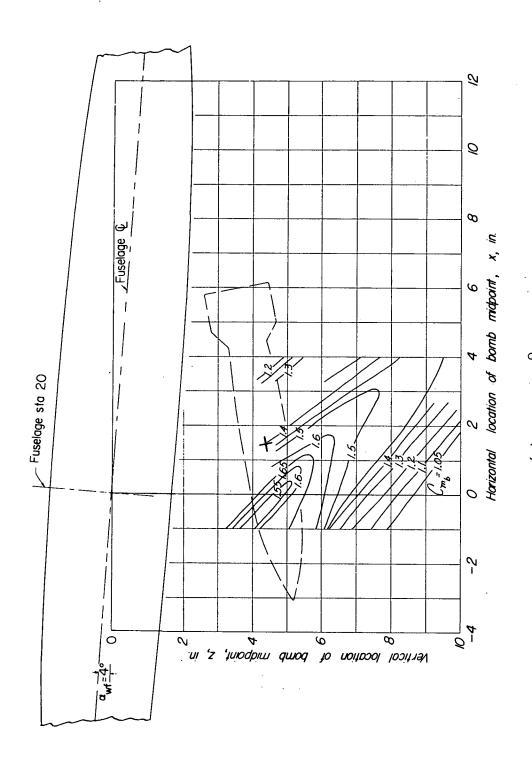
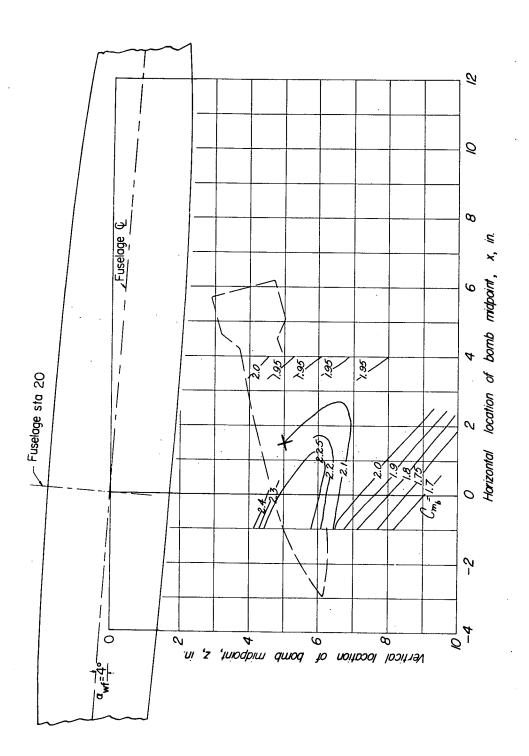
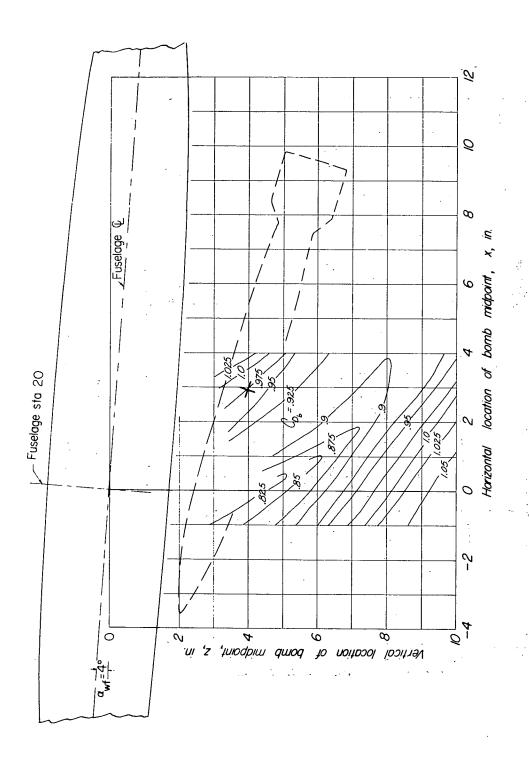


Figure 20.- Continued.



(g) $\alpha_{\rm b} = -15^{\rm o}$.

Figure 20.- Concluded.



ं Figure 21.- Contour plot of drag of bomb 4 in presence of wing-fuselage combination.

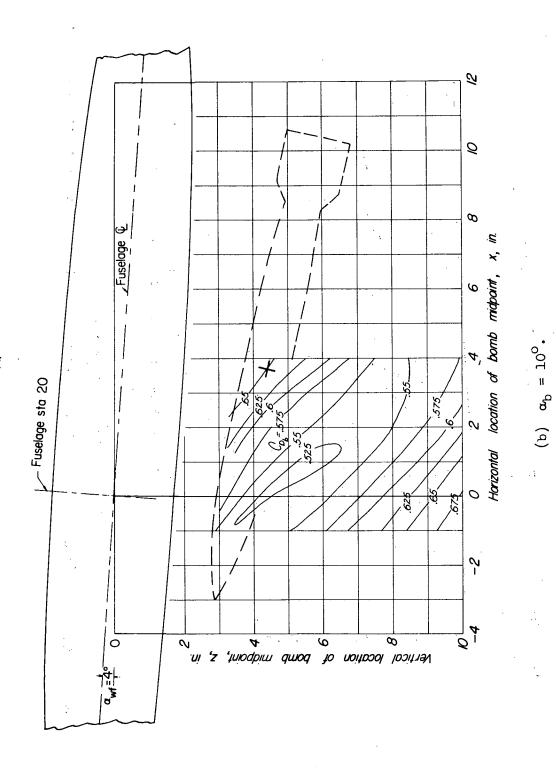


Figure 21.- Continued.

हुनु स्टीन्टर है.

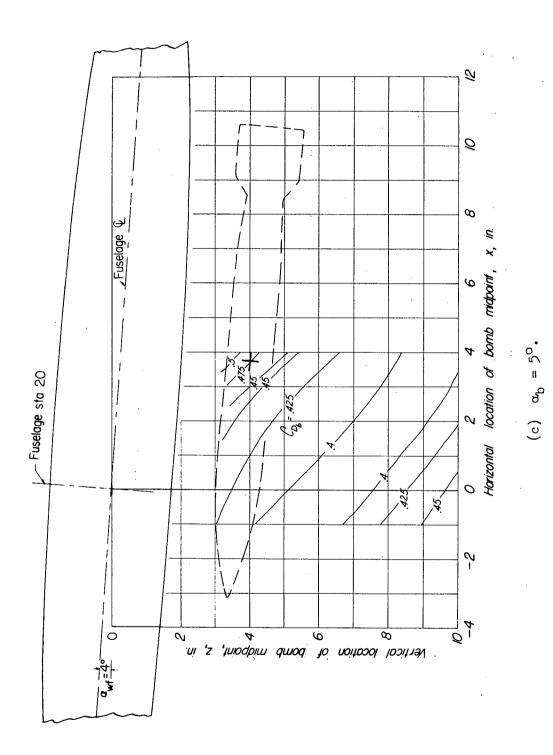


Figure 21.- Continued.

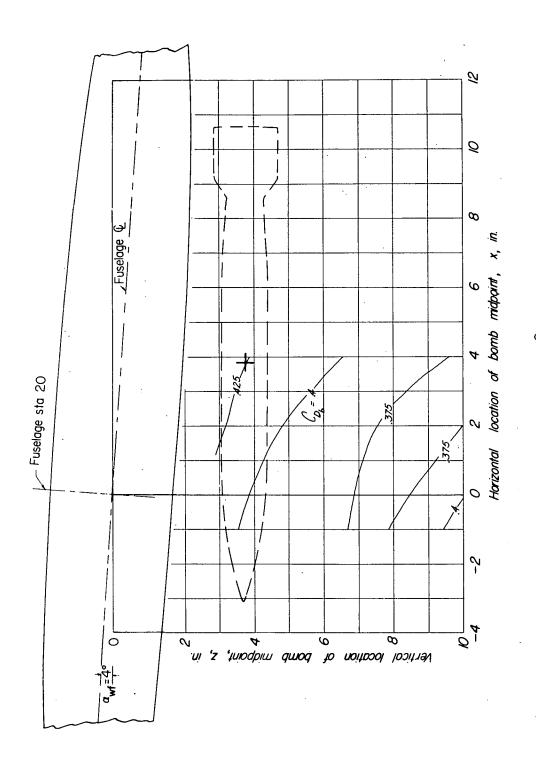


Figure 21.- Continued.

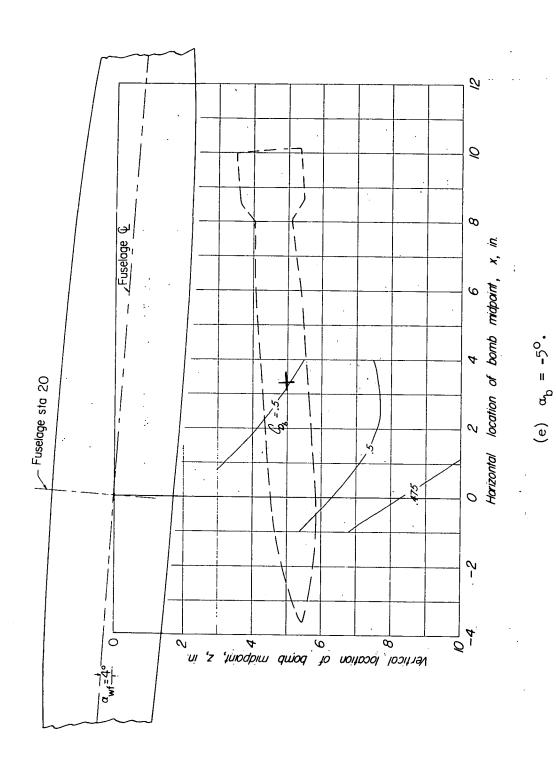


Figure 21.- Continued.

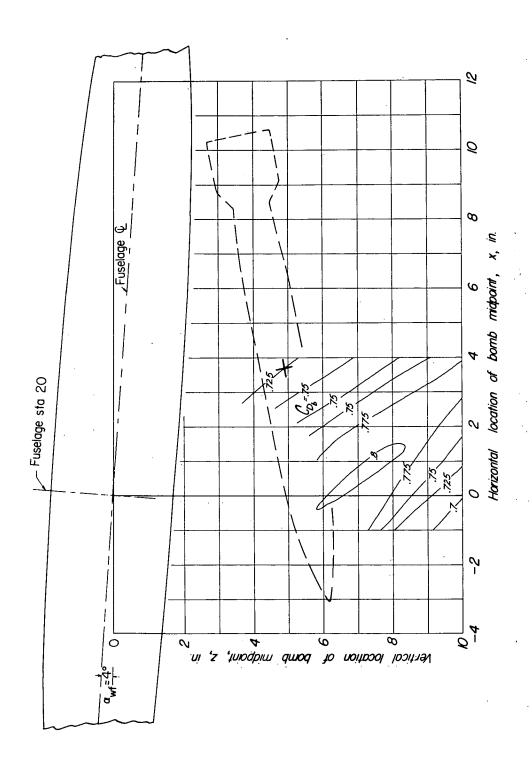


Figure 21.- Continued.

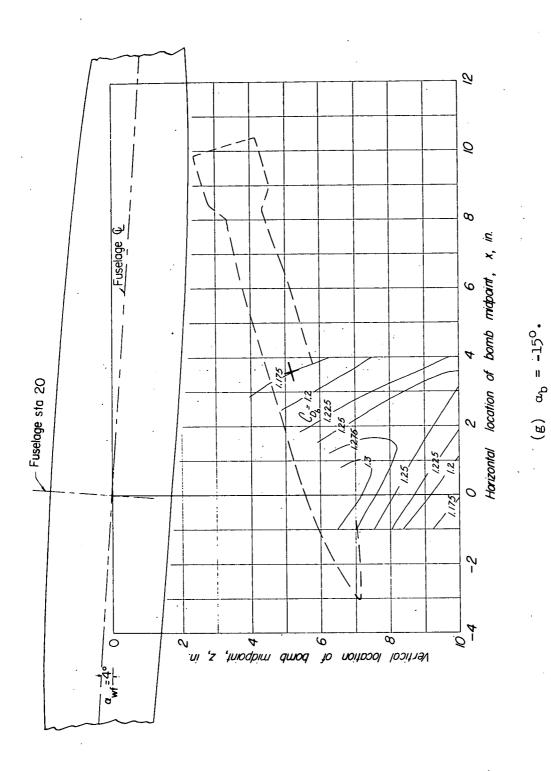
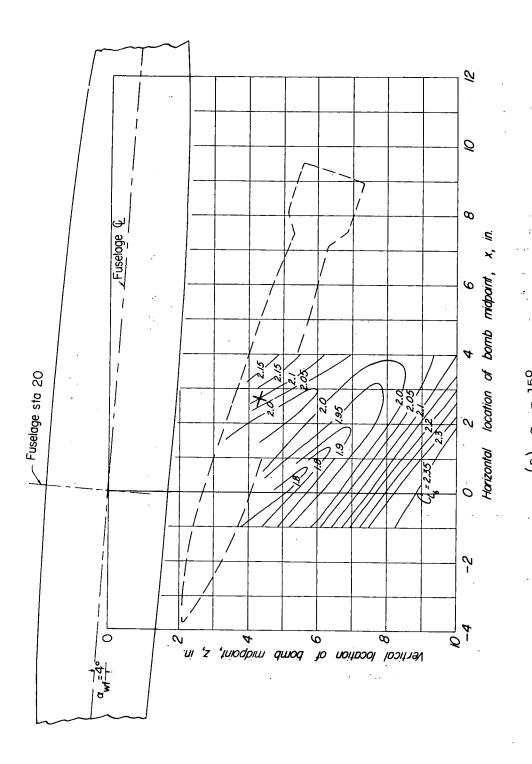


Figure 21.- Concluded.



ं Figure 22.- Contour plot of lift of bomb 4 in presence of wing-fuselage combination.

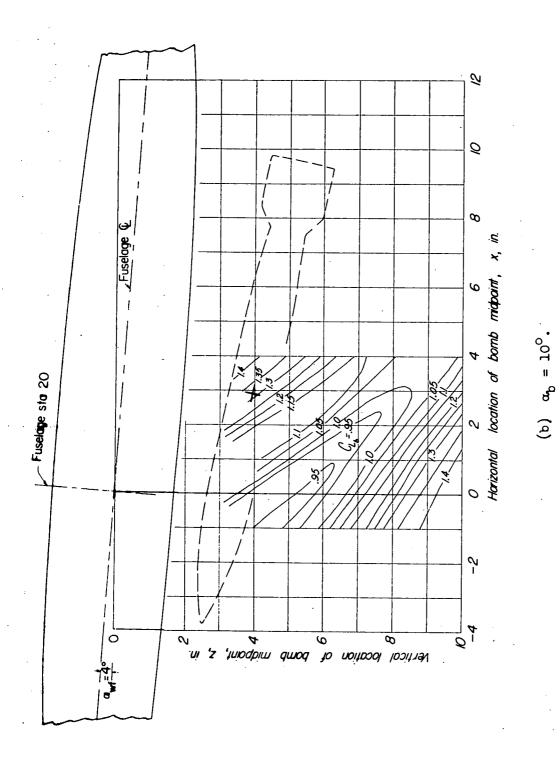


Figure 22.- Continued.

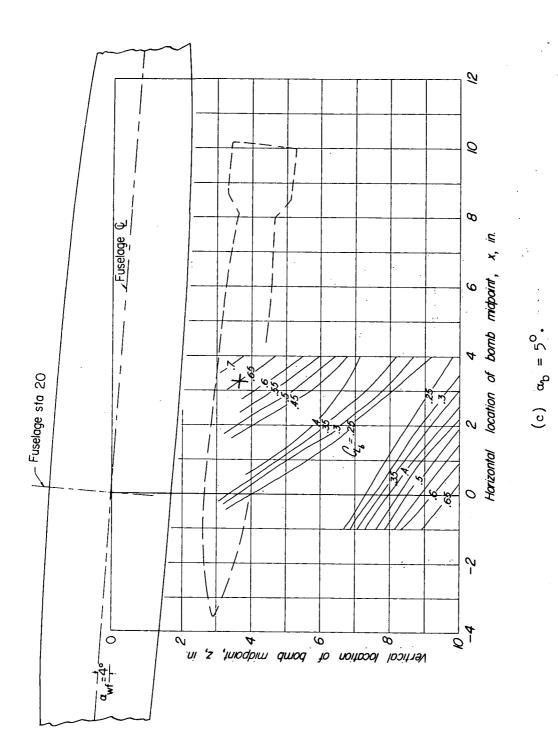


Figure 22.- Continued.

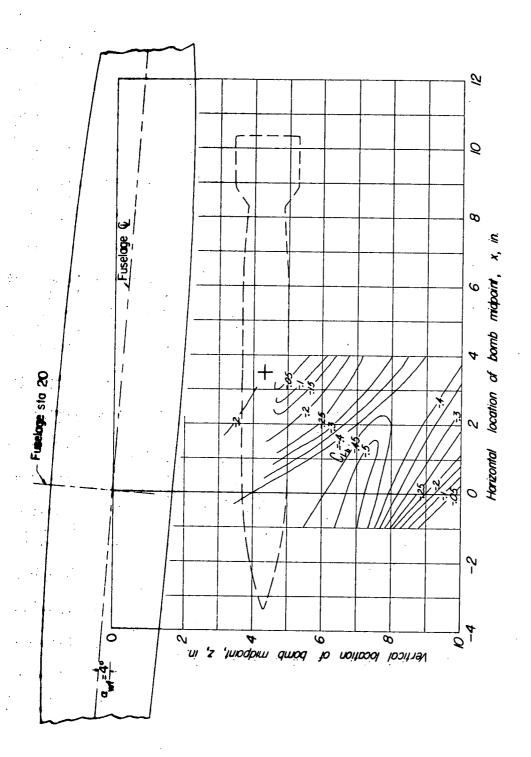


Figure 22.- Continued.

 $(a) a_b = 0^0$

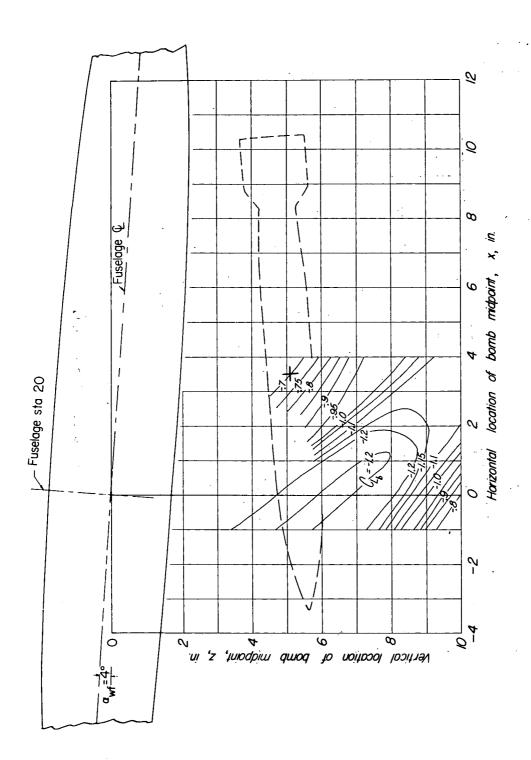


Figure 22.- Continued.

(e) $\alpha_{\rm b} = -5^{\rm o}$.

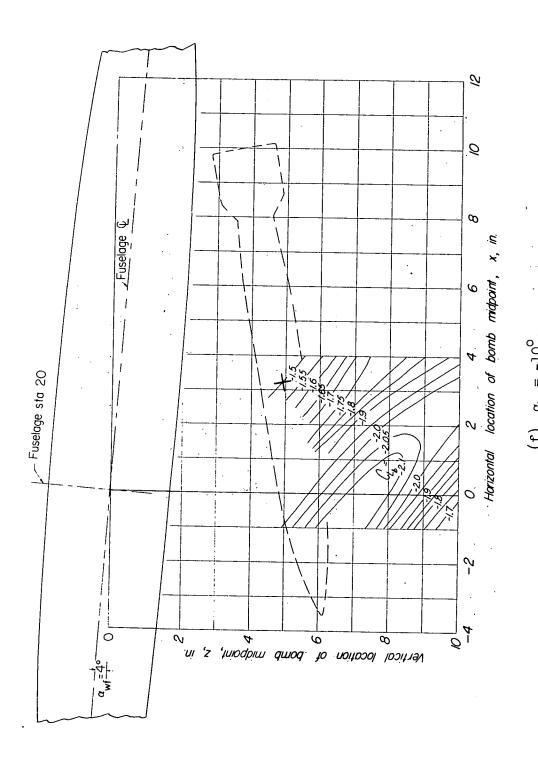


Figure 22.- Continued.

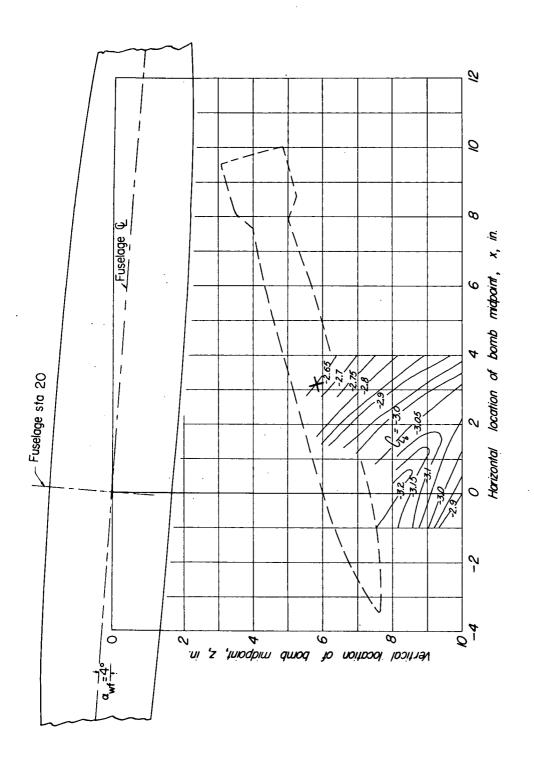


Figure 22.- Concluded.

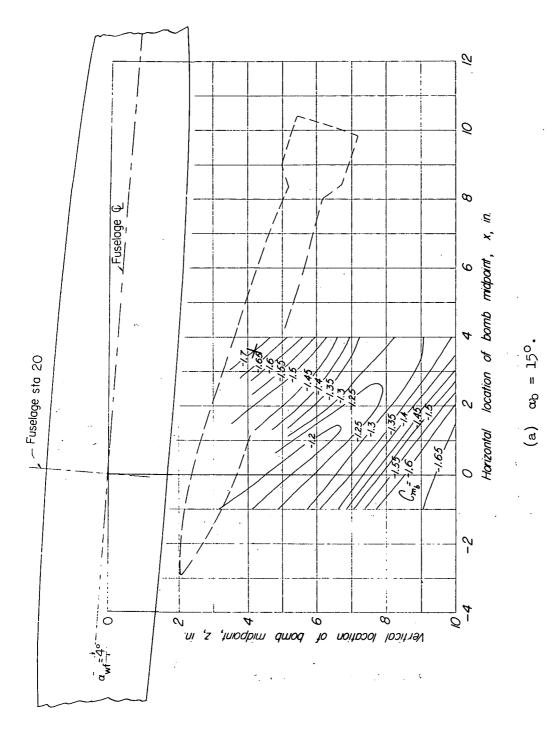


Figure 23.- Contour plot of pitching moment of bomb μ in presence of wing-fuselage combination. y=0.

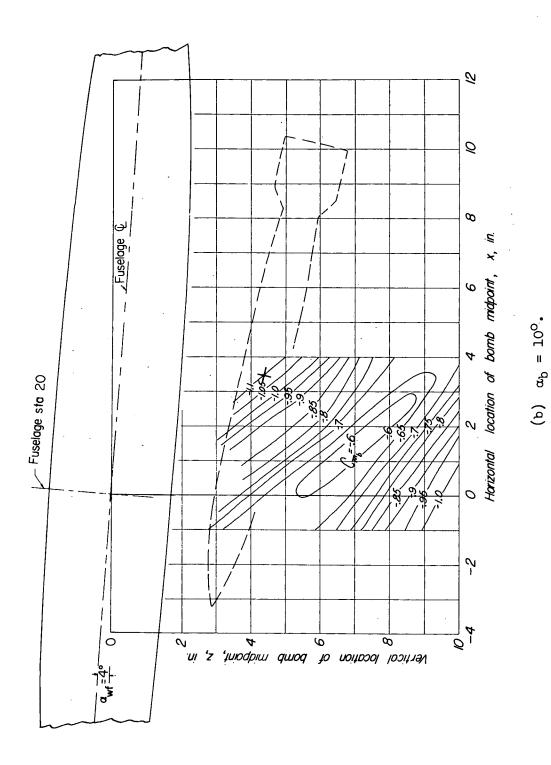


Figure 23.- Continued.

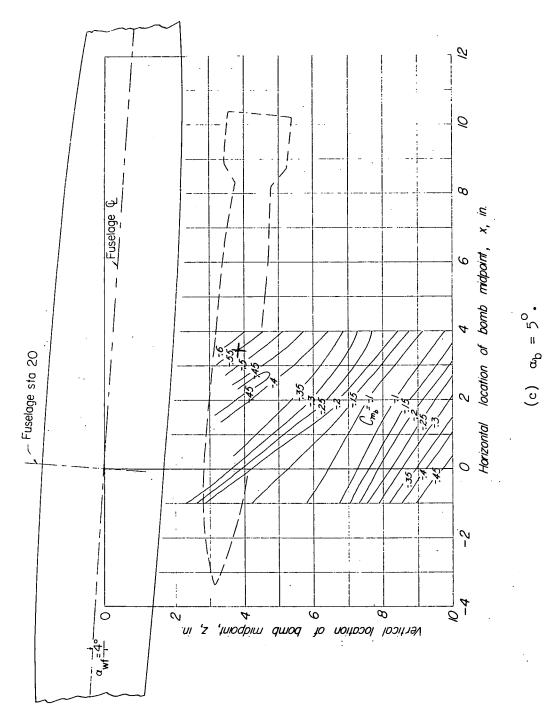


Figure 25.- Continued.

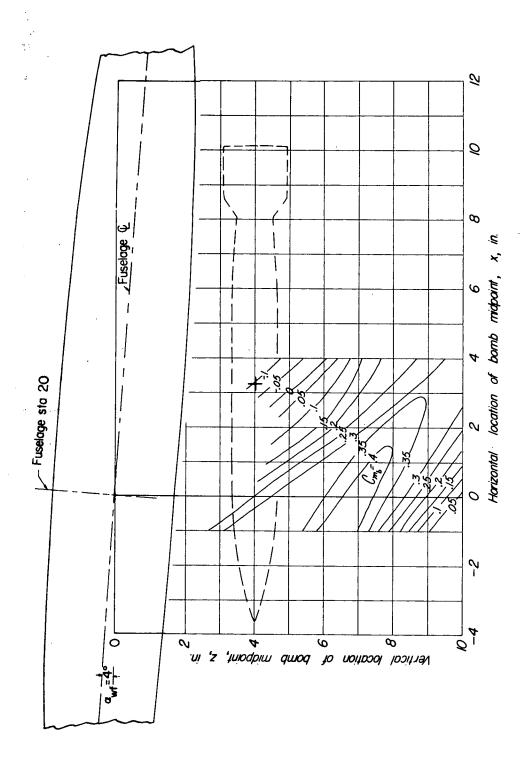


Figure 23.- Continued.

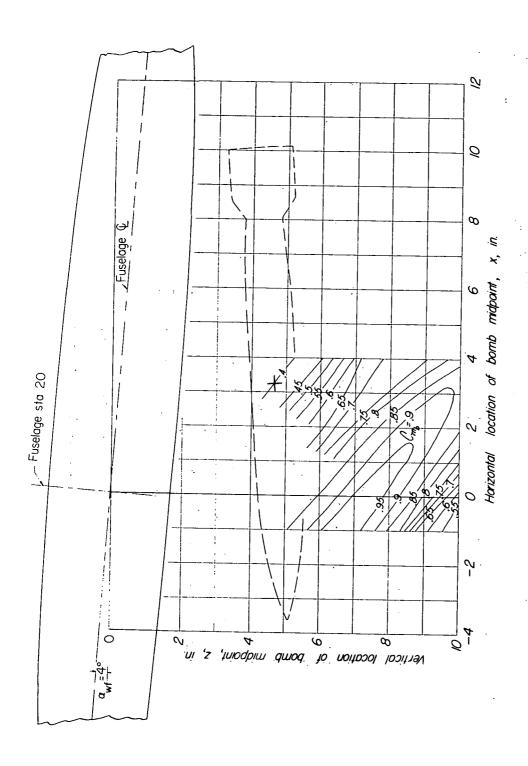


Figure 23.- Continued.

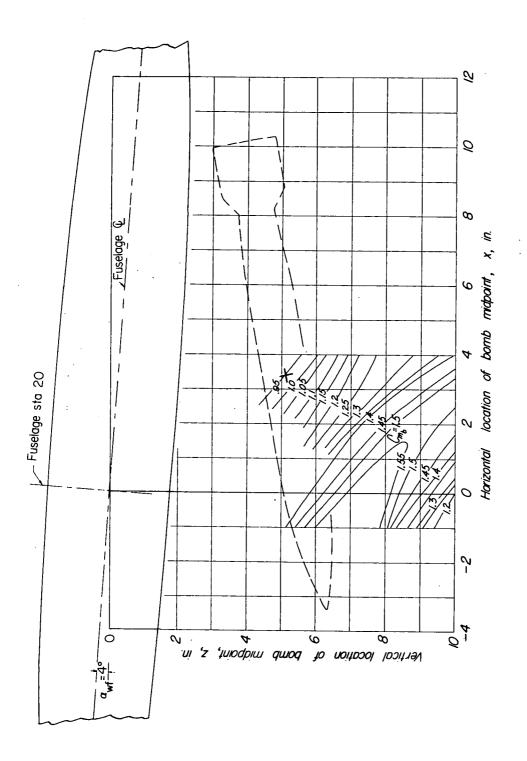


Figure 23.- Continued.

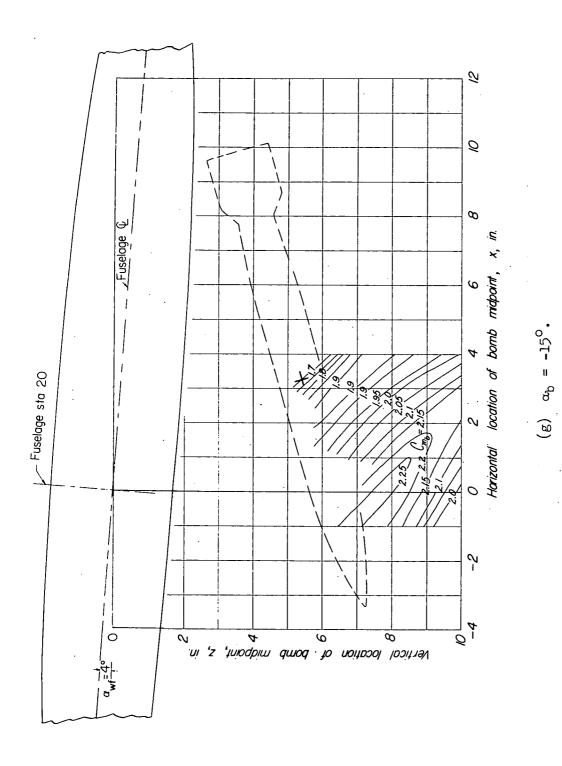
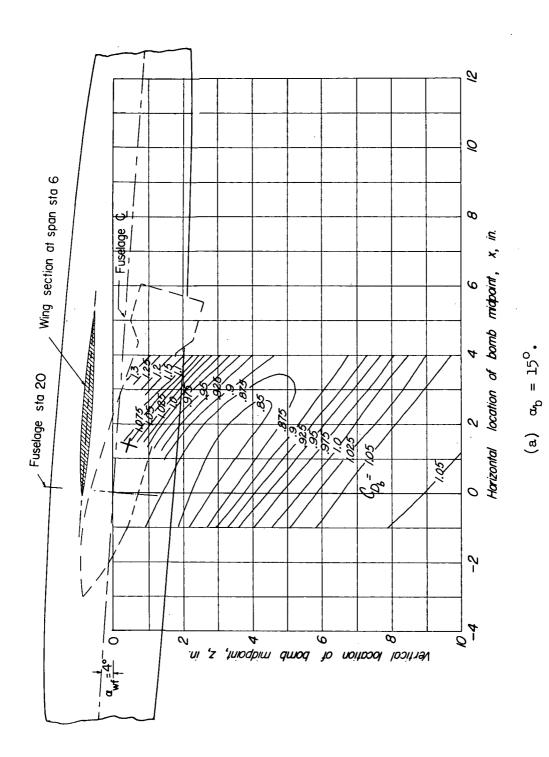


Figure 25.- Concluded.



y = 6 inches. Figure 2^{μ} .- Contour plot of drag of bomb 3 in presence of wing-fuselage combination.

135

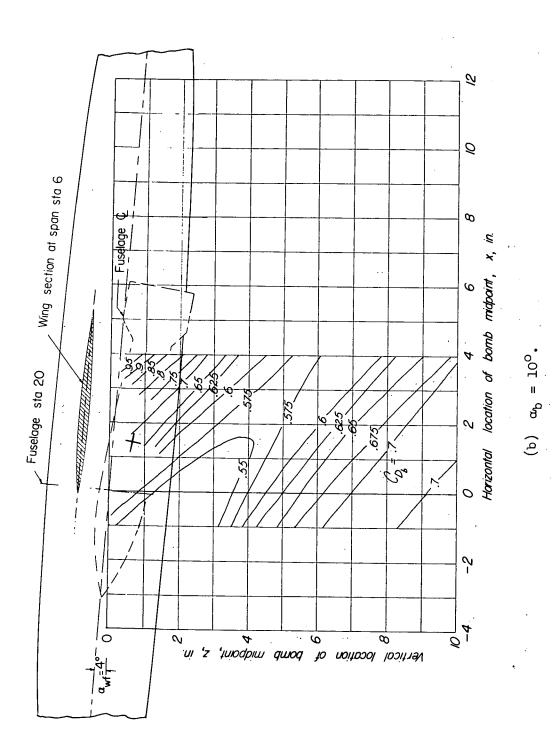


Figure 24.- Continued.

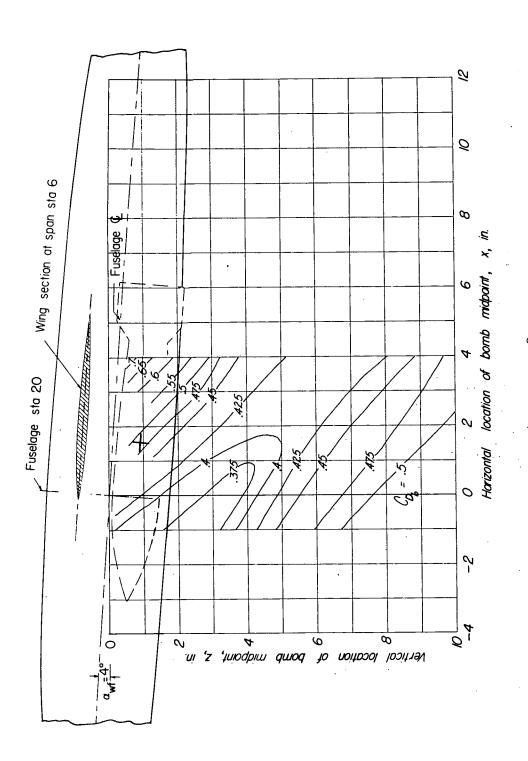


Figure 24. - Continued.

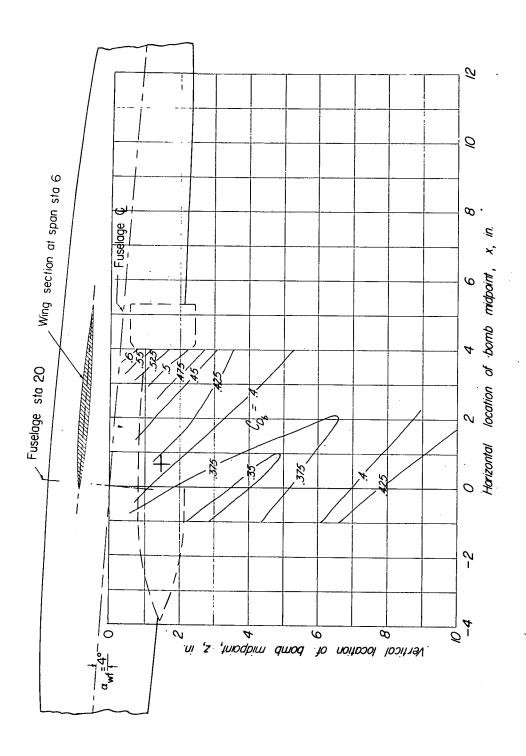


Figure 24.- Continued.

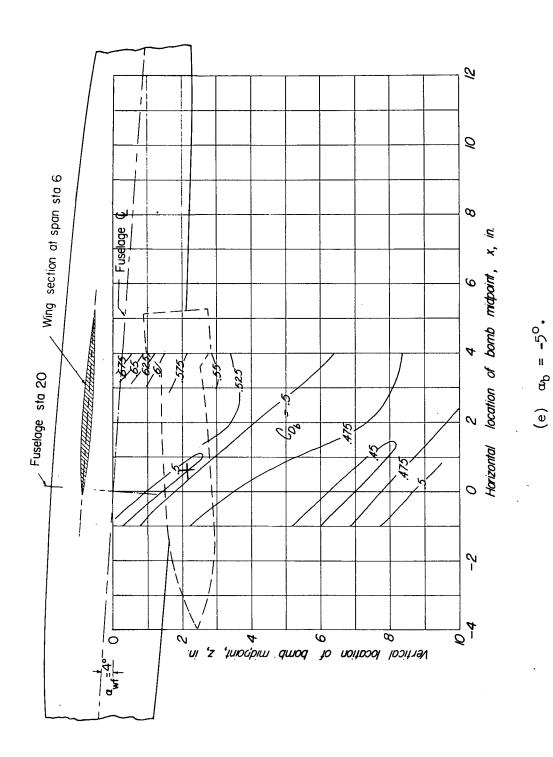


Figure 24.- Continued.

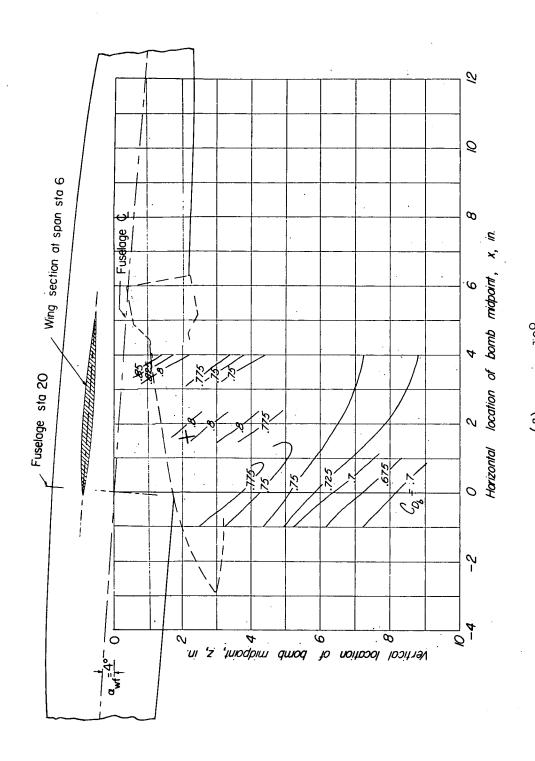


Figure 24.- Continued.

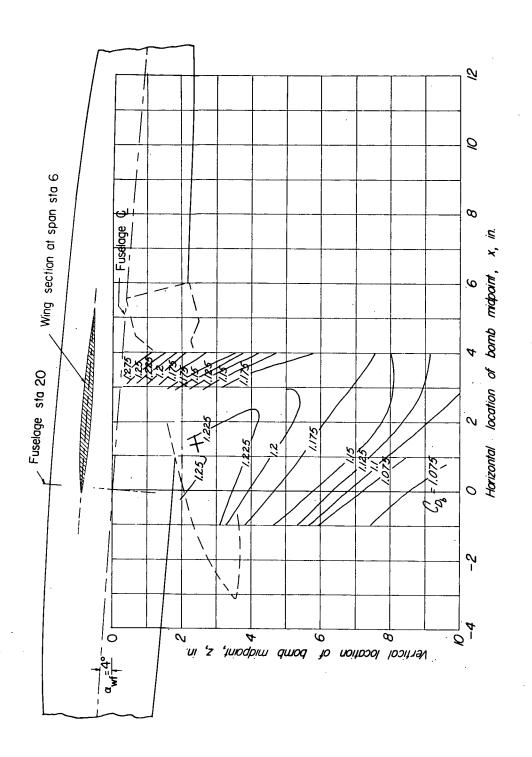


Figure 24.- Concluded.

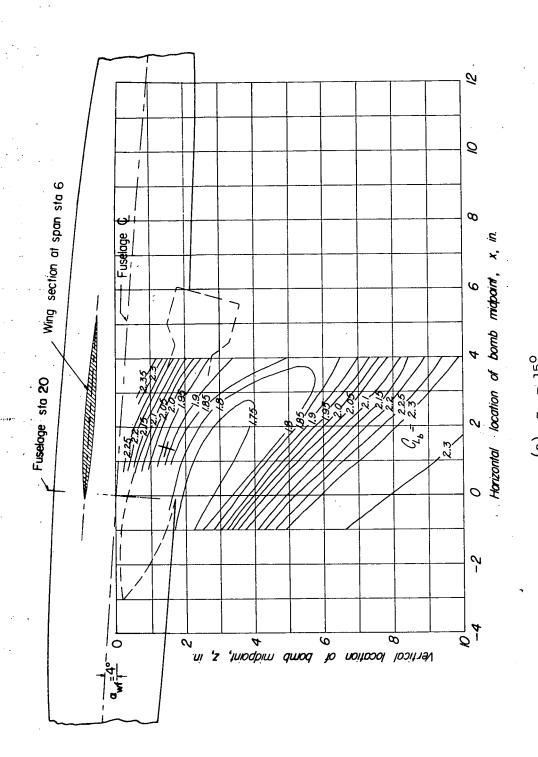


Figure 25.- Contour plot of lift of bomb 3 in presence of wing-fuselage combination. y = 6 inches.

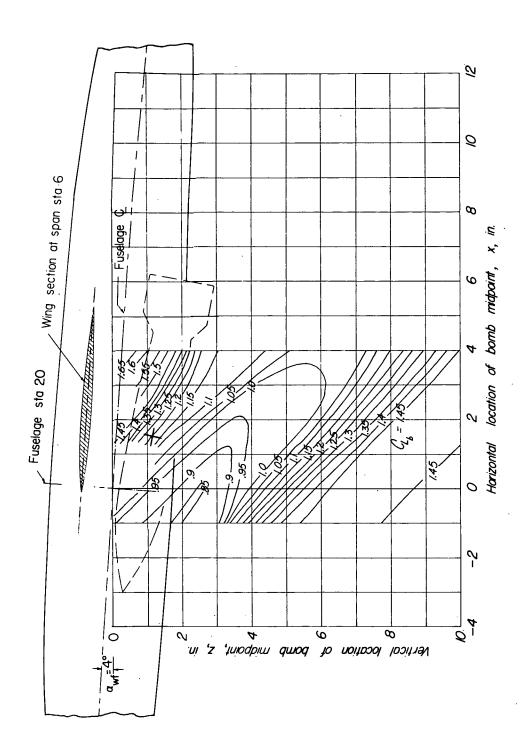


Figure 25.- Continued.

(b) $\alpha_{\rm b} = 10^{\rm o}$.

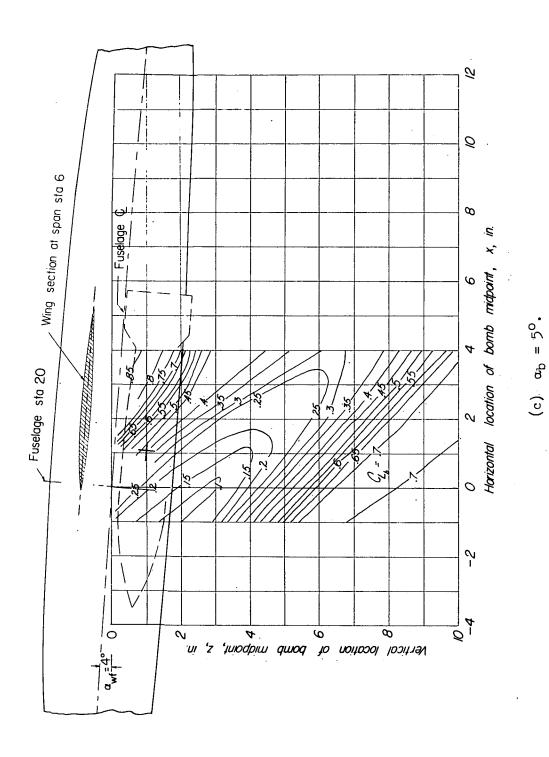


Figure 25.- Continued.

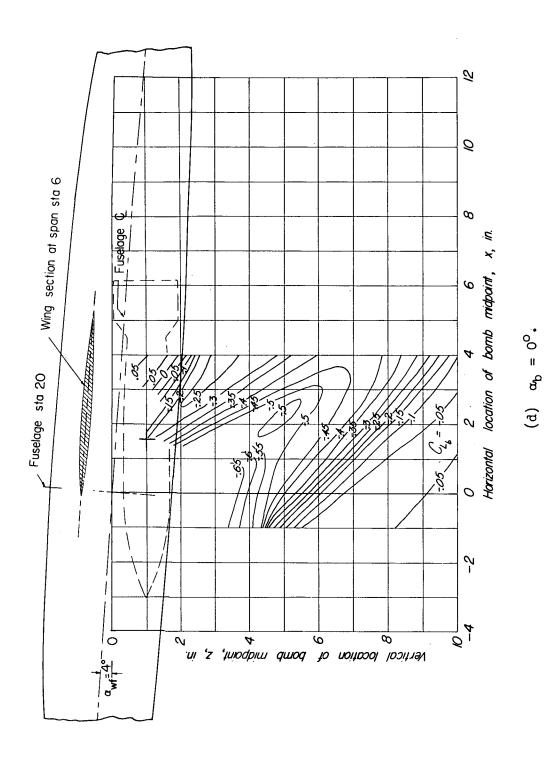


Figure 25.- Continued.

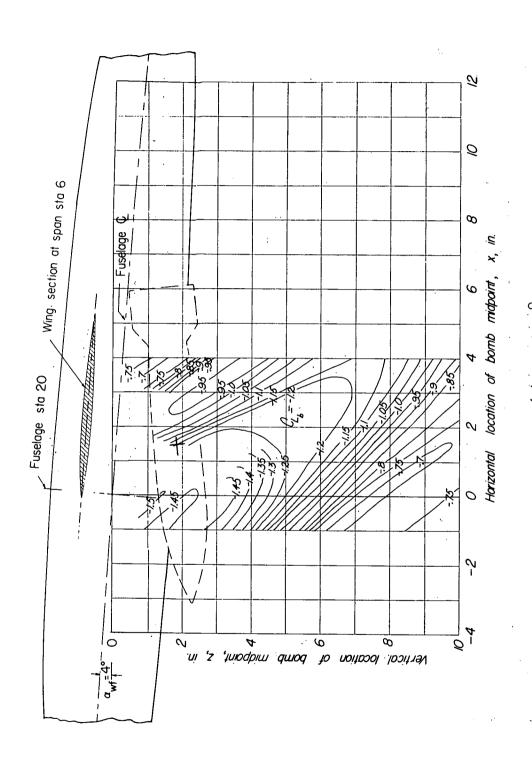


Figure 25.- Continued.

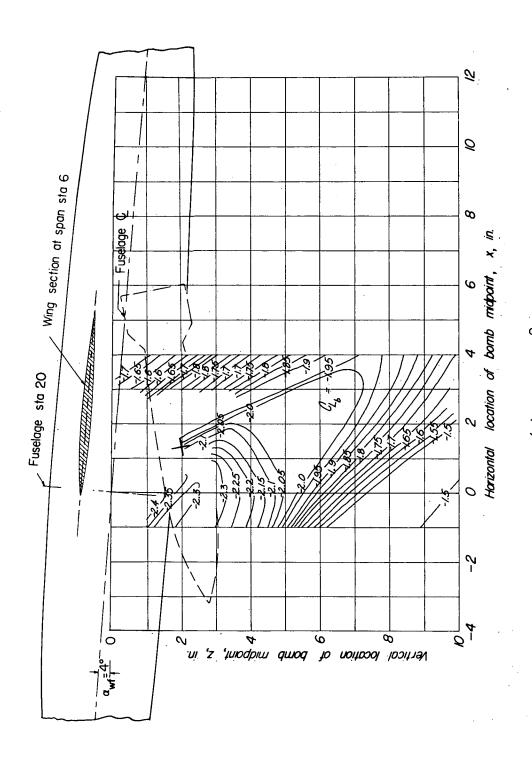


Figure 25.- Continued.

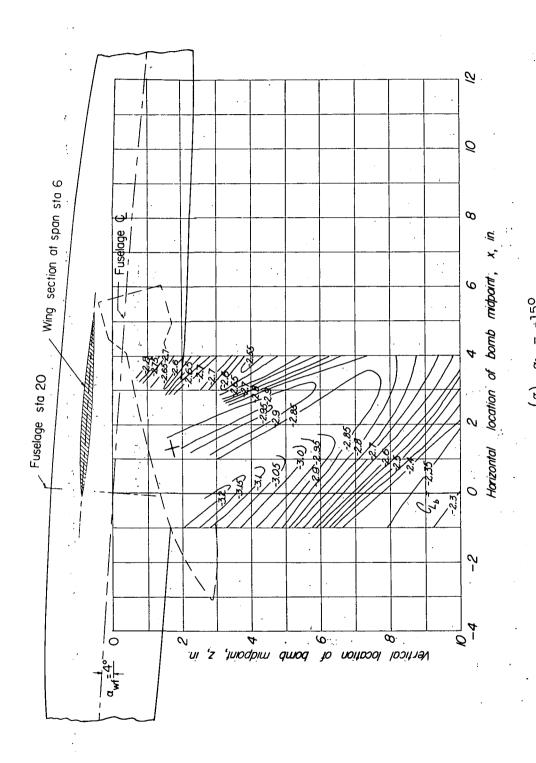


Figure 25.- Concluded.

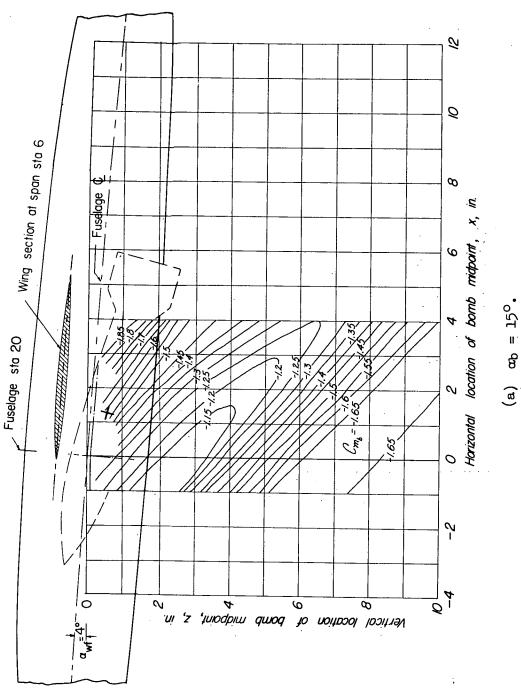


Figure 26.- Contour plot of pitching moment of bomb 3 in presence of wing-fuselage combination. y = 6 inches.

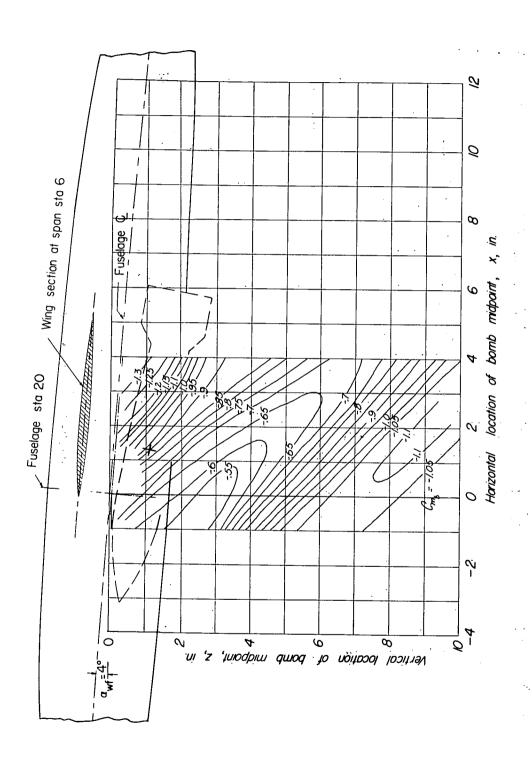


Figure 26.- Continued.

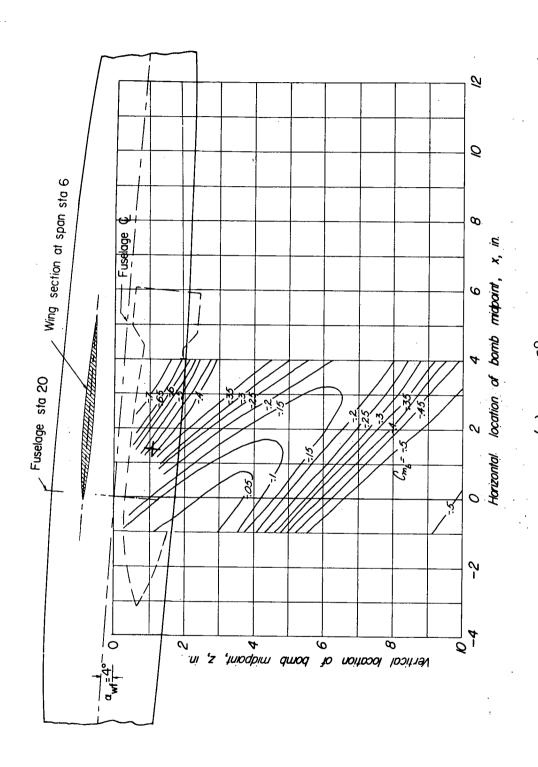
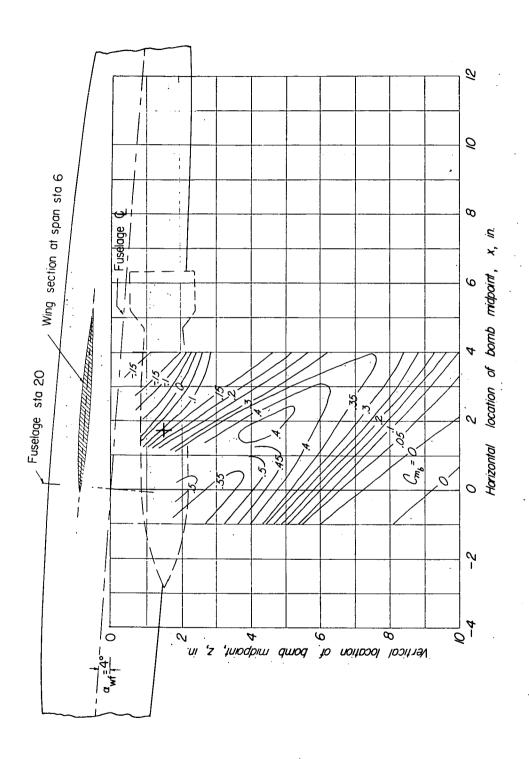


Figure 26.- Continued.



(d) $\alpha_{\rm b} = 0^{\rm o}$. Figure 26.- Continued.

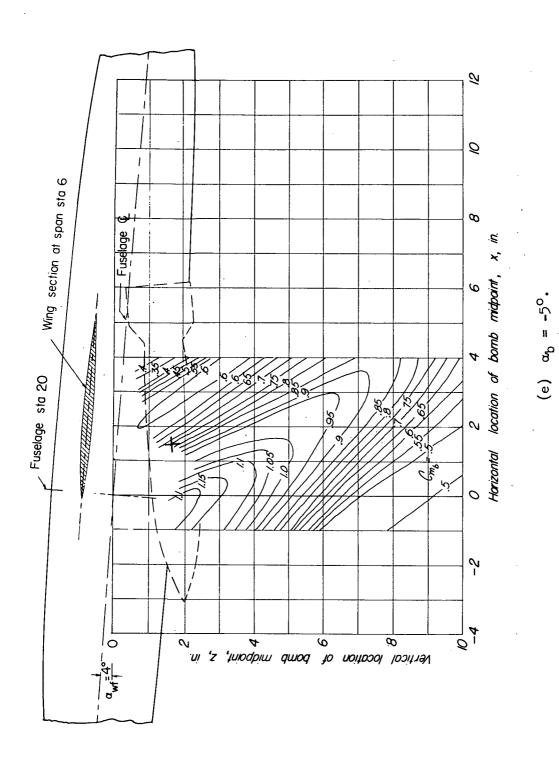


Figure 26.- Continued.

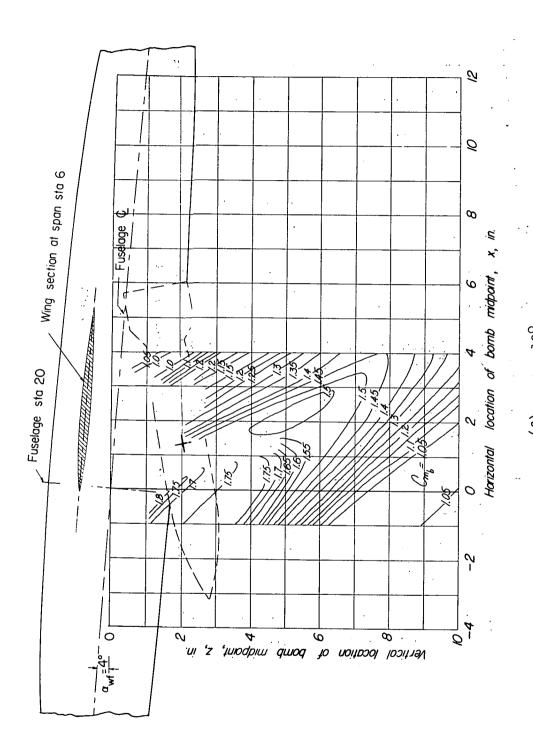


Figure 26.- Continued.

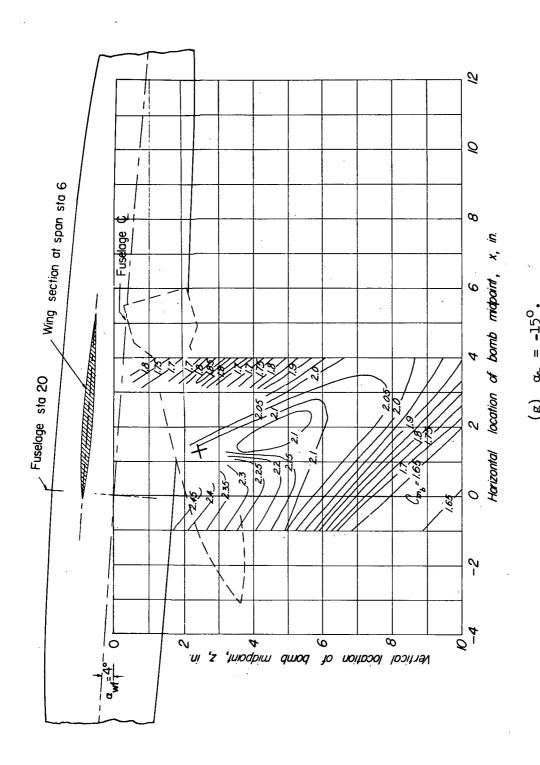


Figure 26.- Concluded.

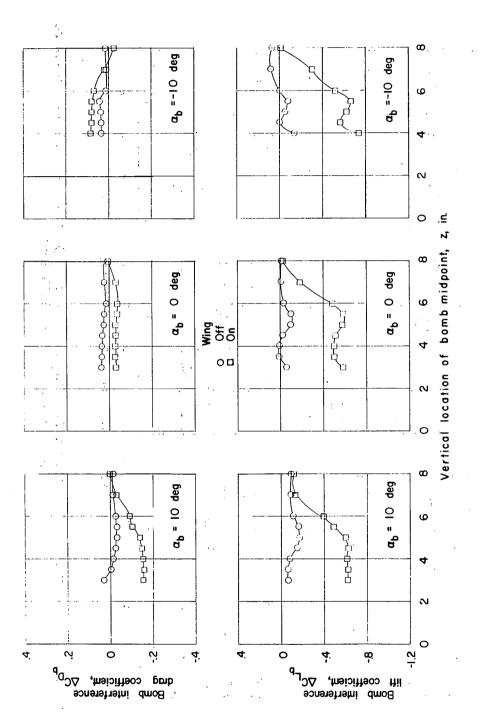


Figure 27.- Interference lift and drag of bomb 3 in presence of wing-fuselage combination and fuselage alone. x = -0.15 inch; $\alpha_{wf} = \mu^0$; y = 0.

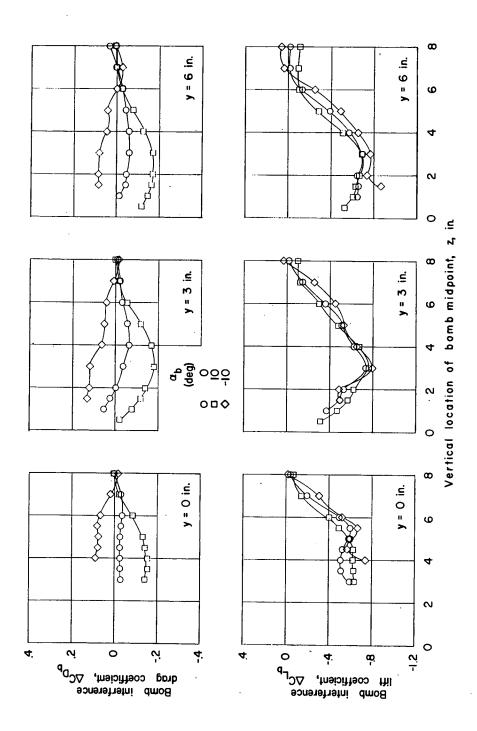


Figure 28.- Comparison of interference lift and drag of bomb 3 at three different spanwise stations. $\alpha_{\rm wf}=4^{\rm o}$; x = -0.15 inch.

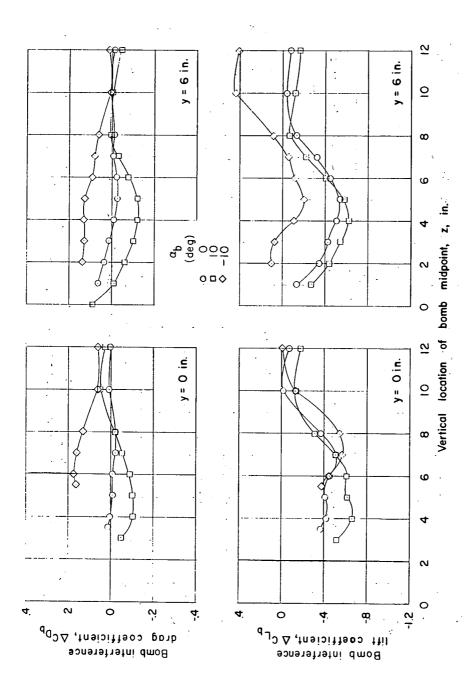


Figure 29.- Comparison of interference lift and drag of bomb μ at two different spanwise stations. $\alpha_{\rm wf} = \mu^{\rm O}$; x = -0.15 inch.

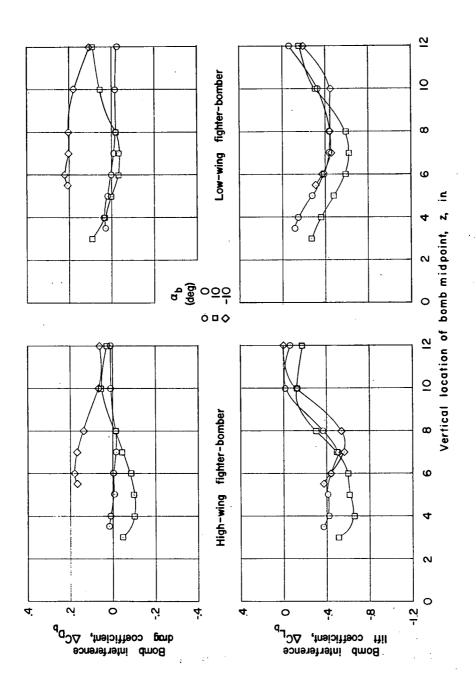


Figure 30.- Comparison of interference lift and drag on bomb 3 in presence at a low- and high-winged fighter-bomber configuration. $\alpha_{\rm wf} = 4^{\rm O}$; x = -0.15 inch; y = 0.

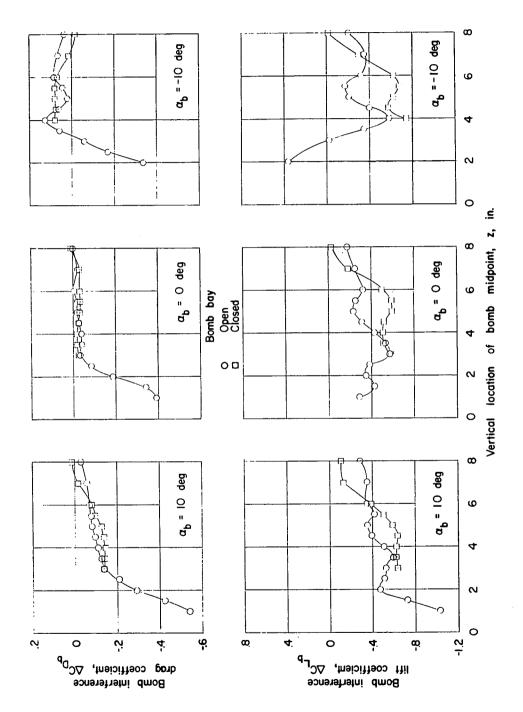


Figure 31.- Comparison of interference lift and drag of bomb 3 in presence of wing-fuselage combination with open and closed bomb bay (open bomb-bay data taken from ref. 2). $\alpha_{\rm wf} = \mu^{\rm o}$; bination with open and closed bomb bay (open bomb-bay data taken from ref. x = -0.15 inch.